Mühle et al., Perfluorocyclobutane (PFC-318, *c*-C_4F_8) in the global atmosphere, Atmospheric Chemistry and Physics, acp-2019-267

Authors' response to reviews:

Below we repeat the suggestions from both reviewers in italic and add our replies in bold. If we quote sentences from the manuscripts, modified parts will be bold, while unmodified parts will not be bold. We thank both reviewers for their overall positive reviews and helpful suggestions.

Reviewer 1:

The authors have brought together an impressive data set for atmospheric observations and modelling of PFC-318, which is global, long-term and consistent. The manuscript is well written but perhaps lacking succinctness a bit, which could be helped by moving some rather technical aspects that are not essential for the narrative to the supplement. A general concern is that the authors focus very much on their hypothesis of PTFE production as the main source of PFC-318 to the atmosphere. Other sources are barely mentioned let alone discussed, whereas the observations in my opinion point to a much more complex picture of emission sources (including unknowns). This should be given some more consideration. Other points are listed below.

We thank the reviewer for the overall positive assessment of our work. We agree that more technical aspect can be moved in the Appendix. In our detailed replies and our revisions to the manuscript we now point out more strongly the limitations of the inversion. Foremost, the further away emissions occur, the more likely the regional inversion method will allocate these emissions to a general diffuse region, rather than identify individual *c*-C_4F_8 point sources. For the Indian subcontinent, the limited number of samples taken onboard the aircraft contributes further to the problem. This needs to be kept in mind when interpreting the inversion results for East Asia and India. We also now emphasize that we cannot categorically exclude an unknown industrial source (Abstract, Section 5.3.5, Summary and Conclusion) and changed or added several statements (Abstract, Sections 5.3.1 and 5.3.5, and Summary and Conclusion), but the data and the inversion results are consistent with the hypothesis that production of TFE/HFP/PTFE/FEP and other fluorochemicals, both historically in developed countries and today in developing countries are likely the main source for *c*-C_4F_8. *c*-C_4F_8 is a by-product of the production of the needed TFE and HFP monomers via the pyrolysis of HCFC-22, industry experts confirm the practice to vent *c*-C_4F_8 from this process into the atmosphere (historically in developed countries and currently in China), emissions are not correlated with population density, and the semi-conductor industries in South Korea, Japan, Taiwan, and Europe do not emit significant amounts of *c*-C_4F_8. We hope that our added explanations and revisions address the concerns of the reviewer.

L119 I don't think a personal communication can be counted as evidence

In hindsight, the evidence was weak and it seems that *c*-C_4F_8 was not used significantly in this application. Lacking other references, we removed this part of the sentence from the Introduction. The evidence for use as geohydrological tracer is also rather weak and we chose to add "perhaps used as a geohydrological tracer**".**

L169-178 Have the authors ascertained that their calibration system has a linear response behaviour over a relevant mole fraction range? How was the calibration scale uncertainty estimated?

As explained in the last paragraph of Section 2.1, the linearity of the analytical system was assessed "with a series of diluted air samples (parent tank at 1.252 ppt, dilutions from 100 % to 6.25 %, Ivy et al., 2012) and a series of different volumes of a working standard (parent tank at 1.60 ppt, sample volumes from 200 % to 5 % of usual 2 L volume). A small deviation from linearity was observed for the most diluted samples and the smallest volumes probably due to a memory or blank of ~0.014 ppt on Medusa 9 was corrected for. Medusa 7 showed an effect of ~0.008 ppt, but as this was just below the detection limits and within the typical precisions, we chose not to correct for this.**". We hope that the reviewer agrees that these tests are sufficient to establish linearity.**

The calibration scale uncertainty was estimated conservatively based on the purity of the reagent, the reproducibility of the dilution technique to prepare the mixtures, measurement precisions, and propagation uncertainties as outlined in Prinn et al., 2000, 2001, and 2018 which we added at the end of the second paragraph of Section 2.1.

L187 "perhaps slightly better"?

We tried to express that the 5975 series MSDs showed slightly better detection limits than 5973 series MSDs. As the range of ~0.01-0.03 ppt includes detection limits estimated for both 5973 and 5975 series MSDs, we changed the sentence to "Detection limits …. were ~0.01–0.03 ppt **for both types of** MSDs.**".**

L210 "perhaps"?

We agree with the reviewer and removed "perhaps". It was redundant as the slight uncertainty in the estimated effect of ~0.008 ppt is already reflected in the approximate sign (~).

L214-249 It is commendable that the authors have carried out these tests. However, the high number of statistical outliers is worrying and casts some doubt on the derived longterm trends, in particular the early parts. Adding uncertainty ranges to the fits based on a) the samples that were included but showed discrepancies between Medusas and b) the sparsity of the measurements, might help here. In addition, I recommend moving this rather technical paragraph to the supplement.

We understand the reviewer's concern, which perhaps arises in part from the lengthy description of the tests we performed to verify that measurements at CSIRO and SIO agree, intermingled with the description of the filtering of the actual air archive measurements. We have now moved the discussion of the tests performed at CSIRO and SIO as well as some of the other details into the Supplement (at the beginning). Following the reviewer's suggestion, this considerably shortened Section 2.2 and streamlined the description of the archive data filtering. As suggested by the reviewer, we have also added the 95% confidence bands to the fits in Fig. 1. It is correct that the "early part" of the record, from the mid-1970s to the late 1970s, is more uncertain as no Cape Grim Air Archive (CGAA) data were available, but we would like to point out that the reconstruction of the "early part" of the record, from the late 1970s until in-situ data became available, is dominated by the

frequent and well behaved CGAA data. The less frequent, filtered NH tank data play a rather unimportant role. In the fits in Fig 1, this was achieved as described in the text by guiding the NH fit with the CGAA data. Note that, in the CSIRO inversion, the same effect was essentially achieved by using larger data uncertainties for the NH data, so that the inversion fits more closely to the SH data. When the NH tank data are left out of the CSIRO inversion, the reconstructed mixing ratios and emissions do not change significantly (see Fig. S3a for the emissions, and we now include the sensitivity test results for the reconstructed mixing ratios as well in a modified Fig. S3b). Moreover, it should be pointed out that most of the filtered NH tanks were filled in 2003 and later, typically many tanks on one or two days in a given year, which would add little information to the reconstruction given the onset of in-situ data at multiple stations in 2011 and the high quality of the CGAA data used to guide the filtering. We added this explanation to the revised text in Section 2.2.

L225 "eigth"

We fixed this typo to "eighth" **and the text has been moved to the beginning of the Supplement.**

L267 "a"

We removed this orphan "a" from Section 2.3.

L513 How high is the interhemispheric gradient and how has it evolved over time? This might e.g. reveal information on changes in emission latitudes. There is a lot of space in Figures 1 and 4 to show this.

We believe that the IH gradient before the onset of in-situ data is too dependent on the more scattered and uncertain NH archive data to draw defendable conclusions. From 2011 to 2017, when full in-situ datasets are available, the IH gradient increased from ~0.05 ppt to ~0.09 ppt, in line with increasing predominantly NH emissions. We added a new inset to Fig. 1 to show this, modified the caption, and added corresponding text to Section 5.1. Unfortunately, we do not believe that we can draw conclusions about changes in emission latitudes from the IH gradient with the 12-box atmospheric model and annually-repeating transport parameters.

L523 Define "good agreement". There are no uncertainty ranges given for the two estimates in Figure S7.

We felt that the old Fig. S7 would be too busy if we had included the uncertainty bands, but we agree with the reviewer that we need to show them. Therefore, we created a new Fig. S7 which shows the reconstructed mole fractions by the two inversions including 2σ uncertainty bands, demonstrating the good agreement of the two inversions. We reference this new Fig. S7 in Section 5.1. We also included the uncertainties of the mean ages (before 1965) and effective ages (after 1965) for the firn samples in the new Fig. S7 with respect to the question of reviewer #1 about L1256. (Note, the old Fig. S7 is now new Fig. S8 and so forth. Due to the insertion of new Fig. S12, old Fig. S11 is now Fig. S13 and old. Fig. S12 is now new Fig. S14.)

L537-538 Again, are these discrepancies within uncertainties?

Yes, the discrepancies in global emissions are within uncertainties as can be seen in Fig. 5. Emissions prior to 1980 rely on archive data that are predominantly NH, relatively sparse and of poor quality compared to later

decades (see Sec 2.2), and, in the case of the CSIRO inversion, firn data that comprises atmospheric air spanning a range of ages of typically about 40 years. To make this more clear to the reader and to also follow reviewer #1's comment on the same sentence, we modified this sentence at the beginning of Section 5.2 to "The Bristol inversion initially reconstructs lower emissions, but **the differences are within the estimated uncertainties for the reconstructed histories (see Fig. 5)."**

L555 GWP-100?

The reviewer is correct. We clarified the text at the end of Section 5.2 accordingly. The use of GWP_{100} was actually specified in the caption of old Fig. S8/new Fig. S9, but now we also added the GWP_{100} for each compound as well as a citation.

L571-574 Given that the largest emissions appear to occur near the sea, is there scope for some emissions being related to ships or submissions? What fraction of emissions did the model initially assign to have occurred over the ocean?

We are wondering if there is a misunderstanding here. Old Fig. S10/new Fig. S11 shows the cumulative footprint map for 2010-2017 for the Gosan station. This is the sensitivity to potential emissions from each area of the grid box on the map, not the emission strength at any given grid box. The sensitivity to potential emissions is related to how often air originates from a certain grid box according to meteorological models. It reflects how much information about distant sources is collected at the receptor site (in this case Gosan station).

The model assigns no emissions over sea a priori, and the inversion does not allow emissions to be placed there, see Fig. 7. The inversion actually infers a spatially resolved scaling of the a priori emissions field, therefore by setting 0 emissions then no matter how it is scaled, the resultant emissions will always be 0 over sea.

L590-591 This appears to be in disagreement with the statement in L576-578.

We actually disagree, but our wording in Section 5.3.1 was probably not clear. On L590-591 we compare a) the combined regional emissions in East Asia with our global emissions estimate and b) the Eastern Chinese emissions with our global emissions estimate. On L576-578, however, we compare Eastern Chinese emissions determined by our inversion with the a-priori emissions for Eastern China estimated from Saito et al. Therefore, the statements are not in disagreement. To make this clearer, we have changed the sentence near the end of the first paragraph of Section 5.3.1 to "The a priori emissions for eastern China of 0.185 Gg yr^{-1} are based on the Saito et al. (2010) estimate for all of China for November 2007 to September 2009, **but the inversion suggests emissions that are** ~62 % **higher** in 2010 and more than tripl**e** in 2017.**".**

L603 FABS?

We thank the reviewer for catching that we did not define the FABS at the first appearance in the text. We now defined it as "semiconductor fabrication plants (FABS)**". It had been defined in the caption for Figure 7.**

L631-638 Please add information such as measurement precisions, observed mole fraction ranges, ions used for identification and quantification, etc. on the HFP measurements to the manuscript. Please provide quantitative evidence instead of "associated with" and "virtually absent".

We apologize for not including more details on the HFP measurements. We now added the new Fig. S12 with a detailed caption. We also modified the main text at the end of Section 5.3.1 and refer to this new Figure. HFP is measured on m/z 131 and 150. On the Porabond Q column it elutes after HFC-125 and before CFC-115. We confirmed the identify of HFP with a spike of ~10 ppt HFP (87,422 area counts) measured at SIO. The working standard used at that time had a small HFP peak equivalent to ~0.03–0.04 ppt (270–380 area counts), while ambient air samples contained ~0.01 ppt HFP (98–123 area counts), just around the estimated detection limit of ~0.01 ppt (3 times baseline noise). The small abundance of HFP in the working standard led to poor precisions of ~20%. From Nov. 2018 until present, ambient air measurements at SIO typically showed 0–0.5 times (0–150 area counts) the response of the working standard used, reaching at most 2.5 times, indicating continuing miniscule ambient mixing ratios. HFP measurements at Aspendale (ASA) have not been calibrated, but the peak responses in ambient air sampled from Feb. 2017 until present were almost always small (ranging from 0 – 300 area counts), indicating similarly small ambient mixing ratios as at SIO. Only occasional small pollution events have been observed at ASA as discussed in Section 5.3.3. HFP measurements at Gosan and Shangdianzi (SDZ) were not calibrated, but several working standards showed significant peak responses (up to 2,500 and 4,000 area counts, respectively). From Aug. 2018 until present, *c*-C_4F_8 pollution events at SDZ always coincide with HFP pollution events. The new Fig. S12 shows the ratios of the area response in ambient air samples relative to the working standard (RL (reported)) for *c*-C_4F_8 (PFC-318), HFP, and HFC-23. Good correlations among the three compounds are evident. We removed references to other compounds from the text for brevity. We changed the wording from "associated with**" to "coincide with" and added a reference to the new Fig. S12 which clearly shows the correlations. As requested we clarified the second sentence to "**virtually absent **(≤0.01 ppt)".**

L639-641 Consistent with emissions from many of these facilities, but clearly not all (as stated in L610-612). Given the problems with associating these sources can the authors confirm that the ratios between m/z 131 and 101 during pollution events were consistent with those observed in clean air? This would help to rule out interferences during pollution events.

We can confirm that even during the highest pollution events measured at Gosan, the ratios of the mass over charge ratios m/z 131 over m/z 100 show no deviation from those observed in bracketing standards or during background conditions.

L661 How much smaller?

We thank the reviewer for pointing out this omission at the end of Section 5.3.2, which made us also realize that we had not defined the list of countries for the North Western European emissions given in this Section. We have now added this information and we also reran the European inversion as a mistake had been found.

This leads to a slight upward revision of the emissions (from 0.02 ± 0.01 Gg yr^{-1} to 0.026 ± 0.013 Gg yr^{-1}) and an updated Fig. 8. We adjusted the wording in Section 5.3.2 to reflect the updated results. We have also added that “The inversion is broadly consistent with emissions from PTFE/FEP production and FABS, but emissions from other industrial sources may also play a role”. As requested, we have now added UNFCCC and bottom-up emissions for comparison: 0.0007 Gg yr^{-1} (UNFCCC, 2013–2014) and 0.0017 Gg yr^{-1} (Bottom-up emission inventories, Section 3, 2013–2014)) for the inversion domain.

L697 That is a very optimistic way of looking at that Figure.

The sensitivity of the emissions generally decreases with distance from the measurement location, which leads to increased uncertainty in the inversion, both in the spatial distribution of emissions and their overall magnitude. The further away emissions occur, the more likely the regional inversion method will allocate these emissions to a general diffuse region, rather than identify individual c-C_4F_8 point sources. We added this explanation to Section 4.4 to point out more clearly the limitations of the regional inversion method. Due to the limited number of samples taken onboard the aircraft, the regional inversion for the Indian subcontinent may have more difficulty identifying individual point sources (which also may not be emitting at all times). We added this information in Section 4.6. We modified the sentence in Section 5.3.5. to stress these limitations “Given the limitations of the inversion method to identify distant point sources from a relatively small number of samples (see Sections 4.4 and 4.6), the posterior emissions …**”. As pointed out in the text “**Emissions predominantly occur outside of the Indo-Gangetic plain, the most densely populated region of India” **and we now add** “**, which excludes potential sources that scale with population. Instead the inversion allocates emissions in a much less densely populated region in which multiple likely industrial point sources for c-C_4F_8 are located.” We hope that these additional explanations address the reviewer’s concern with respect to Fig. 9 and Section 5.3.5.**

L706-707 This is not very clear from the Figure, which is rather indicating an unknown source.

Given that all the potential PTFE/FEP producing facilities we found in India are located within the emissive region identified by the inversion (Fig. 9), while none are in the heavily populated Indo-Gangetic Plain, and keeping the limitations of the inversion in mind (see our reply above), we are confident that the inversion results support our hypothesis that production of PTFE/FEP and other fluorochemicals is the likely dominant source of c-C_4F_8 emissions. Still, we modified the sentence to “While we cannot categorically exclude an unknown industrial source, these results **are consistent with the chemistry of** PTFE/**FEP** production as dominant emission source of c-C_4F_8**.”. We also modified two sentences in the Summary and conclusions section accordingly following the reviewer’s advice. Based on new information, we also added “Note, that one of the facilities in western India (Navin Fluorine International, Surat, Gujarat) is known to also produce HFO-1234yf since 2016, using a process which starts out with the same chemistry, that is the pyrolysis of HCFC-22 to TFE and HFP, with c-C_4F_8 as potential by-product (see Supplement)”. We added a short section in the Supplement with citations about HFO-1234yf. We also added a similar sentence in Section 5.3.1 about the PTFE production facilities of the Juhua Group Corporation in Zhejiang province which also produce HFO-**

1234yf since 2016. Other facilities licensed by Honeywell to produce HFO-1234yf using this route with potential *c*-C_4F_8 emissions may exist in East Asia, but any such production is relatively recent and cannot explain historic *c*-C_4F_8 emissions.

L713 What is the main purpose of this direct c-C_4F_8 production?

The main purpose *c*-C_4F_8 produced is unfortunately not listed on the HaloPolymer website. We contacted the company, but received no reply. The website broadly states that "R318C is used in air-conditioners, heat pumps and energy units. It is also used for synthesis of fluororganic compounds". The website lists CF_4, C_2F_6, *c*-C_4F_8, SF_6, and WF_6 as "specialty gases (that) are organic and inorganic fluorinated gases widely used as dielectrics and fire extinguishing agents, in dry etching processes during production of microelectronics.", but does not specify for which of these applications exactly *c*-C_4F_8 is used. The only use that was not included in the Introduction is "for synthesis of fluororganic compounds". When searching for chemical reactions on scifinder.cas.org, several reactions can be found in which *c*-C_4F_8 is used to introduce -CF_3 group into larger organic molecules. The reaction of *c*-C_4F_8 with TFE to HFP, as described in the Introduction, is also found. Three other reactions are described which lead to a variety of products, including desired products such as the hydrofluoroolefin HFO-1234yf, a fourth generation refrigerant used in newer mobile air conditioners (MACs) or HFP, but also various other products. While it is not clear which of these, or other reactions, using *c*-C_4F_8 as feedstock are commercially important, we added this new information to the Introduction. We have also added short discussions on possible *c*-C_4F_8 emissions from HFO-1234yf production in recent years.

L729 Which ones did PFC-318 correlate best with (also for other pollution events in Asia etc)?

The best correlation was observed between PFC-318 (*c*-C_4F_8) and HFC-23 at ZEP. Other compounds, such as HCFC-22, CFC-13, CH_2Cl_2, $CHCl_3$, or TCE showed weaker correlations. We added Fig. S15 to show PFC-318 (*c*-C_4F_8), HFC-23, and HCFC-22 concentrations at ZEP and now refer to this figure. We also added Fig. S12 which shows the good correlations between PFC-318 (*c*-C_4F_8), HFP, and HFC-23 enhancements at SDZ.

L740-741 How much larger?

We have modified the sentence and added this information in the main text: "These global emissions are significantly larger **than what can be compiled from available** bottom-up inventory information **(70 ± 17 times, 1990–1996, 29 ± 5 times, 1997–2010, 15 ± 1 times, 2011–2014)".**

L1236 Figure 1 is mostly demonstrating quality assurance purposes and one cannot see most station data anyway as it is on top of each other. As the long-term trend is shown again in Figures 3 and 4 I suggest moving it to the supplement.

We believe that demonstrating data quality assurance and showing the underlying raw data is very important. Moreover, as requested we have added the confidence bands and the interhemispheric gradients to Fig. 1 and therefore would like to retain Fig. 1 in the main text.

L1256 Is it necessary to show years from 1900 if the first data point is after 1930? What is the uncertainty of the calculated effective ages?

As *c*-C_4F_8 mixing ratios are not much different from zero in the early decades of the 1900s, we have changed Fig. 3 to show mixing ratios reconstructed by the CSIRO inversion from 1930. We would like to point out though that firn measurements are not associated with discrete age values, rather they relate to atmospheric mole fraction from a range of times in the atmosphere. The oldest data point is from South Pole and has a mean age of 1890 (it is mentioned in the Fig. 3 caption that it is not plotted). The data point with mean age 1933 reflects a mix of air from about 1900–1950. So although the measurements do contain information about mole fraction before the 1930s, there is not much change occurring in mole fraction or emissions.

Effective ages before about 1965 are very uncertain, as they depend on the growth rate of *c*-C_4F_8 in the atmosphere which itself is quite uncertain and small at this time. However, as described at the end of the second paragraph in Section 4.3.1, mean ages are shown in Fig. 3 (and the new Fig. S7) for firn data that would have an age before 1965 (for the best case estimate). Effective ages after 1965 are also dependent on the atmospheric growth rate, but this is known quite well from the inversion. Note that the firn data are shown versus mean or effective age in Fig. 3 and new Fig. S7 for illustrative purposes only; the CSIRO inversion uses Green's functions (also called age distributions) from the firn model to characterize the age of the air in each firn sample, with the ensemble of Green's functions used to incorporate uncertainty (as described in Section 4.3.1). Therefore uncertainty in effective age is only relevant for the comparison in Fig. 3 and new Fig. S7 and not for the CSIRO inversion. The 2 sigma range for effective ages varies between about ±0.2 and ±4 ppt, with a mean value of ±1.4 ppt (see new. Fig S7).

Supplement

Figure S1 The caption is actually an entire section and should perhaps have its own heading.

We now give the Section its own heading "Details on the tuning of the CSIRO firn model for the Summit13 site" and moved the heading "Supplemental Figures" and Fig. S1 just below this Section.

Figure S3 There is quite some uncertainty in the 1960s and 70s. Has this been reflected in the emission uncertainties?

Yes, uncertainty in the diffusion coefficient for *c*-C_4F_8 relative to CO_2 is included in the Green's function ensemble that is used in the bootstrap method to calculate uncertainties in emissions inferred by the CSIRO inversion. To clarify this, we modified the last sentence of the first paragraph of Section 4.3.1 to "… different firn model parameters **including relative diffusivity** (Trudinger et al., 2013, …)**".**

Figure S7 Please also show the published observational data set of Saito et al.

Note, old Fig. S7 is now new Fig. S8. As requested, we added the baseline trends given in Saito et al., 2010. However, we would like to point out that these data had calibration drift problems, see our reply to L547 below, which is why we did not include them in the inversion. We also believe that the baseline algorithm used for these data did not work as well as the AGAGE baseline algorithm, perhaps exacerbated by the significant

pollution observed and worse precisions. Therefore, the seemingly large differences between the Saito et al. trend lines themselves and the AGAGE and Oram et al. data are misleading. Note, we also added citations for Saito et al. and Oram et al. under new Fig. S8.

Table S3 RoW is not explained and web pages should be cited with the date on which they were accessed.

We thank the reviewer for this comment as it made us revisit Tables S3 and S4. We realized that we made mistakes with the references and corrected those. We now include the names of the two market reports and when each of the three sources was accessed. We also include definitions of RoW (Rest of the World). For the two market research reports, RoW includes the market share for India and Russia. For www.qianzhan.com, North America and Europe are also included in RoW as they could not be separated.

Reviewer 2:

The manuscript entitled "Perfluorocyclobutane (PFC-318, c-C_4F_8) in the global atmosphere" by Mühle et al. has been evaluated by this reviewer. The paper presents a substantial piece of measurement and modeling work on the atmospheric abundance and emission rates of perfluorobutane. The authors have developed an independent gravimetric c-C_4F_8 calibration scale and characterized the abundance of c-C_4F_8 with high precision in both hemispheres in order to determine historical emissions (archived samples) and recent global emissions. Using inversion modeling techniques, regional emission patterns (and pollution events) are investigated in detail, revealing that major c-C_4F_8 sources are found in heavily industrialized provinces of China (and perhaps Russia), due to the production of PTFE and other fluoropolymers. They predict c-C_4F_8 emissions will continue to rise and that c-C_4F_8 will become the second most important PFC emitted to the atmosphere in terms of CO2 equivalent emissions.

General Comments: The manuscript is a pleasure to read, has very few technical errors, and presents and an impressive amount of interesting data. The authors have done a commendable job to present a succinct and encompassing description of the methods and the results. The conclusions follow elegantly from the data presented and form a compelling narrative, especially considering the magnitude of difference in the potential emissions sources involved. I have only few scientific comments/questions. Those are listed below here, followed by technical (suggested) corrections:

We thank the reviewer for the very positive overall evaluation of our research article. We are very pleased that the reviewer agrees with our line of reasoning and conclusions.

Specific Comments:

L55: ": : :. explaining the increase in emissions." Presumably the authors here refer to the early/pre 1980's?

This indeed needed a clarification. We added "in the 1960s/70s" in the Abstract.

L65: "Significant emissions" must be inferred significant emissions?

Yes, this is correct as in the difference between global emissions and the sum of regional emissions. We changed as suggested by the reviewer to "significant emissions **inferred" in the Abstract.**

L115: What is "aerolyzed foods"? Please explain (very briefly), or used more common term.

We thank the reviewer for pointing out this mistake in the Introduction. We meant aerosolyzed foods which refers to foamed food products and sprayed food products, but this is perhaps not very commonly used. Therefore, we have replaced this with "foamed/sprayed foods**".**

L262: Please explain what is meant by "above bubble close-off".

Throughout the firn (compacted snow), air is contained in tiny channels that are open to the atmosphere. As more snow accumulates at the surface, the weight of the snow above causes the channels to be compressed and they eventually close to form discrete bubbles of air embedded in ice. Below this point the air cannot be pumped out anymore. We have modified the sentence in third paragraph in Section 2.3 to "… from 19 depth levels in the firn from **the** surface to **80.06 m (below this depth firn air can no longer be collected as the open channels in the firn have closed off and formed discrete air bubbles embedded in ice).”**

L396-397: “it was assumed that emissions were constant from year to year”. This seems confusing to me. Perhaps I’m not understanding this inversion correctly. I can see that the emissions would be assumed constant during the year, but why from year to year? How does this work?

We agree that this sentence at the beginning of Section 4.3.2 could be better worded. When a Bayesian inversion is performed, certain “a priori” assumptions need to be made to inform the inversion. These are often times emissions from a bottom-up inventory, which are believed to be reasonably close to reality, but bottom-up emissions for c-C_4F_8 are significantly too low. Therefore our approach, which has been used extensively in the literature, was to assume that emissions in any given year are similar to the previous and the next year, but to allow for a certain change (year-to-year emissions growth), that is we expect emissions to only change gradually. We rephrased the sentence to “A priori, it was assumed that emissions were **similar** from year to year **such that** the ***a priori*** year-to-year **emissions** growth rate **was assumed to be zero with an uncertainty** of 200 t yr^{-2} (0.2 Gg yr^{-2}, **1σ**), approximately twice the bottom-up estimate in Sect. 3.**”. Note, that we also corrected the unit from t yr^{-1} to t yr^{-2} (Gg yr^{-1} to Gg yr^{-2}), as it is an uncertainty in the emissions growth rate, and specified that it is a 1σ uncertainty.**

L440: “We do not report emission estimates outside of eastern Asia due to large posterior uncertainties but include them assisted with determination of the boundary conditions”. I do not understand this approach. Please clarify and explain.

We agree that this sentence in the third paragraph of Section 4.4 was rather confusing. Emission estimates far from the measurement station will be highly uncertain, both in terms of their spatial distribution and magnitude. We therefore choose to only report emissions for a region where the uncertainty is small enough that we are able to draw conclusions from the estimates, here eastern Asia. Nevertheless, the emissions outside of the reported region are still estimated in the inversion as they may contribute to pollution events measured at GSN. The contribution to the absolute error to the modelled mole fraction from distant emissions sources is small, but the resultant uncertainty in their inferred emissions is large. This leads to larger uncertainty in the reported regional emissions if they are included, which may hinder interpretation of results. To clarify, we changed to sentence to “While we do not report emission estimates outside of eastern Asia due to large posterior uncertainties, **they are still estimated in the inversion as they are useful when modelling emissions in eastern Asia and their uncertainties that we do report.”.**

L538: Please explain why not incorporating the firn data has this impact on the emissions estimates.

Prior to 1980, the Bristol inversion is based on sparse, uncertain NH archive data, and the CSIRO inversion on the same NH archive data plus firn data with age distributions covering roughly 40 years. The differences between the inversions before the early 1980s are within the estimated uncertainties for these reconstructions as can be seen in Fig. 5. We modified the sentence at the beginning of Section 5.2 to “The Bristol inversion initially reconstructs lower emissions, but **the differences are within the estimated uncertainties for the reconstructed histories (see Fig. 5).".**

L547: How can the mole fractions of this very unreactive compound change in the tanks?

The ratio of NIES/AGAGE *c*-C_4F_8 calibration assignments for two tanks exchanged between NIES and AGAGE (SIO) changed by more than 10% between 2008 and 2016, which is completely unacceptable. On the contrary, the IN/OUT values assigned by AGAGE (at the beginning and end of each tank's service time), agree for both tanks within precisions of 0.02 ppt (~1.1 to 1.7%). Therefore, we concluded that there must have been an internal calibration drift problem at NIES for *c*-C_4F_8 in tanks NIES used to assign calibrations to the two tanks exchanged with AGAGE/SIO. Unfortunately, we do not have enough data to characterize this further. One possible explanation for the drift (change of concentration) of such an inert perfluorinated compound could be the presence of Christo-Lube MCG111, which had been used by the manufacturer on a limited number of Essex tanks to deal with leak problems at the valve flange. MCG111 is a mixture of perfluorinated polyether (PFPE) and polytetrafluoroethylene (PTFE). We showed, without a doubt, that it is able to produce polyfluorinated compounds including *c*-C_4F_8 and CF_4 at ppt level, which caused a good deal of grieve for the AGAGE network. We still think that the sentence in the manuscript describes what the likely cause is, even though we did not include any of the details for brevity sake as we did not use the data. We slightly modified this and the previous sentence in the second paragraph of Section 5.2.

L553: C_2F_6 is here listed as a minor PFC, however in L122, it was a major. Which are the majors and the minors?

We agree that this is not consistent. In terms of mixing ratios, there is only one major PFC, CF_4, currently at ~86 ppt in the Northern Hemisphere, while the other three PFCs could all be called minor PFCs with C_2F_6 at ~4.9 ppt, *c*-C_4F_8 at ~1.8 ppt, and C_3F_8 at ~0.69 ppt. In terms of GWP_{100} CO_2 equivalent emissions, see old Fig. S8/new Fig. S9, CF_4 is also in its own league, while C_2F_6 and *c*-C_4F_8 CO_2-eq. emissions are similar but smaller and C_3F_8 CO_2-eq. emissions are even smaller. Therefore, we modified the sentence on L122 (Introduction) to "While the major atmospheric **PFC**, tetrafluoromethane (CF_4) **as well as the minor PFCs** hexafluoroethane (C_2F_6) and octafluoropropane (C_3F_8) are …**". The use of "minor" in the two statements is now consistent with each other (last sentence of Section 5.2 and seventh paragraph of the Introduction).**

L558: To make clear what we are talking about, I suggest inserting "from a climate forcing standpoint" before "will become the second most important PFC: : :".

We chose to modify the sentence at the end of Section 5.2 to: "*c*-C_4F_8 **CO_2-eq.** emissions have been …, so that *c*-C_4F_8 will become the second most important PFC emitted into the global atmosphere **in terms of CO_2-eq. emissions."**

"Technical" Comments:

L42-43: The propagated uncertainties on the emissions should be given in the abstract.

Agreed. We added 1σ uncertainties to the Abstract: "… the 1960s to 1.2 ± **0.1 (1σ)** Gg yr^{-1} in the late 1970s to late 1980s, then declined to **0.77 ± 0.03** Gg yr^{-1} in the mid-1990s to early 2000s, … rise since the early 2000s to 2.2**0 ± 0.05** Gg yr^{-1} in 2017**". We changed this accordingly in the "Summary and Conclusions" section.**

L61: " in agreement with our analysis". This seems like an obvious statement. Suggest deleting.

Agreed. We deleted it from the Abstract. We also deleted this in the "Summary and Conclusions" section.

L102: "Recently there is also further evidence: : :". This sentence begins awkwardly – suggest rewording it.

We changed the sentence in the Introduction to "Today we also have further evidence that …**".**

L249: "Fig.1." Other places in the manuscript "Figure" is used. Check for consistency.

Our understanding is that ACP requires the use of "Figure" when it stands at the beginning of a sentence and "Fig." when it stands anywhere else in a sentence.

L302: Perhaps "default" is a better word in place of "definition".

We agree that "by definition" was not the right choice of words, but "by default" does not seem right either. We modified the sentence in Section 3 to "However, these data are **inherently** not representative of total global emissions **since** developing countries do not…**".**

L311: Move the definition of 1t =0001Gg to the introduction paragraph, where Gg is first used.

Done. We moved this to the Introduction.

L316: replace "similar to" with "analogous to what has been observed for".

Done. We also modified the beginning of the sentence in Section 3: "As has been **found** by Saito et al. (2010) and Oram et al. (2012), we show in Sect. 5.2 and 5.3 that measurement based ("top-down") global and most regional emissions are significantly larger than the compiled bottom-up **c-C_4F_8 emissions** inventory information (see Fig. 5), **analogous to what has been found for** other PFCs (Mühle et al., 2010), reflecting the shortcomings of current emission reporting requirements and inventories".

L641: Insert "occurring" before ": : :in China: : :)

Done (last sentence in Section 5.3.1).

Line 689-691: These two sentences belong more appropriately in sections 5.35 and 5.3.6.

On one hand, we agree with the reviewer. On the other hand, these two sentences at the end of Section 5.3.4 serve as transition from 5.3.4 to 5.3.5 and 5.3.6. Moreover, the first sentence applies to both 5.3.5 and 5.3.6 and would have to be repeated if moved. Unless the reviewer feels strongly about this, we prefer to leave it as is.

Figures:

Figures 1 is nicely formatted, but the formatting is inconsistent with that applied in Figures 2-4. Moreover Figure 5 has a completely different formatting style. This figure formatting ought to be "harmonized".

For Fig. 1, we increased the fonts sizes and stroke of the box and tick marks (it was also updated following reviewer #1's request to add interhemispheric gradient and confidence bands). For Fig. 5, we adjusted the fonts, changed the color of the box and tick marks, added an axis at the right and top, and removed the outer box. Both Figures now more closely resemble Figures 2 – 4. We hope that no further changes will be needed.

Figure 1 caption: What are the error bars?

We added to the figure caption "**For individual samples, error bars reflect measurement precisions. For monthly means, error bars represent standard deviations.**"

Perfluorocyclobutane (PFC-318, *c*-C_4F_8) in the global atmosphere

Jens Mühle[1], Cathy M. Trudinger[2], Luke M. Western[3], Matthew Rigby[3], Martin K. Vollmer[4], Sunyoung Park[5], Alistair J. Manning[6], Daniel Say[3], Anita Ganesan[7], L. Paul Steele[2], Diane J. Ivy[8], Tim Arnold[9,10], Shanlan Li[5], Andreas Stohl[11], Christina M. Harth[1], Peter K. Salameh[1], Archie McCulloch[3], Simon O'Doherty[3], Mi-Kyung Park[5], Chun Ok Jo[5], Dickon Young[3], Kieran M. Stanley[3], Paul B. Krummel[2], Blagoj Mitrevski[2], Ove Hermansen[11], Chris Lunder[11], Nikolaos Evangeliou[11], Bo Yao[12], Jooil Kim[1], Benjamin Hmiel[13], Christo Buizert[14], Vasilii V. Petrenko[13], Jgor Arduini[15,16], Michela Maione[15,16], David M. Etheridge[2], Eleni Michalopoulou[3], Mike Czerniak[17], Jeffrey P. Severinghaus[1], Stefan Reimann[4], Peter G. Simmonds[3], Paul J. Fraser[2], Ronald G. Prinn[8], and Ray F. Weiss[1]

Deleted: Luke M. Western[3],

[1]Scripps Institution of Oceanography, University of California, San Diego, La Jolla, CA, USA
[2]Climate Science Centre, CSIRO Oceans and Atmosphere, Aspendale, Victoria, Australia
[3]School of Chemistry, University of Bristol, Bristol, UK
[4]Laboratory for Air Pollution and Environmental Technology, Empa, Swiss Federal Laboratories for Materials Science and Technology, Dübendorf, Switzerland
[5]KNU, Kyungpook Institute of Oceanography, College of Natural Sciences, Kyungpook National University, South Korea
[6]Met Office Hadley Centre, Exeter, UK
[7]School of Geographical Sciences, University of Bristol, Bristol, UK
[8]Center for Global Change Science, Massachusetts Institute of Technology, Cambridge, MA, USA
[9]National Physical Laboratory, Teddington, Middlesex, UK
[10]School of GeoSciences, University of Edinburgh, Edinburgh, UK
[11]NILU, Norwegian Institute for Air Research, Kjeller, Norway
[12]Meteorological Observation Centre (MOC), China Meteorological Administration (CMA), Beijing, China
[13]Department of Earth & Environmental Sciences, University of Rochester, Rochester, NY, USA
[14]College of College of Earth, Ocean, and Atmospheric Sciences, Oregon State University, Corvallis, OR, USA
[15]Department of Pure and Applied Sciences, University of Urbino, Urbino, Italy
[16]ISAC-CNR, Bologna, Italy
[17]Edwards LTD, Burgess Hill, West Sussex, UK

Correspondence to: Jens Mühle (jmuhle@ucsd.edu)

Atmospheric Chemistry and Physics, acp-2019-267

Abstract. We reconstruct atmospheric abundances of the potent greenhouse gas c-C_4F_8 (perfluorocyclobutane, perfluorocarbon PFC-318) from measurements of in situ, archived, firn, and aircraft air samples with precisions of ~1–2 % reported on the SIO-14 gravimetric calibration scale. Combined with inverse methods, we found near zero atmospheric abundances from the early 1900s to the early 1960s, after which they rose sharply, reaching 1.66 ppt (parts per trillion dry-air mole fraction) in 2017. Global c-C_4F_8 emissions rose from near zero in the 1960s to 1.2 ± 0.1 (1σ) Gg yr^{-1} in the late 1970s to late 1980s, then declined to 0.77 ± 0.03 Gg yr^{-1} in the mid-1990s to early 2000s, followed by a rise since the early 2000s to 2.20 ± 0.05 Gg yr^{-1} in 2017. These emissions are significantly larger than inventory-based emission estimates. Estimated emissions from eastern Asia rose from 0.36 Gg yr^{-1} in 2010 to 0.73 Gg yr^{-1} in 2016 and 2017, 31 % of global emissions, mostly from eastern China. We estimate emissions of 0.14 Gg yr^{-1} from Northern and Central India in 2016 and find evidence for significant emissions from Russia. In contrast, recent emissions from North Western Europe and Australia are estimated to be small (≤ 1 % each). We suggest that emissions from China, India and Russia are likely related to production of polytetrafluoroethylene (PTFE, "Teflon") and other fluoropolymers and fluorochemicals that are based on the pyrolysis of hydrochlorofluorocarbon HCFC-22 ($CHClF_2$) in which c-C_4F_8 is a known by-product. The semiconductor sector, where c-C_4F_8 is used, is estimated to be a small source, at least in South Korea, Japan, Taiwan, and Europe. Without an obvious correlation with population density, incineration of waste containing fluoropolymers is probably a minor source, and we find no evidence of emissions from electrolytic production of aluminum in Australia. While many possible emissive uses of c-C_4F_8 are known and though we cannot categorically exclude unknown sources, the start of significant emissions may well be related to the advent of commercial PTFE production in 1947. Process controls or abatement to reduce c-C_4F_8 by-product were probably not in place in the early decades, explaining the increase in emissions in the 1960s/70s. With the advent of by-product reporting requirements to the United Nations Framework Convention on Climate Change (UNFCCC) in the 1990s, concern about climate change and product stewardship, abatement, and perhaps the collection of c-C_4F_8 by-product for use in the semiconductor industry where it can be easily abated, it is conceivable that emissions in developed countries were stabilized and then reduced, explaining the observed emission reduction in the 1980s and 1990s. Concurrently, production of PTFE in China began to increase rapidly. Without emission reduction requirements, it is plausible that global emissions today are dominated by China and other developing countries. We predict that c-C_4F_8 emissions will continue to rise and that c-C_4F_8 will become the second most important emitted PFC in terms of CO_2-equivalent emissions within a year or two. The 2017 radiative forcing of c-C_4F_8 (0.52 mW m^{-2}) is small but emissions of c-C_4F_8 and other PFCs, due to their very long atmospheric lifetimes, essentially permanently alter Earth's radiative budget and should be reduced. Significant emissions inferred outside of the investigated regions clearly show that observational capabilities and reporting requirements need to be improved to understand global and country-scale emissions of PFCs and other synthetic greenhouse gases and ozone depleting substances.

Deleted: ~

Deleted: ~

Deleted: 8

Comment [JM11]: *Rev. #2: L42-43: The propagated uncertainties on the emissions should be given in the abstract.*

Deleted: ~

Deleted:

Deleted: conclude

Comment [JM12]: *Rev. #2: L55: ": : :. explaining the increase in emissions." Presumably the authors here refer to the early/pre 1980's?*

Comment [JM13]: *Rev. #2: L61: " in agreement with our analysis". This seems like an obvious statement. Suggest deleting.*

Deleted: , in agreement with our analysis

Comment [JM14]: *Rev. #2: L65: "Significant emissions" must be inferred significant emissions?*

Deleted:

1 Introduction

The perfluorocarbon (PFC) perfluorocyclobutane (c-C_4F_8, PFC-318, octafluorocyclobutane, CAS 115-25-3) is a very long-lived and potent greenhouse gas (GHG) regulated under the Paris Agreement of the United Nations Framework Convention on Climate Change (UNFCCC). Ravishankara et al. (1993) concluded that the most important atmospheric loss process of c-C_4F_8 is Lyman-α photolysis resulting in an atmospheric lifetime of 3200 years. Later, Morris et al. (1995) argued that if reactions of c-C_4F_8 with electrons and positive ions in the mesosphere and aloft are irreversible, the lifetime could be reduced to 1400 years, which, on human timescales, is still essentially infinite. c-C_4F_8 has a radiative efficiency of 0.32 W m^{-2} ppb^{-1} (parts per billion) and, assuming a 3,200 year lifetime, a global warming potential of 9,540 on a 100-year timescale (GWP_{100}) (Myhre and Shindell et al., 2013; Engel and Rigby et al., 2018). Due to the long lifetime and high radiative efficiency, emissions of c-C_4F_8 (and other perfluorinated compounds) essentially permanently alter the radiative budget of Earth (Victor and MacDonald, 1999).

Deleted: ^{1}

Lovelock (1971) predicted the accumulation of c-C_4F_8 in the global atmosphere, but to the best of our knowledge, the earliest atmospheric measurements of c-C_4F_8 were presented in Sturges et al. (1995) and in the Ph.D. theses of Travnicek (1998) and Oram (1999, discussed further below). Sturges et al. (2000) determined from one vertical balloon-borne profile in 1994 that c-C_4F_8 mole fractions declined from ~1.1 ppt (parts per trillion) in the lower atmosphere of the Northern Hemisphere (NH) to ~0.6 ppt in the stratosphere, while Harnisch (1999) reported that Sturges et al. (1995) had found 0.4 ppt in the troposphere decreasing to ~0.1 ppt at 25 km in 1994, suggesting a revised calibration scale. Harnisch et al. (1998; 1999) estimated from this atmospheric gradient global emissions of 1–2 Gg yr^{-1} (kt yr^{-1}, 1 t = 0.001 Gg). Travnicek (1998) reported ~0.2 ppt in 1977 and ~0.7 ppt in 1997 in the NH troposphere, from which Harnisch (2000) estimated average global emissions of 0.7 Gg yr^{-1}. Despite differences in early measurements and emissions estimates, perhaps due to different calibration scales and analytical methods, these studies were consistent with the accumulation of c-C_4F_8 in the global atmosphere.

Comment [JM15]: *Rev. #2: L311: Move the definition of 1t =0001Gg to the introduction paragraph, where Gg is first used.*

Harnisch (1999, 2000) stated that c-C_4F_8 had limited economic relevance, with some use for plasma etching in the semiconductor industry, that c-C_4F_8 can be formed via dimerization of tetrafluoroethylene (TFE), and that thermal decomposition or combustion of polytetrafluoroethylene (PTFE) and other fluoropolymers (Morisaki, 1978) (during waste disposal) possibly led to the accumulation of atmospheric c-C_4F_8.

Today we have stronger evidence for c-C_4F_8 emissions from the semiconductor and microelectronics industry as it has been increasingly used since the 1990s for dry etching, chemical vapor deposition chamber cleaning and as deposition gas (Bosch process). Compared to other fluorinated gases used for these processes, more selective etching, cost reduction in plasma cleaning, easier abatement and hence potentially lower contribution to global warming have been cited as advantages of c-C_4F_8 (e.g. Sasaki et al., 1998; Christophorou and Olthoff, 2001; Raju et al., 2003; Kokkoris et al., 2008; and references therein). However, due to efficient abatement with modern emission controls (up to 90 %), today's c-C_4F_8 emissions from this industry could also be small (Zhihong et al., 2001).

Today we also have further evidence that the thermal decomposition of PTFE and other fluoropolymers can lead to the formation of c-C_4F_8, TFE and hexafluoropropylene (HFP) (van der Walt et al., 2008; Bezuidenhoudt et al., 2017); the resultant c-C_4F_8 could therefore be emitted to the atmosphere.

Comment [JM16]: *Rev. #2: L102: "Recently there is also further evidence: : :". This sentence begins awkwardly – suggest rewording it.*

Deleted: Recently there is also

One potentially major source of c-C_4F_8 that seems to have received too little attention is the production of TFE and HFP monomers, the building blocks for PTFE, fluorinated ethylene propylene (FEP, TFE/HFP copolymer) and other fluoropolymers, which involves pyrolysis of hydrochlorofluorocarbon 22 (HCFC-22, $CHClF_2$) as c-C_4F_8, the dimer of TFE, is a by-product/intermediate of this process (Chinoy and Sunavala, 1987; Broyer et al., 1988; Gangal and Brothers, 2015). This reaction can be steered towards HFP or c-C_4F_8 by controlling the dimerization of TFE to c-C_4F_8 and the co-pyrolysis of c-C_4F_8 with TFE to HFP (Jianming, 2006). c-C_4F_8 could therefore be emitted during TFE/HFP/PTFE/FEP production if it is not abated or recovered, e.g. for use in the semiconductor industry or for pyrolysis with TFE to HFP at a later stage, perhaps at a different facility.

Several other, perhaps minor, emissive uses of c-C_4F_8 are also known (see Lewis, 1989; Chung and Bai, 2000; Harnisch, 2000; Christophorou and Olthoff, 2001; Kim et al., 2002; Liu et al., 2008; and reference therein), e.g. in foamed/sprayed foods, as a food packaging gas, in retinal detachment surgery, for contrast-enhanced ultrasound imaging, in radar systems, as a specialty refrigerant (e.g. in submarines where R-405A (43 % c-C_4F_8) can replace pure HCFC-22 and the chlorofluorocarbon CFC-12, CCl_2F_2), as an electrically insulating dielectric gas (e.g. in mixtures with sulfur hexafluoride, SF_6), as a medium for polymerization reactions, in fire extinguishers, and perhaps as a geohydrological tracer (Kass, 1998). Several chemical reactions in which c-C_4F_8 is used to introduce $–CF_3$ groups into organic molecules are known (chemfinder.cas.org, accessed 2019/06/19) as well as reactions leading to desirable products such as HFO-1234yf, a fourth generation refrigerant used in newer mobile air conditions (MACs, see Supplement) or HFP, but also various other compounds. Production of c-C_4F_8 for these uses, via the pyrolysis of HCFC-22 or perhaps from 1,2-dichlorotetrafluoroethane (CFC-114) (Siegemund et al., 2016), may cause emissions as well. While the major atmospheric PFC tetrafluoromethane (CF_4) as well as the minor PFCs hexafluoroethane (C_2F_6) and octafluoropropane (C_3F_8) are released during primary aluminum production (Holliday and Henry, 1959; Tabereaux, 1994; Fraser et al., 2013), no evidence for c-C_4F_8 emissions has been presented so far. Cai et al. (2018) presented evidence for negligible emissions of c-C_4F_8 from the similar electrolytic production of rare earth elements in China. There are no known natural sources of c-C_4F_8. In summary, there may be multiple c-C_4F_8 emission sources, but the extent and time evolutions of these various potential emission sources are unclear.

Saito et al. (2010) reported the first continuous, approximately four year long, in situ measurement record of c-C_4F_8 at two stations in the NH, with mean baseline 2006–2009 mole fractions of ~1.22 ppt at Cape Oshiishi (43.1° N, 145.3° E) and ~1.33 ppt at Hateruma Island (24.1° N, 123.8° E) (NIES calibration scale). Saito et al. (2010) determined increase rates of 0.01–0.02 ppt yr^{-1} and global emissions of 0.6 ± 0.2 Gg yr^{-1}.

Oram et al. (2012) published the first multi-decade long atmospheric record of c-C_4F_8 in the Southern Hemisphere (SH). They combined previous measurements of sub-samples of the Cape Grim Air Archive (CGAA) for the SH with air dates prior to 1994 (from Oram, 1999, converted to a new, 19.6 % lower calibration scale with an estimated uncertainty of ≤7 %) with newer measurements of CGAA sub-samples with air dates after 1994 and a change of analytical method after 2006. They found an increase of c-C_4F_8 at Cape Grim from 0.35 ppt in 1978 to ~0.8 ppt in 1995 and 1.2 ppt in 2010, with a current increase rate of ~0.03 ppt yr^{-1}. They reported that global c-C_4F_8 emissions increased from ~0.9 Gg yr^{-1} in the early 1980s to ~1.7 Gg yr^{-1} in 1986 before declining to a minimum of ~0.4 Gg yr^{-1} in 1993, after which they increased to ~1.1 Gg yr^{-1} in 2006 and 2007 and may have stabilized. Oram et al. (2012)

Deleted: ,

Deleted: ,

Comment [JM17]: *Rev. #2: L115: What is "aerolyzed foods"? Please explain (very briefly), or used more common term.*

Deleted: aerolyzed

Deleted: ,

Deleted: ,

Comment [JM18]: *Rev. #1: L119 I don't think a personal communication can be counted as evidence*

Deleted: to estimate the size of natural gas and oil reservoirs, for leak detection of nuclear waste containers (Schmidbauer, N., personal communication, 2011)

Deleted: two

Deleted: s

Deleted: and

Comment [JM19]: *Rev. #2: L553: C_2F_6 is here listed as a minor PFC, however in L122, it was a major. Which are the majors and the minors?*

Deleted: ,

Deleted: the minor PFC

Deleted: from primary aluminum production noted that the global emissions determined by Saito et al. (2010) were lower than their estimate and suggested that the underlying atmospheric rise rate measured by Saito et al. may be too small.

In summary, calibration differences between previous studies are significant, no multi-decadal c-C_4F_8 record for the NH has been published, and global emissions have not been reassessed since Oram et al. (2012). Therefore our primary goals have been to develop an independent gravimetric c-C_4F_8 calibration scale and to characterize the abundances of c-C_4F_8 with high precisions in both hemispheres in order to determine updated historic and recent global emissions. We present measurements of c-C_4F_8 with precisions of ~1–2 % on the SIO-14 calibration scale (~2 % accuracy) developed by the Scripps Institution of Oceanography (SIO) using instrumentation and calibration methods of the Advanced Global Atmospheric Gases Experiment (AGAGE) program (Prinn et al., 2018). We discuss historic atmospheric mole fractions of c-C_4F_8 based on measurements of the CGAA for the extra-tropical SH, archived air samples from various sources for the extra-tropical NH, continuous atmospheric measurements in both hemispheres at multiple remote AGAGE stations since mid-2010, combined with measurements of air extracted from firn from both hemispheres. Using our measurements and inverse modelling methods, we infer global c-C_4F_8 emissions since the beginning of the 20th century until 2017. To improve our understanding of prominent c-C_4F_8 sources and source regions, we investigate regional c-C_4F_8 emission strengths as observed by the global AGAGE network in eastern Asia, Europe, parts of Australia and Russia and by an aircraft campaign over India. We also summarize and discuss available inventory based "bottom-up" emissions and compare them to the emissions we determined with our atmospheric measurement based "top-down" approach.

2 Experimental methods

2.1 Instrumentation, data availability, and calibration

c-C_4F_8 and ~40 other halogenated compounds were measured by AGAGE in 2 L air samples with the "Medusa" cryogenic pre-concentration system with gas chromatograph (GC, Agilent 6890) and quadrupole mass selective detector (MSD) (Miller et al., 2008; Prinn et al., 2018). Data from twelve in situ measurements sites and fourteen Medusa instruments were used. At Monte Cimone, Italy, c-C_4F_8 was measured with a commercial Adsorption-Desorption System with gas chromatograph and mass spectrometer (ADS-GC/MS) (Maione et al., 2013). Table 1 shows the availability of in situ, archived air (Sect. 2.2), firn air (Sect. 2.3) and aircraft air sample (Sect. 2.4) measurements with information for each site. For all measurements, each sample was alternated with a reference gas (Prinn et al., 2000; Miller et al., 2008), resulting in up to 12 fully calibrated samples per day (Medusa and ADS-GC/MS). The reference gases at each site were calibrated relative to parent standards at SIO.

c-C_4F_8 measurements are reported on the SIO-14 calibration scale as ppt dry-air mole fractions. The calibration scale is based on four gravimetric halocarbon/nitrous oxide (N_2O) mixtures via a stepwise dilution technique with large dilution factors for each step (10^3 to 10^5) (Prinn et al., 2000; 2001). High purity c-C_4F_8 (99.999 %, Matheson Trigas) and N_2O (99.9997 %, Scott Specialty Gases) were further purified by repeated cycles of freezing (-196° C), vacuum removal of non-condensable gases, and thawing. Artificial air (Ultra Zero Grade, Airgas) was further purified via an absorbent trap filled with glass beads, Molecular Sieve (MS) 13X, charcoal, MS 5Å, and Carboxen 1000 at -80° C

Comment [JM110]: *Rev. #1: L169-178 Have the authors ascertained that their calibration system has a linear response behaviour over a relevant mole fraction range? How was the calibration scale uncertainty estimated?*

See our reply.

(ethanol/dry ice). Zero air was measured to verify insignificant c-C_4F_8 and other halocarbon blank levels before being spiked with the c-C_4F_8/N_2O mixtures. The resulting mixtures of c-C_4F_8 in artificial air have prepared values of ~1.3 ppt and the relative standard deviation of the calibration scale is 0.23 %. We estimate the uncertainties of the calibration scale propagation from SIO to the sites to be ~0.6 % and the calibration scale uncertainty to be ~2 % (see Prinn et al., 2000, 2001, 2018).

The primary calibration instrument for the AGAGE network at SIO (La Jolla, California), Medusa 1, and all field instruments used a Porabond Q (25 m, 0.32 mm I.D., 5 µm film thickness, Varian) chromatographic main column and, initially Agilent 5973, later 5975 series MSDs. The original Medusa design is described by Miller et al. (2008); subsequently all Medusas were converted or newly built to measure nitrogen trifluoride (NF_3) (Arnold et al., 2012), but this did not affect the c-C_4F_8 measurements methodology or the results. While 5975 MSDs are beneficial for samples and compounds with very low mole fractions, precisions for c-C_4F_8 measurements of archived air samples (3–7 replicates, see next section) were similar, i.e. better than ~0.01 ppt. Daily reference gas measurement precisions slightly improved from ~0.02 ppt (~1.5–2 %) to ~0.01 ppt (~1–1.5 %) with the 5975 MSDs. Detection limits (3 times baseline noise) for 2 L air samples were ~0.01–0.03 ppt for both types of MSDs.

Comment [JM111]: *Rev. #1:L187 "perhaps slightly better"?*

Deleted: , perhaps slightly better for 5975

In addition to calibrations, Medusa 1 was also used to measure in situ local ambient air and several archived air samples (see Sect. 2.2). However, analysis of most archived air samples at SIO occurred on a second instrument, Medusa 7, as it was equipped with a more sensitive 5975 MSD at that time. For these measurements, we temporarily converted Medusa 7 to use a GasPro GSC (60 m, 0.32 mm I.D., Agilent) main column as it promised better separation performance for several higher PFCs (Ivy et al., 2012) measured along with c-C_4F_8. Similarly, Medusa 9, the instrument used to measure most CGAA samples at the Commonwealth Scientific and Industrial Research Organisation (CSIRO, Aspendale) and ambient air after October 2010, had been converted to use a GasPro column. On both types of main columns, c-C_4F_8 was measured on mass over charge ratios (m/z) of 131 ($C_3F_5^+$) and 100 ($C_2F_4^+$) and reported by height using carefully chosen integration parameters as perfluorobutane (C_4F_{10}) shares both m/z and elutes on the tail of c-C_4F_8. The m/z ratios remained the same despite the very different separation principles of these two main columns. Measurements of archived air samples on Medusa 7 with both main columns agreed within less than 0.01 ppt (ratio of 1.0016, $R^2 = 1.0000$, n = 4, 0.237–1.11 ppt). In situ c-C_4F_8 measurements at SIO with Medusa 1 (Porabond Q) and 7 (with the GasPro column) continued to agree within typical precisions. We also compared archived air measurements on Medusa 1 and 7, both before and while Medusa 7 used the GasPro column, and results agree within precisions of 0.02 ppt or better (Medusa 1 vs. Medusa 7, both Porabond Q, ratio of 1.0001, $R^2 = 0.9987$, n = 95, 0.237–1.616 ppt, Medusa 1, Porabond Q vs. Medusa 7, GasPro, ratio of 1.0018, $R^2 = 0.9979$, n = 39, 0.239–1.515 ppt). These tests show that the different main columns did not cause any bias.

The analytical systems showed no significant c-C_4F_8 blanks. The linearity of Medusa 7 (SIO) and 9 (CSIRO) used to measure archived air samples was assessed with a series of diluted air samples (parent tank at 1.252 ppt, dilutions from 100 % to 6.25 %, Ivy et al., 2012) and a series of different volumes of a working standard (parent tank at 1.60 ppt, sample volumes from 200 % to 5 % of usual 2 L volume). A small deviation from linearity was observed for the most diluted samples and the smallest volumes, probably due to a memory or blank of ~0.014 ppt on Medusa 9, for which a correction was applied. Medusa 7 showed an effect of ~0.008 ppt, but as this was just below the detection limits and within the typical precisions, we chose not to correct for this.

Comment [JM112]: *Rev. #1: L210 "perhaps"?*

Deleted: was

Deleted: ed for

Deleted: perhaps

2.2 Archived air samples of the extra-tropical Southern Hemisphere (SH, Cape Grim Air Archive, CGAA) and extra-tropical Northern Hemisphere (NH)

To reconstruct the atmospheric history of c-C_4F_8 in the extra-tropical SH, 41 unique CGAA samples (collected 1978–2009, Langenfelds et al., 2014) were measured at CSIRO in 2011 (Ivy et al., 2012). In addition, 8 subsamples of CGAA parent tanks and four additional SH samples were measured at SIO to demonstrate that measurements at CSIRO and SIO agree (for details see the Supplement). Based on an iterative filtering process designed to reject outliers greater than 2σ deviations from curve fits through the results for all 60 SH samples (41 at CSIRO and 19 at SIO) and pollution filtered monthly mean measurements (O'Doherty et al., 2001; Cunnold et al., 2002) at the extra-tropical stations CGO and ASA (Australia), 13 SH samples were rejected as outliers, leaving 47 SH samples (78 %). To reconstruct the atmospheric history in the extra-tropical NH, 126 unique air samples mostly filled at SIO and THD (1973–2016) were measured at SIO. Additionally, 3 NH samples (filled in 1980 and 1999) were measured at CSIRO to demonstrate that measurements at CSIRO and SIO agree (for details see the Supplement). Most of the NH samples had been filled during baseline conditions for various purposes using modified diving compressors (RIX Industries, US, SA-3 and SA-6, Weiss and Keeling laboratories) and did not show any artefacts for many gases (e.g. Mühle et al., 2010; O'Doherty et al., 2014; Vollmer et al., 2016). For c-C_4F_8, however, comparisons with concurrent in situ measurements at MHD, THD, SIO and JFJ revealed artefacts for most of these samples and the iterative filtering process only retained c-C_4F_8 data for eleven NH samples. In contrast, CGAA tanks were filled with a cryogenic method which did not produce any bias. Due to the sparse NH data and poor data quality before in situ measurements started in the NH, the fits used for the iterative filtering process of NH data had to be guided by the final SH fit shifted by 1.5 years to allow for the delay of c-C_4F_8 accumulation between the SH and NH due to inter-hemispheric transport (Mühle et al., 2010; Vollmer et al., 2016). Without this guidance, initial NH fits were dominated by high outliers, resulting in bad fits. It should be pointed out that most of the filtered NH tanks were filled in 2003 and later, typically many tanks on one or two days in a given year, which would add little information to the reconstruction given the onset of in situ data at multiple stations in 2011 and the high quality of the CGAA data used to guide the filtering. Fig. 1 shows the filtered data and the final suggested fits and 95% confidence bands.

2.3 Air extracted from firn

To augment the data set of in situ and archived air measurements, we measured c-C_4F_8 in samples from a subset of the firn sites described in Trudinger et al. (2016), namely NEEM08 in the NH and DSSW20K and SPO01 in the SH, plus one new site in the NH, Summit13, Greenland. We used the CSIRO firn model (Trudinger et al., 1997; Trudinger et al., 2013) to characterize the age of the air in these samples (detailed in Sect. 4.1). Here, we give a brief description of the firn sites. For a full description of the calibration of the CSIRO firn model for NEEM08, DSSW20K, and SPO01 see Trudinger et al. (2013), and for Summit13 see Fig. S1.

NEEM08: Firn air was extracted from the EU borehole in July 2008 in northern Greenland, drilled near the North Greenland Eemian Ice Drilling Project (NEEM) deep ice core drilling site (77.45° N, 51.06° W) (Buizert et al., 2012). This site has a moderate snow accumulation rate of 199 kg m^{-2} yr^{-1}.

Summit13: Firn air was collected in May 2013 at Summit, Greenland from a borehole (72.66° N, 38.58° W) drilled 10 km NNW of Summit Station, Greenland. The US Firn Air system (Battle et al., 1996) was used to extract the air

Comment [JM113]: *Rev. #1: L214-249 It is commendable that the authors have carried out these tests. However, the high number of statistical outliers is worrying and casts some doubt on the derived longterm trends, in particular the early parts. Adding uncertainty ranges to the fits based on a) the samples that were included but showed discrepancies between Medusas and b) the sparsity of the measurements, might help here. In addition, I recommend moving this rather technical paragraph to the supplement.*

Deleted: Three CGAA tanks were measured at the beginning, in the middle, and towards the end of the measurements at CSIRO, with agreements within typical precisions or better (0.01–0.02 ppt).

Deleted: SH

Deleted: were measured at SIO which were sub-sampled from

Deleted: (fill dates 1986–2008, 0.60–1.17 ppt) into evacuated stainless steel (SS) tanks (4.5 L, Essex Industries, USA) with a vacuum manifold and pressure regulator shown not to produce any c-C_4F_8 artefacts. They were measured at SIO on Medusa 7 to take advantage of the more sensitive MSD and to evaluate the agreement with Medusa 9 measurements at CSIRO. Four of these CGAA subsamples measured at SIO agreed within precisions (delta mole fractions, Δx = 0.00–0.01 ppt, ratio = 1.0047, R^2 = 0.9994) with their CGAA parents measured at CSIRO, 2 subsamples showed a larger differences (0.018 and 0.027 ppt). The measurements of the seventh subsample and its CGAA parent were rejected, perhaps due to problems during the subsampling or with the parent tank. While we did not measure the CGAA parent of the eights subsample at CSIRO, we found agreement (Δx = 0.01 ppt) with another CGAA tank of similar air age (Δt = 63 days) measured at CSIRO. F

Deleted: (fill dates 1995–2010, 0.84–1.25 ppt)

Deleted: .

Deleted: Three were also in very good agreement with CGAA samples of similar fill date measured at CSIRO (Δx < 0.006 ppt, Δt = 7–23 days) and one showed a larger difference (Δx = 0.05 ppt).

Deleted: Two of these tanks measured at CSIRO were filled together at SIO in 1999 with 2 tanks measured at SIO and the agreement is excellent (Δx = <0.007 ppt). The third tank, filled in 1980 at Cape Meares, Oregon, agreed within 0.034 ppt with another NH tank (filled at SIO within 9 days) measured at SIO. Despite this larger difference, the overall good agreement of NH and SH samples measured at SIO and CSIRO shows that measurements on the involved instruments were comparable and that calibration scales were properly propagated.

Deleted: had been

from 19 depth levels in the firn from the surface to just above 80.06 m (below this depth firn air can no longer be collected as the open channels in firn have closed off and formed discrete bubbles embedded in ice). The 3 in borehole was drilled with the Eclipse Ice Drill (IDDO) and new rubber bladders (1/8 in thick) were fabricated (Greene Rubber Co., Woburn, MA) for use in this campaign. 2.5 L glass flasks were filled at all depths for high resolution measurements of gases performed by the National Oceanic and Atmospheric Administration (NOAA) (CO_2, CH_4, CO, N_2O, SF_6, H_2). Larger volume samples from pre-selected depth levels were filled in 35 L electro-polished SS tanks using a KNF Neuberger pump (with neoprene diaphragms). These samples were measured at SIO for c-C_4F_8 and other trace gases (including CH_4, N_2O, CFCs, HFCs, HCFCs, and SF_6). For quality control purposes, the sample line was measured on site for CO_2 and CH_4 by cavity ring-down spectroscopy (CRDS, Los Gatos Research, µ-GGA) and [CO] by a reducing compound photometer (Peak Labs, RCP1) prior to filling the flasks. Summit has a moderate snow accumulation rate of 211 kg m^{-2} yr^{-1}. CSIRO firn model calculations for Summit use the density profile from Adolph and Albert (2014) and mean annual temperature and pressure of 241.75 K and 665 mbar. The diffusivity profile and related parameters were calibrated using the measurements described above of CO_2, CH_4, N_2O, SF_6, CFC-11, CFC-12, CFC-113, CH_3CCl_3, HFC-134a, HCFC-141b, and HCFC-142b. Firn model results for these tracers are shown in Fig. S1.

Comment [JM114]: *Rev. #2: L262: Please explain what is meant by "above bubble close-off".*

Deleted: bubble close-off (80.06 m

Deleted: a

Deleted: [

Deleted:]

Deleted: [

Deleted:]

Deleted: (

Deleted: R

Deleted: Gas

Deleted: Detector

DSSW20K: Firn air was collected in January 1998 in Eastern Antarctica (66.73° S, 112.83° E) from a borehole drilled 20 km west of the deep Dome Summit South (DSS) drill site near the summit of Law Dome (Smith et al., 2000; Sturrock et al., 2002; Trudinger et al., 2002). This site has a short firn column and a moderate snow accumulation rate of 150 kg m^{-2} yr^{-1}.

SPO01: We only measured one sample collected in 2001 from 120 m from a borehole at the South Pole, Antarctica (90° S, 119° W) (Aydin et al., 2004; Sowers et al., 2005). This site has a deep firn column and a low snow accumulation rate of 75 kg m^{-2} yr^{-1}, resulting in old firn air.

Firn air extracted from the DSSW20K, NEEM08, and SPO01 sites was measured at CSIRO in 2012 (Medusa 9), while Summit13 firn air was measured at SIO (Medusa 7), see Table 1. c-C_4F_8 firn measurement data are included in the data file listed in the Supplement. Other gases such as CH_4 and N_2O were measured as well.

2.4 Air samples collected over India and the Indian Ocean

Air samples were collected on-board the UK FAAM (Facility for Airborne Atmospheric Measurements) BAe-146 aircraft during eleven flights conducted from June 12, 2016 to July 9, 2016 (9–28° N, 72–86° E) into 3 L pre-evacuated electropolished SS flasks (SilcoCan, Restek) sealed with metal bellow valves (SS-BNVVCR-4, Swagelok). During the time it took to compress the air samples to 41 psig (30–60 s, depending on altitude) using a metal bellows pump (PWSC 28823-7, Senior Aerospace, USA), the aircraft travelled ~7 km. Nine flights occurred over Northern India and two over Southern India and the Indian Ocean. In total, 176 flask samples were collected, with the majority (>90 %) of these samples filled below 1.5 km altitude. The size of the subsamples analyzed with the Medusa 21 at University of Bristol was reduced to 1.75 L (from 2 L) and the sampling rate to 50 ml min^{-1} (from 100 ml min^{-1}) to allow for triplicate analyses of each flask and to accommodate for the lower flask pressure. c-C_4F_8 measurements are reported on the SIO-14 calibration scale. Detection limits, blanks, and precisions were similar to those stated above. For further details, see Say et al. (2019).

3 Bottom-up emission inventories (UNFCCC, EDGAR, NIRs, WSC)

Emissions of compounds, such as c-C_4F_8, into the atmosphere are often estimated by so called “bottom-up” methods, which are based on information such as purchased, produced or imported amounts, industrial activities referred to as activity data and estimated emissions factors for each emissive process. Developed countries report annual emissions of GHG, including c-C_4F_8, to the UNFCCC using such bottom-up methods. However, these data are inherently not representative of total global emissions since developing countries do not have the same comprehensive UNFCCC reporting requirements, including countries such as South Korea, China, and Taiwan with sizable electronics and PTFE manufacturing capacities and thus with potentially significant c-C_4F_8 emissions. An additional complication is that several countries report unspecified mixes of PFCs or of PFCs and HFCs and other fluorinated compounds, making it difficult or impossible to estimate emissions of individual compounds, such as c-C_4F_8. In the Supplement, we gather available inventory information from submissions to UNFCCC, National Inventory Reports (NIRs), the Emissions Database for Global Atmospheric Research (EDGAR), the World Semiconductor Council (WSC), and the US Environmental Protection Agency (EPA) in an effort to estimate contributions from unspecified mixes and countries not reporting to UNFCCC to compile a meaningful bottom-up inventory. Globally these add up to 10–30 t yr^{-1} (0.01–0.03 Gg yr^{-1}) from 1990 to 1999, 30–40 t yr^{-1} (0.03–0.04 Gg yr^{-1}) from 2000 to 2010, and 100–116 t yr^{-1} (~0.1 Gg yr^{-1}) from 2011 to 2014 (with a substantial fraction due to the U.S. emissions from fluorocarbon production reported by US EPA). As has been found by Saito et al. (2010) and Oram et al. (2012), we show in Sect. 5.2 and 5.3 that measurement based (“top-down”) global and most regional emissions are significantly larger than the compiled bottom-up c-C_4F_8 emissions inventory information (see Fig. 5), analogous to what has been found for other PFCs (Mühle et al., 2010), reflecting the shortcomings of current emission reporting requirements and inventories.

Comment [JM115]: *Rev. #2: L302: Perhaps “default” is a better word in place of “definition”.*

Deleted: and ozone depleting substances (ODS)

Deleted: T

Deleted: however, by definition,

Deleted: as

Comment [JM116]: *Rev. #2: L311: Move the definition of 1t =0001Gg to the introduction paragraph, where Gg is first used.*

Deleted: , 1 t = 0.001 Gg

Deleted: Similar to what

Deleted: d

Deleted: pointed out

Deleted: will

Comment [JM117]: *Rev. #2: L316: replace “similar to” with “analogous to what has been observed for”.*

Deleted: similar

Deleted: to

Deleted: emission

4 Modelling studies

4.1 CSIRO firn model

The CSIRO firn model and its use in global inversion frameworks has been described in detail (Trudinger et al., 2013; Trudinger et al., 2016; Vollmer et al., 2016; Vollmer et al., 2018; Vollmer et al., 2019). Air samples taken far away from pollution sources represent the background atmospheric trace gas composition at that time. Once air enters the firn, vertical diffusion and other physical processes in the firn lead to mixing of air of different ages. Therefore, air extracted from firn must be described with an age distribution. We used the CSIRO firn model to describe the relationship between trace gas mole fractions measured in each extracted air sample from a given depth and the corresponding age distribution of high-latitude atmospheric mole fractions. The diffusion coefficient of c-C_4F_8 relative to that of CO_2 in air at 253 K used here was 0.47 with an estimated uncertainty of ~10 %. This value was determined using Equation 4 from Fuller et al. (1966) with Le Bas volume increments (e.g. Table 1.3.1, Mackay et al. (2006) and a multiplier for the Le Bas increments of 0.97 (which minimizes the difference of calculated relative diffusion coefficients of a number of compounds from values measured by Matsunaga et al. (1993, 2002, 2005)).

Figure 2 shows the measured depth profile of *c*-C_4F_8 (ppt) in air extracted from polar firn sites in the NH (Greenland) and the SH (Antarctica), for site details see Table 1. All samples showed *c*-C_4F_8 mole fractions above the detection limit. The firn reconstructed depth profiles are discussed in Sect. 4.3.1.

4.2 AGAGE 12-box model of the global atmosphere

The AGAGE 12-box two-dimensional model (Cunnold et al., 1983; Cunnold et al., 1997; Rigby et al., 2013) describes the transport and loss of trace gases in the global atmosphere. The model divides the atmosphere into four latitudinal bands at 0° and 30° S/° N and three altitude bands at 500 hPa and 200 hPa and calculates the mole fractions in each box. The AGAGE background sites (MHD, THD, RPB, SMO and CGO, see Table 1) were historically chosen to represent the trace gas mole fractions in the four lower (tropospheric) model “boxes”. Model transport parameters were varied seasonally, but repeated annually. Given the very long atmospheric lifetime of *c*-C_4F_8 compared to the study period, the lifetime of *c*-C_4F_8 was assumed to be infinite in the model.

4.3 Global inversion methods

We used the AGAGE 12-box model in two different Bayesian inversions, denoted as the “CSIRO” and “Bristol” inversions, to estimate historic *c*-C_4F_8 emissions from our observations and to reconstruct historic abundances. Both inversions used in situ and archive data and the CSIRO inversion additionally used firn data. The observations need to be representative of clean background air at each sampling location. For in situ data, the AGAGE statistical method was used to remove pollution events and to calculate pollution-free monthly mean background air mole fractions for each AGAGE station (O'Doherty et al., 2001; Cunnold et al., 2002). As explained in Sect. 2.2, an iterative filtering algorithm starting out with all the archived air data and the pollution-free monthly means was then used to reject outliers for the extra-tropical SH and NH, mostly from the NH archive data. Due to the remoteness of the firn sample sites, we assumed background conditions without any filtering.

4.3.1 CSIRO inversion

The CSIRO inversion was developed to infer annual emissions at the global scale from firn, ice core and atmospheric measurements (Sturrock et al., 2002; Trudinger et al., 2002; Trudinger et al., 2016). Green’s functions from the CSIRO firn model were used to relate the measured air in the firn samples to air in the atmosphere in the past, and Green’s functions from the AGAGE 12-box model were used to relate global emissions with a specified latitudinal distribution to mole fraction in the extra-tropical SH and NH. The inversion included constraints to avoid negative mole fractions, negative emissions and unrealistic changes in emissions; these constraints were required due to the characteristics of inverting firn data and sparse archive data. The uncertainties in reconstructed mole fractions and inferred emissions were calculated using a bootstrap method that included the uncertainty in firn measurements, annual mean mole fraction (this uncertainty is temporally-correlated, see Supplement in Vollmer et al., 2019), calibration scale (±2 %), and the firn model through the use of an ensemble of Green’s functions corresponding to different firn model parameters including relative diffusivity (Trudinger et al., 2013; Trudinger et al., 2016; Vollmer et al., 2016).

Deleted: y

Deleted: as

Figure 3 shows the data that were used in the CSIRO inversion: annual values based on 10-year smoothing spline fits (i.e. 50 % attenuation at periods of 10 years) to monthly means of pollution-free in situ measurements at the AGAGE background sites CGO (SH) and MHD (NH), annual values based on 10-year smoothing spline fits to measurements of the CGAA and archived NH air samples, and air extracted from polar firn in both hemispheres. Annual means from the spline were only used in the inversion when there were pollution-free archive or in situ measurements around that time. Figure 3 also shows the final reconstructed abundances for the extra-tropical SH (solid black line) and NH (dashed black line) based on the optimized emissions. The measured mole fractions in firn air are plotted against their effective atmospheric ages if that age is after 1965, where the effective ages are calculated using the reconstructed history of atmospheric mole fractions determined by the CSIRO inversion (Trudinger et al., 2002). Before 1965, the growth rate in the atmosphere was small and uncertain; this makes it difficult to determine effective ages, so the earlier firn measurements are plotted against their mean ages (see also Fig. S7). Firn depth profiles for each firn site corresponding to the CSIRO inversion results are shown in Fig. 2 (solid lines) and they typically agree with the measurements within precisions (1σ, shown as error bars).

Overall, the abundances reconstructed with the CSIRO inversion agree very well with the measurement data (see also Fig. S2). In Fig. S3, we show the effect of excluding different sites from the inversion on reconstructed emissions and mixing ratios and the sensitivity of the inversion to the relative diffusion coefficient of c-C_4F_8. It should be pointed out that the deepest NEEM08 firn air sample for the NH showed slightly lower mole fractions (0.0085 ppt) than the deepest DSSW20K samples for the SH (0.021 ppt and 0.0185 ppt), although the mean ages are similar (1930s). The same applies to the second deepest NEEM08 (0.0105 ppt) and DSSW20K (0.018 ppt) samples (1940s), which is unexpected for a long-lived anthropogenic compound predominantly emitted in the NH. While the differences seem significant within the nominal precisions (0–0.0014 ppt) achieved for these firn samples measured only 1–2 times, they are not significant within typical precisions achieved for archive samples (~0.01–0.02 ppt) which are typically measured 3 or more times and these data are just at or below the typical detection limits of 0.01–0.03 ppt. Based on the order in which the firn samples were measured and the absence of detectable blanks, it seems unlikely that a small blank, memory, calibration, or measurement problem could have caused this small discrepancy. The early part of the reconstructed record, with near-zero mole fractions, is also most susceptible to small uncertainties in the calibrated diffusivity profiles versus depth for all sites used in the firn model, uncertainties in the firn model structure (e.g. physical properties being invariant of time), or uncertainties in the diffusivity of different tracers relative to each other. Thus, there are a number of possible reasons for the higher mixing ratio in the SH firn data at this time, and we do not interpret this as evidence of higher mole fraction in the SH in the 1930s or 1950s.

4.3.2 Bristol inversion

The Bristol inversion was used to estimate annual fluxes of c-C_4F_8 using archive and in situ observations only (Rigby et al., 2011; Rigby et al., 2014; Vollmer et al., 2018). A priori, it was assumed that emissions were similar from year to year such that the a priori year-to-year emissions growth rate was assumed to be zero with an uncertainty of 200 t yr^{-2} (0.2 Gg yr^{-2}, 1σ), approximately twice the bottom-up estimate in Sect. 3. The derived emissions uncertainties include contributions from the measurement repeatability, the calibration scale uncertainty, and the model-measurement representation error (Rigby et al., 2014). Furthermore, because some archive air samples exhibit

Deleted:

Deleted:

Deleted: see

Deleted:

Deleted: ,

Deleted: constant

Comment [JM118]: *Rev. #2: L396-397: "it was assumed that emissions were constant from year to year". This seems confusing to me. Perhaps I'm not understanding this inversion correctly. I can see that the emissions would be assumed constant during the year, but why from year to year? How does this work?*

Deleted: , with an uncertainty in

Deleted: ^{1}

Deleted: ^{1}

substantial short-timescale (< 1 year) variations that are unlikely to represent real changes in the background atmosphere (Fig. 1), the minimum uncertainty was set to the maximum deviation of the archive air samples from the smooth curve in Fig. 1 (0.03 ppt). Model representation errors were estimated as the variability of the pollution-free monthly baseline means determined by the AGAGE pollution algorithm (O'Doherty et al., 2001; Cunnold et al., 2002) from the high-frequency in situ data at each station for each given month. For periods without in situ data, the representation error was assumed to be equal to the average baseline variability from in situ data in the same latitudinal band scaled by the measured *c*-C_4F_8 abundance. The calibration scale propagation uncertainty is estimated based on propagation uncertainties of the *c*-C_4F_8 calibration scale from primary gravimetric standards to secondary standards within the “R1” relative calibration framework used in AGAGE and on propagation uncertainties from the R1 framework to the standards used to measure individual samples. Figure 4 shows that there is good agreement between the archived air samples (Sect. 2.2) and the pollution-free monthly mean in situ data from the AGAGE background sites (MHD and THD, RPB, SMO, and CGO) used in the Bristol inversion and the reconstructed mole fractions for the four latitudinal bands which these samples represent (see also Fig. S4).

Deleted:

4.4 Regional model and inversion study using NAME-HB for eastern Asia

To investigate regional emissions in eastern Asia (20° N–50° N and 110° E–160° E) from our observations we used an inversion method based on Bayesian inference. We estimated annual mean emissions, assuming that emissions are constant in both space and magnitude during each calendar year. Here, the inversion used observations from the Gosan station as this site was operated with relatively few interruptions from October 2010 to the end of 2017, with best data coverage from 2011 to 2015. These observations were binned into 12 hourly averages. The inversion method requires an atmospheric transport model to derive the sensitivity of the observations to a surface emissions field. We used the Lagrangian NAME (Numerical Atmospheric dispersion Modelling Environment) model from the UK Met Office (Jones et al., 2007), driven by meteorology from the Met Office Unified Model (Walters et al., 2014). The sensitivity was derived by releasing 20,000 hypothetical air parcels per hour of measurement from Gosan station, which were transported backwards in time for up to 30 days. The model recorded the time and location that air parcels interacted with the surface (below 40 m above ground level at a spatial resolution of 0.352° by 0.234°), and these data were used to form an aggregated 30-day sensitivity or “footprint” map for each hour of measurement. In addition, the model recorded the time and location that air parcels left the domain boundaries to provide the sensitivity to the boundary conditions. The footprint maps, generated over the domain 5° S–74° N and 55° E–192° E and up to 19 kilometres, were aggregated into 12 hourly averages.

We used a trans-dimensional hierarchical Bayesian method (NAME-HB) with a Metropolis-Hastings Markov chain Monte Carlo (MCMC) algorithm (Metropolis et al., 1953; Hastings, 1970) to solve the inverse problem. This allowed spatial emission estimates of *c*-C_4F_8 to be derived, whilst considering the uncertainties in the model, measurements, and a priori information and, importantly, the uncertainty in these uncertainties. Bayesian methods require a priori knowledge, here the emissions and boundary conditions. As little information on eastern Asia’s *c*-C_4F_8 emissions (see Sect. 3) was available, we based our mean a priori emissions on those estimated by Saito et al. (2010). We spread their emissions for each reported country uniformly over the area of each country, rather than use population density (as in Saito et al., 2010) as that is not likely a good proxy of *c*-C_4F_8 emissions. We also spread

Deleted: to be

0.11 Gg yr^{-1} of emissions over the rest of the domain where the footprint was calculated. The value of 0.11 Gg yr^{-1} is an approximate scaling of the global total emissions based on population in this outer domain, i.e. the remainder of the domain not defined as eastern Asia. While we do not report emission estimates outside of eastern Asia due to large posterior uncertainties, they are still estimated in the inversion as they are useful when modelling the emissions in eastern Asia and their uncertainties that we do report. We assigned a large uncertainty to these a priori emissions (Table S1), which were governed by a log-normal distribution, so that they were uninformative and the observations dominated the estimation. We set a priori boundary conditions to be the mean background mole fractions measured at MHD on each vertical boundary (N, E, W, S) of the NAME domain. Offsets to the boundary conditions on each boundary were estimated in the inversion on a monthly basis.

Comment [JM119]: *Rev. #2: L440: "We do not report emission estimates outside of eastern Asia due to large posterior uncertainties but include them assisted with determination of the boundary conditions". I do not understand this approach. Please clarify and explain.*

Deleted: but including them assisted with determination of the boundary conditions (or non-proximal emissions)

The hierarchical nature of the inversion method means that hyper-parameters were also incorporated to include uncertainties in the NAME sensitivities, which are described by a multivariate normal distribution (see Ganesan et al., 2014). The reversible jump, or trans-dimensional, aspect of the inversion means that the underlying resolution at which the emissions are estimated is itself explored during inference (Lunt et al., 2016). Table S1 shows the a priori probability distributions assigned to the emissions and boundary conditions scaling factors, model uncertainty and the underlying grid. The posterior emissions estimates and their uncertainties were governed by exploring the spaces of each of these parameters and hyper-parameters. The sensitivity of the emissions generally decreases with distance from the measurement site, which leads to increased uncertainty in the inversion, both in the spatial distribution of emissions and their overall magnitude. The further away emissions occur, the more likely the regional inversion method will allocate these emissions to a general diffuse region, rather than identify individual c-C_4F_8 point sources.

Deleted: N

4.5 Regional model and inversion study using InTEM for Western Europe

To investigate regional emissions in Western Europe (36° N–66° N and -14° E–31° E) we used InTEM, an inversion framework (Arnold et al., 2018) based on the NAME Lagrangian transport model (Jones et al., 2007), together with observations from MHD, Tacolneston (TAC), Jungfraujoch (JFJ) and Monte Cimone (CMN). A priori estimates were considered unknown (see Sect. 3 and the Supplement) and therefore set to a uniform distribution of 0.2 Gg yr^{-1} over the whole land area within the inversion domain with an uncertainty of 0–0.62 Gg yr^{-1}. Observational uncertainty was time varying and estimated as the variability of the observations in a 6 hour moving window plus the measurement repeatability determined from repeat measurements of the on-site calibration standards. Model uncertainty was estimated every 2 hours as the larger of the median of all pollution events at each station in a year or 16.5 % of the magnitude of the pollution event. A temporal correlation of 12 hours was assumed in the model uncertainty at each station. An analytical solution was found that minimized the residual between the model and the observations and the difference between the posterior and the a priori flux estimate, balanced by the uncertainties of both. The baseline was estimated in the inversion following Arnold et al. (2018). The variable resolution of the inversion grid was calculated and refined within InTEM based on the magnitude of the footprint and emissions from each grid box. The inversions were run 24 times per year, each time with a randomly generated sub-sample (90 %) of the available observations from each station (10 % removed in 5-day blocks), to further explore the uncertainty. Emissions and uncertainties were averaged across the 24 individual inversions thereby assuming 100 % correlation between uncertainties in these separate inversions. 1-year inversions were performed covering the period 2013–2017.

4.6 Regional model and inversion study using NAME-HB for India

To investigate regional emissions from the Indian subcontinent from the samples taken on-board a research aircraft in June and July 2016 (see Sect. 2.4) we used the NAME-HB inversion method described in Sect. 4.4 and Table S1. Here, the domain spanned from 6° N to 48° N and from 55° E to 109° E with an altitude up to 19 kilometers and emissions were estimated as the mean over the 2-month period. As with eastern Asia and Western Europe studies, the sensitivity of the atmospheric measurements to surface emissions was derived using the NAME model. Back-trajectories were simulated for each minute of each flight path for up to 30 days backward in time. To account for the motion of the aircraft, hypothetical air parcels were released from a cuboid whose dimensions were defined as the change in latitude, longitude and altitude of the aircraft during each 1 minute period, at a release rate of 1000 air parcels min^{-1}. Wherever possible, samples were collected during periods of level flight, to minimise the altitude component of the release volume. India's a priori emissions were set to 18 % of global *c*-C_4F_8 emissions (from Sect. 5.2), equal to India's fraction of the global population, but uniformly distributed over India. A large uncertainty was assigned (Table S1) to reflect the lack of information on India's current *c*-C_4F_8 emissions. A priori vertical boundary conditions were assigned using background mole fractions from MHD (N, E and W) and CGO (S). Offsets to these boundary conditions were estimated in the inversion. Due to the limited number of samples taken onboard the aircraft, the regional inversion for the Indian subcontinent may have more difficulty identifying individual point sources (see Section 4.4), which also may not be emitting at all times. We report only emissions for Northern and Central India (NCI) as the inversion has low sensitivity over southern India and Sri Lanka and the north western edge of the domain, and no sensitivity beyond the Himalayas (see Fig. S5). Sensitivity tests indicate that *c*-C_4F_8 emissions determined for NCI are insensitive to the choice of a priori emissions (see Fig. S6).

Deleted: only

4.7 Pollution events at Zeppelin station

The Zeppelin (ZEP) station is located in a clean Arctic environment and receives air masses representative mostly of the Arctic background. Nevertheless, 10 cases of enhanced *c*-C_4F_8 mole fractions were observed with the arrival of air masses from Eurasia. To trace the origin of these events, we used 3-hourly 50-day backward simulations for a passive tracer with version 10 of the Lagrangian particle dispersion model FLEXPART (Stohl et al., 2005). The model was driven with operational meteorological analyses of the European Centre for Medium Range Weather Forecasts (ECMWF, https://www.ecmwf.int/). The model set-up was similar to that typically used for inversion studies (Stohl et al., 2009), but the number of events observed at the station was too small for a sensible regional inversion. Instead, we inserted unit emission sources (~1 kg s^{-1}) at two facilities in Russia producing PTFE and halogenated chemicals including *c*-C_4F_8 (HaloPolymer, Kirovo-Chepetsk, Kirov Oblast and Galogen Open Joint-Stock Company, Perm), one or both of which we suspect to be responsible for the observed enhancements. We then scaled the modeled *c*-C_4F_8 mole fractions based on these two unit sources to the observed enhancements to estimate the source strength required to explain the observations. The two sources are quite close to each other and thus very much correlated so it was impossible to quantify the influence of each source individually, but it turned out that each source required about the same flux to produce a similar good match with the observations.

Deleted: most of

5 Results and discussion

5.1 Atmospheric histories of *c*-C_4F_8 in both hemispheres

Figure 1 shows the atmospheric histories of *c*-C_4F_8 in the extra-tropical NH and SH determined from several sets of archive measurements and pollution filtered data from six in situ measurement stations. As detailed in Sect. 2.2, the data shown have gone through an iterative filtering process which mostly removed outliers from the NH record. The pollution-free monthly mean in situ data for the four extra-tropical NH stations shown here and ZEP agree within precisions, although JFJ data tends to be at the lower range since early 2015 for unknown reasons. The two extra-tropical SH stations, CGO and ASA also agree well with each other. Mole fractions measured in both hemispheres show a clear and consistent interhemispheric gradient reflecting the high precision of the measurements and indicating that emissions of *c*-C_4F_8 predominantly occur in the NH. These data form a consistent atmospheric record of *c*-C_4F_8 from the late 1970s to 2017 in both hemispheres, albeit with very sparse data for the NH before in situ measurements started at JFJ and at other NH stations. The inset in Fig. 1 shows that the interhemispheric gradient, based on in situ measurements at high-latitude stations in the NH (MHD, THD, SIO) and SH (CGO) has been rising from ~0.05 ppt in 2011 to ~0.09 ppt in 2017, which suggests increasing, predominantly NH, emissions.

To augment our *c*-C_4F_8 data set and to extend our reconstruction further backwards in time, we measured air samples extracted at several firn sites from both hemispheres and interpreted the data with the CSIRO global inversion framework. The CSIRO inversion (see Sect. 4.3.1) yields the atmospheric history of *c*-C_4F_8 starting in 1900 until present, although abundances are essentially not different from zero (<0.02 ppt) until the early 1960s (Fig. 3). Average global *c*-C_4F_8 mole fractions from the CSIRO inversion reached 0.45 ppt in 1980, 0.74 ppt in 1990, 0.97 ppt in 2000, 1.29 ppt in 2010, and 1.66 ppt in 2017. The Bristol inversion (see Sect. 4.3.2) does not incorporate firn data, still atmospheric histories of the two inversions generally are in good agreement (see Fig. S7).

The CSIRO inversion reconstructs that the global rise rate of *c*-C_4F_8 accelerated from near zero before the late 1960s to ~0.03–0.04 ppt yr^{-1} in the mid-1970s to late 1980s, after which the rise rate slowed to ~0.02 ppt yr^{-1} in the early 1990s to mid-2000s. It increased again in the early 2000s and reached ~0.07 ppt yr^{-1} in 2017.

Compared to Oram et al. (2012), our work extends the SH record from 2008 until present and, arguably, from 1978 back to 1900. Furthermore, it adds the full NH record. SH mole fractions reconstructed by Oram et al. (2012) are very similar in 1978 and 1990, but ~0.06 ppt lower in the mid-1980s (~11 %) and the late 1990s to late 2000s (~5 %, see Fig. S8). Although the stated precision in Oram et al. (2012) of 0.8 % (~0.01 ppt at 1.2 ppt) is similar to the 0.01–0.02 ppt achieved here, the resulting precisions of the CGAA measurements achieved here are significantly improved, e.g. the noise in the CGAA reconstruction by Oram et al. (2012) is about as large as the interhemispheric gradient determined here (see Fig. S8). The estimated accuracy of the SIO-14 *c*-C_4F_8 calibration scale of ~2 % also compares favorably to previous calibration scale uncertainties.

5.2 Global *c*-C_4F_8 emissions

Global *c*-C_4F_8 emissions (Fig. 5 and Supplement) started to increase in the early 1960s (CSIRO inversion) from near zero to ~1.2 Gg yr^{-1} in the late 1970s to the late 1980s. The Bristol inversion initially reconstructs lower emissions, but the differences are within the estimated uncertainties for the reconstructed histories (see Fig. 5). Afterwards,

Deleted:

Comment [JM120]: *Rev. #1: L513 How high is the interhemispheric gradient and how has it evolved over time? This might e.g. reveal information on changes in emission latitudes. There is a lot of space in Figures 1 and 4 to show this.*

Comment [JM121]: *Rev. #1: L523 Define "good agreement". There are no uncertainty ranges given for the two estimates in Figure S7.*

Now shown in new Fig. S7.

Deleted: down

Deleted: S7

Deleted: ,

Deleted: S7

Comment [JM122]: *Rev. #2: L538: Please explain why not incorporating the firn data has this impact on the emissions estimates.*

Comment [JM123]: *Rev. #1: L537-538 Again, are these discrepancies within uncertainties?*

Deleted: catches up by the early 1980s, perhaps because firn data were not incorporated.

Deleted: this

emissions determined by both inversions declined to ~0.8 Gg yr^{-1} in the mid-1990s to early 2000s. Since then emissions kept increasing, reaching ~2.2 Gg yr^{-1} in 2017. Both inversions reconstruct emissions which are significantly larger than available bottom-up inventory information (see Sect. 3 and the Supplement), reflecting the shortcomings of the current UNFCCC reporting requirements and bottom-up inventories.

Emissions presented by Oram et al. (2012) agree very well from 2001 to 2007 with our results and on average also from 1978 to 2001, although they show larger variability. Global emissions roughly estimated by Harnisch (2000) based on measurements by Travnicek (1998) of ~0.7 Gg yr^{-1} from 1978 to 1997 are 30% lower than our estimate of 1.01 ± 0.10 Gg yr^{-1}. Saito et al. (2010) estimated global emissions of 0.6 ± 0.2 Gg yr^{-1} from January 2006 to September 2009, about half of our 1.16 ± 0.09 Gg yr^{-1} estimate. This difference is likely due to slowly changing *c*-C_4F_8 mole fractions in calibration tanks used by NIES (Takuya Saito, personal communication, 2018), which would significantly affect the background rise rate and thus global emissions, but would have had less influence on the regional emissions estimated by Saito et al. (2010) as these are mostly dependent on the magnitude of the much larger pollution events above background.

Comment [JM124]: *Rev. #2: L547: How can the mole fractions of this very unreactive compound change in the tanks?*

See our reply.

Global emissions of *c*-C_4F_8 have clearly not levelled off at 2005–2008 levels as had been suggested by Oram et al. (2012), but kept rising. In contrast, emissions of other minor PFCs, C_2F_6 and C_3F_8, have decreased since the early 2000s and stabilized in recent years (Trudinger et al., 2016), reflecting that emission sources and/or use patterns of *c*-C_4F_8 are different from those of the other minor PFCs. Weighted by GWP$_{100}$ (100-year timescale) estimated 2017 emissions of *c*-C_4F_8, C_3F_8, C_2F_6, and CF_4 were 0.021, 0.005, 0.022, and 0.083 billion tonnes of CO_2-eq., respectively (see Fig. S9). *c*-C_4F_8 CO_2-eq. emissions have been larger than those of C_3F_8 since 2004 and, assuming continued growth, will also surpas C_2F_6 emissions within a year or two, so that *c*-C_4F_8 will become the second most important PFC emitted into the global atmosphere in terms of CO_2-eq. emissions. In the next section, we will investigate regional emissions of *c*-C_4F_8 to gain a better understanding how individual regions and sources may contribute to the global emissions.

Comment [JM125]: *Rev. #2: L553: C2F6 is here listed as a minor PFC, however in L122, it was a major. Which are the majors and the minors?*

Comment [JM126]: *Rev. #1: L555 GWP-100?*

Deleted: S8

Deleted: outpace

Comment [JM127]: *Rev. #2: L558: To make clear what we are talking about, I suggest inserting "from a climate forcing standpoint" before "will become the second most important PFC: : :".*

5.3 Regional *c*-C_4F_8 emission studies

5.3.1 Emissions from eastern Asia

Within the AGAGE network, the two stations in eastern Asia, Gosan (GSN) and Shangdianzi (SDZ), show by far the most frequent and most pronounced pollution events of up to ~14 ppt above NH background, indicating significant regional emissions (see Fig. S10). Therefore, we use a regional inverse method (NAME-HB) to infer the emissions in this region (20° N–50° N and 110° E–160° E, see Sect. 4.4). We focus on the observations from GSN as this site was operated with relatively few interruptions from June 2010 to the end of 2017 and had almost full coverage for each year from 2011 to 2015. Significantly longer data gaps exist for SDZ, which would have made interpretation of inversion results more difficult. The sensitivity of the inversion generally decreases with distance to the receptor station resulting in relatively low sensitivity for emissions from western China, eastern Japan and Taiwan (the cumulative footprint map for 2010–2017 is shown in Fig. S11). Therefore, we report in Table 2 and Fig. 6 estimated emissions for eastern China, western Japan, South Korea, North Korea, and Taiwan. *c*-C_4F_8 emissions in this eastern Asian domain increased from 0.36 ± 0.07 Gg yr^{-1} in 2010 to 0.73 ± 0.13 Gg yr^{-1} in 2016 and 2017 and were

Deleted: S9

Deleted: S10

dominated by emissions from eastern China. The a priori emissions for eastern China of 0.185 Gg yr^{-1} are based on the Saito et al. (2010) estimate for all of China for November 2007 to September 2009, but the inversion suggests emissions that are ~62 % higher in 2010 and more than triple in 2017. Note, that if we were to sum up emissions for all regions of China, including those where the inversion has low sensitivity, total emissions would be another ~50–75 % higher. In contrast, the EDGAR 4.2 emissions inventory, the only available bottom-up information (see Sect. 3 and the Supplement), suggests no significant emissions from China.

For western Japan we find emissions of ~0.02 Gg yr^{-1} (no trend), ~30 % lower than the a priori emissions (from Saito et al. 2010, see Sect. 4.4). While total country emissions are likely higher, the available bottom-up information (see Sect. 3 and Supplement) suggests an order of magnitude lower emissions for all of Japan. For South Korea, the inversion adjusts emissions down to 0.01–0.02 Gg yr^{-1} in most years and up to ~0.04 Gg yr^{-1} in 2014 and 2015. Except perhaps for 2012 and 2017, emissions from South Korea are significantly higher than the 0.003–0.008 Gg yr^{-1} suggested by the available bottom-up information. Emissions from Taiwan show no trend and are relatively small with ~0.01 Gg yr^{-1}, which is ~50 % of ~0.02 Gg yr^{-1} indicated by the Taiwanese NIR, though it should be noted that the inversion has relatively low sensitivities for some parts of Taiwan (see Fig. S11). Overall, emissions from western Japan, South Korea, and Taiwan are small, despite their large semiconductor industries (see also Fig. 7), suggesting that this industry sector is not a major emitter of *c*-C_4F_8. Emissions from North Korea are also small.

Combined regional *c*-C_4F_8 emissions doubled from 2010 to 2016, driven by Chinese emissions. They represent 31 ± 4 % of global emissions (2010–2017), while eastern China's emissions represent 28 ± 4 %. The difference between global and eastern Asian emissions remained relatively consistent, ranging from ~1.04 Gg yr^{-1} in 2010 to 1.47 Gg yr^{-1} in 2017 with an average of 1.20 ± 0.14 Gg yr^{-1} from 2010 to 2017 and 1.15 ± 0.03 Gg yr^{-1} from 2011 to 2015, the years with the best data coverage at GSN and thus highest confidence in the results. This means that the increase in global emissions is essentially explained by the increase in eastern Asian emissions, i.e. mostly from China, but also that significant emissions of ~1.16 Gg yr^{-1} exist outside of the investigated region (a fraction of which may stem from industries located in parts of China and perhaps Japan where the inversion has low sensitivity).

Figure 7 shows that from 2010 to 2017 emissions in eastern China occur from the highly industrialized provinces Shandong, Tianjin, and parts of Henan and Hebei (south/southwest of Beijing) as well as from Shanghai and neighboring Jiangsu (to the north), Anhui (to the west) and Zhejiang (to the south) in the Yangtze River Delta region. Also shown are locations of potential industrial *c*-C_4F_8 point sources. For South Korea, western Japan and Taiwan, semiconductor fabrication plants do not seem to be dominant *c*-C_4F_8 emitters as they are not co-located with large *c*-C_4F_8 emissions (though the inversion has low sensitivity for eastern Japan, where many more semiconductor fabrication plants (FABS) and several PTFE and HCFC-22 plants are located, hence emissions from this region cannot be analyzed).

In China, the picture is less clear than in South Korea, Japan and Taiwan, as several semiconductor fabrication plants in the Yangtze River Delta region are co-located with strong *c*-C_4F_8 emissions, while those near Beijing are not. Many of the potential production facilities of TFE and HFP monomers and PTFE and FEP polymers are co-located with areas where strong *c*-C_4F_8 emissions occur. This is consistent with information from the second largest producer of PTFE in China that they do not recover *c*-C_4F_8 by-product, but do emit *c*-C_4F_8 to the atmosphere (Hu, J., personal communication, 2018). Still, the two facilities north east of Beijing do not seem to emit *c*-C_4F_8, perhaps reflecting

Comment [JM128]: *Rev. #1: L571-574 Given that the largest emissions appear to occur near the sea, is there scope for some emissions being related to ships or submissions? What fraction of emissions did the model initially assign to have occurred over the ocean?*

See our reply.

Deleted: Compared to t

Deleted: , which

Deleted: this represents an increase of

Deleted: a

Deleted: ing

Deleted: 1

Deleted: S10

Comment [JM129]: *Rev. #1: L590-591 This appears to be in disagreement with the statement in L576-578.*

See our reply.

Comment [JM130]: *Rev. #1: L603 FABS?*

that some producers minimize *c*-C_4F_8 emissions, e.g to increase yield or to use *c*-C_4F_8 for other purposes, such as for the semiconductor industry. Several facilities are also located in provinces for which the inversion has low sensitivity. Most HCFC-22 production facilities are not co-located with strong *c*-C_4F_8 emissions, while $CHCl_3$ production facilities tend to be in areas with *c*-C_4F_8 emissions. This may reflect that $CHCl_3$ production has shifted from use as a feedstock to produce HCFC-22 for dispersive applications (refrigeration or foam blowing), where no *c*-C_4F_8 emissions occur, to production of TFE/HFP/PTFE/FEP via HCFC-22 pyrolysis, where *c*-C_4F_8 by-product emissions occur, perhaps at the same or close-by facilities. This would be consistent with the start of the HCFC phase-out for dispersive applications in developing countries mandated by the Montreal Protocol on the Protection of Ozone Layer. Then again, $CHCl_3$ has other uses, e.g. as solvent (Tsai, 2017), without any potential *c*-C_4F_8 emissions.

Note, that at one or both of the PTFE production facilities in Zhejiang province (Juhua Group Corporation) HFO-1234yf is produced since 2016, using a process which starts out with the same chemistry needed for PTFE/FEP production, that is the pyrolysis of HCFC-22 to TFE and HFP, with *c*-C_4F_8 as potential by-product (see Supplement).

There is no strong correlation between *c*-C_4F_8 emissions distribution and population density, e.g. emissions from Henan and Hebei provinces are significantly lower than those from Shandong despite similar total population, which may indicate that combustion of fluoropolymers in waste incineration facilities (Morisaki, 1978; Kannan et al., 2005; van der Walt et al., 2008; Ji et al., 2016; Bezuidenhoudt et al., 2017) is not a dominant source of *c*-C_4F_8 emissions.

If *c*-C_4F_8 emissions in eastern Asia are predominantly associated with TFE/HFP/PTFE/FEP production via the pyrolysis of HCFC-22, *c*-C_4F_8 emissions may co-occur with small emissions of TFE and HFP. HFC-23 emissions may also co-occur as HCFC-22 is produced from $CHCl_3$ and HFC-23 is a by-product that in developing countries is probably again vented to the atmosphere since the UNFCCC Clean Development Mechanism (CDM) funding to avoid HFC-23 emissions has expired (Simmonds et al., 2018; Say et al., 2019). While the global atmospheric lifetime of TFE is only ~2 days, the lifetime of HFP is ~6 days (Acerboni et al., 2001), so that HFP may be detectable near strong emission sources and serve as a sensitive marker for regional TFE/HFP/PTFE/FEP production. After adding HFP to the measurements in late 2018, we find that HFP pollution events at SDZ always coincide with *c*-C_4F_8 and HFC-23 pollution events (see Fig. S12 and its caption in the Supplement). HFP pollution events at GSN are much weaker, reflecting the short atmospheric lifetime and the more distant source region, but they also coincide with *c*-C_4F_8 and HFC-23 pollution events. At both sites, however, *c*-C_4F_8 pollution events also coincide with enhancements of other anthropogenic compounds which may just point to generally polluted air in the region, so it is difficult to draw definitive conclusions. Still it is clear that HFP is emitted in eastern Asia, likely in China, and HFP as well as *c*-C_4F_8 emissions can be explained by PTFE/FEP production. Measurements of HFP at SIO and ASA, confirm that it is virtually absent (<0.01 ppt) from the global background atmosphere even in urban environments.

Overall, the strong c-C_4F_8 emissions in eastern China and their source regions are consistent with our hypothesis of emissions from TFE/HFP/PTFE/FEP production facilities due to little or no recovery or abatement of *c*-C_4F_8 by-product and the significant fraction of global PTFE production (53–67 % in 2015) occurring in China (see Table S3).

5.3.2 Emissions from North Western Europe

Outside of eastern Asia, the TAC station in East Anglia, UK shows by far the most frequent and most pronounced *c*-C_4F_8 pollution events of any AGAGE station, with a few reaching ~5 to 10 ppt above NH background, indicating

Deleted: ,

Deleted: indeed

Deleted: HCFC-22,

Deleted: $CHCl_3$ and

Deleted: strong

Deleted: which are

Deleted: associated

Deleted: ,

Deleted: $CHCl_3$, HCFC-22 and

Deleted: are

Deleted: associated

Deleted: ,

Deleted: $CHCl_3$, HCFC-22

Deleted: co-occur

Deleted: are associated with

Comment [JM131]: *Rev. #1: L631-638 Please add information such as measurement precisions, observed mole fraction ranges, ions used for identification and quantification, etc. on the HFP measurements to the manuscript. Please provide quantitative evidence instead of "associated with" and "virtually absent".*

Comment [JM132]: *Rev. #2: L641: Insert "occurring" before ": : :in China: : :)*

Comment [JM133]: *Rev. #1 L639-641 Consistent with emissions from many of these facilities, but clearly not all (as stated in L610-612). Given the problems with associating these sources can the authors confirm that the ratios between m/z 131 and 101 during pollution events were consistent with those observed in clean air? This would help to rule out interferences during pollution events.*

close-by emissions. Data from the TAC, MHD, JFJ and CMN stations and the InTEM regional inverse method (see Sect. 4.5) were used to estimate emissions from North Western Europe (42° N to 59° N and -11° E to 15° E) based on to the areas of highest sensitivity to the observations (see Fig. S13). Compared to eastern Asia, we find only small emissions of 0.026 ± 0.013 Gg yr^{-1} (Ireland, UK, France, Germany, Belgium, the Netherlands, Luxemburg, and Denmark, 2013–2017) without any significant temporal trend, corresponding to only ~1 % of global emissions, despite an estimated 14 % of global PTFE production in 2015 (see Table S3). The mean distribution of emissions is shown in Fig. 8. Similar to eastern Asia, many identified semiconductor FABS in Europe are not co-located with *c*-C_4F_8 emission hotspots, while several FABS in Northern France, the UK, Ireland, and the Netherlands seem to be co-located. Producers of PTFE and FEP and facility locations in Europe were determined from company websites (3M/Dyneon, AGC/Asahi Glass, Arkema, Chemours/DuPont, Saint-Gobin, Solvay) and the European Pollutant Release and Transfer Register (https://prtr.eea.europa.eu), but it is very difficult to determine at which of the many facilities PTFE or FEP are actually produced and thus where *c*-C_4F_8 may be emitted. It seems that several facilities in The Netherlands, Belgium, the UK, France, and Italy which likely produce PTFE are co-located with identified *c*-C_4F_8 emission hotspots (Fig. 8). Still, many mismatches exist, reflecting the uncertainties in determining the exact facility locations, the relatively small emission strength and uncertainties of the inversion. As in eastern Asia, there seems to be no correlation with population density, which suggests that waste incineration of fluoropolymers is not a dominant *c*-C_4F_8 source here either. The inversion is broadly consistent with emissions from TFE/HFP/PTFE/FEP production and FABS, but emissions from other industrial sources may also play a role. While emissions of 0.026 ± 0.013 Gg yr^{-1} are relatively small, it is noteworthy that UNFCCC reporting suggest much smaller *c*-C_4F_8 emissions (0.0007 Gg yr^{-1} (UNFCCC, 2013–2014) vs. 0.0017 Gg yr^{-1} (bottom-up emission inventories, Section 3, 2013–2014)).

5.3.3 Emissions from South Eastern Australia

Other urban locations of the AGAGE network, such as SIO, USA and ASA, Australia show much smaller pollution events above global background (up to ~2.5 ppt) than those seen at TAC, suggesting even lower emissions. Still, the few pollution events at ASA and even CGO are interesting as production of PFCs in Australia has never been recorded. CFC-11, CFC-12, and HCFC-22 were manufactured starting in 1962 at two facilities in Sydney, but production ceased in 1995 and trace gas emissions from Sydney are rarely if ever observable at CGO or ASA. Without any currently known fluorocarbon production, any *c*-C_4F_8 pollution events observed at CGO or ASA should not be due to fugitive emissions. *c*-C_4F_8 imports to Australia are ~4 to 50 kg yr^{-1} (2011–2015), likely for minor refrigeration uses. In contrast, small but identifiable *c*-C_4F_8 pollution episodes at CGO suggest Melbourne emissions of ~2 t yr^{-1} (0.002 Gg yr^{-1}) in 2016 (down from ~5 t yr^{-1} in 2009, Inter Species Correlation method, ISC, c.f., Fraser et al., 2014; Dunse et al., 2018). Scaled by population to Australia (for lack of a better proxy), emissions from 2009 to 2016 could be ~10–25 t yr^{-1} (0.01–0.025 Gg yr^{-1}), 2–3 orders of magnitude higher than import data suggests. Since early 2017, HFP has been measured at ASA (see Fig. S12 caption). Occasional, small HFP pollution events, which are often, but not always, associated with *c*-C_4F_8 pollution events, may point to small scale production of TFE/HFP/PTFE/FEP in Melbourne or perhaps these small emissions stem from incineration of waste containing fluoropolymers. Another possible explanation could be that more *c*-C_4F_8 is imported in products for minor applications than identified in import data due to inadequate labelling. On a global scale, estimated Australian *c*-C_4F_8

Deleted: S11

Deleted: ~

Deleted: As in

Deleted: most

Deleted: except perhaps

Deleted: and

Deleted: by The Netherlands, the UK, Belgium, and France

Comment [JM134]: *Rev. #1: L661 How much smaller?*

Formatted: Font: Italic

Deleted: c

Formatted: Superscript

Deleted: /TFE/HFP

emissions of ~0.015 Gg yr^{-1} are small, ~0.7 % of global emissions. PFC (CF_4, C_2F_6) pollution episodes at Cape Grim and Aspendale due to PFC emissions from South Eastern Australian aluminum smelters (Portland and Pt. Henry, Victoria and Bell Bay, Tasmania) do not show any evidence of c-C_4F_8 emissions (Fraser et al., 2013; CSIRO unpublished data).

5.3.4 Emissions from under-sampled regions such as the US, India, Russia

The AGAGE network does not closely monitor large areas of the globe where c-C_4F_8 emissions may occur. For example, many semiconductor FABS are located in the western, southern, and eastern US and chemical facilities located in the southern and eastern US are estimated to account for ~10 % of global PTFE production in 2015, while facilities in India and Russia are estimated to account for ~8 % and ~6 %, respectively (see Tables S3 and S4). The two AGAGE stations in California are only able to capture a fraction of these emissions due to predominant westerly winds and therefore we cannot estimate c-C_4F_8 emissions from the continental US. If PTFE production facilities in the US are operated as in NW Europe, emissions should be similarly small. If facilities in India and Russia are operated as in China, emissions could be significant as well. In the case of Russia this seems likely as the original technology for fluoropolymer production in China apparently stems from Russia (Buznik, 2009).

5.3.5 Emissions from India

Say et al. (2019) recently presented measurements from an aircraft campaign in June and July 2016 (see Sect. 2.4) over the Indian subcontinent to determine emissions of ODS and HFCs. Here we use their c-C_4F_8 measurements and the NAME-HB inversion (see Sect. 4.6) and estimate emissions of 0.14 (0.09–0.20) Gg yr^{-1} for Northern and Central India (NCI). Data are only available for two months in 2016, but seasonality in industrial emissions of c-C_4F_8 is not expected. Given the limitations of the inversion method to identify distant point sources from a relatively small number of samples (see Sections 4.4 and 4.6), the posterior emissions distribution (Fig. 9) is consistent with emissions from facilities producing PTFE. Several of the HCFC-22 production facilities are co-located or very close to these PTFE producing facilities, suggesting that a fraction of HCFC-22 is pyrolyzed to produce monomers for PTFE and FEP. Two HCFC-22 production facilities are outside of areas with strong c-C_4F_8 emissions, possibly because these two sites focus on production of HCFC-22 for dispersive applications (refrigeration or foam blowing), where no c-C_4F_8 emissions occur. The single FAB in India we are aware of is not co-located with significant c-C_4F_8 emissions. As in eastern Asia and North Western Europe, there is no apparent correlation of c-C_4F_8 emissions with population density. Emissions predominantly occur outside of the Indo-Gangetic plain, the most densely populated region of India, which excludes potential sources that scale with population. Instead the inversion allocates emissions in a much less densely populated region in which multiple likely industrial point sources for c-C_4F_8 are located. The derived emissions account for 6.8 (4.4–9.7) % of global c-C_4F_8 emissions in 2016, in comparison to the estimated ~8 % of 2015 global PTFE production capacity (see Table S3). While we cannot categorically exclude an unknown industrial source, these results are consistent with the chemistry of TFE/HFP/PTFE/FEP production as dominant c-C_4F_8 emission source. Note, that one of the facilities in western India (Navin Fluorine International, Surat, Gujarat) is known to also produce HFO-1234yf since 2016, using a process which starts out with the same chemistry, that is the pyrolysis of HCFC-22 to TFE and HFP, with c-C_4F_8 as potential by-product (see Supplement). All known Indian

Comment [JM135]: *Rev. 2: Line 689-691: These two sentences belong more appropriately in sections 5.35 and 5.3.6.*

See our reply.

Deleted: T

Comment [JM136]: *Rev. #1: L697 That is a very optimistic way of looking at that Figure.*

Deleted: known

Deleted: Perhaps even clearer than in eastern Asia,

Deleted: point to

Comment [JM137]: *Rev. #1: L706-707 This is not very clear from the Figure, which is rather indicating an unknown source.*

Deleted:

Deleted: of c-C_4F_8

PTFE manufacturers are located within the NCI domain, hence the estimated emissions are likely to be roughly representative of India's national total, though further atmospheric measurements would be required to confirm this.

5.3.6 Emissions from facilities in Russia

Measurements at the ZEP site in remote Svalbard show ten small c-C_4F_8 pollution events above NH background of up to ~0.4 ppt. FLEXPART backward simulations could trace some of these events to two facilities in Russia which produce PTFE and halogenated chemicals including c-C_4F_8 itself (HaloPolymer, Kirovo-Chepetsk, Kirov Oblast and Galogen Open Joint-Stock Company, Perm). Figure S14 shows the FLEXPART footprint emission sensitivity map for the largest observed c-C_4F_8 enhancement on November 19, 2016, suggesting direct transport from the two sites. The emission sensitivity maps indicate that for six of the ten observed pollution events the air had clearly passed over one or both of these two sources, even though the timing of the observed events was often not well matched by the model, which was sometimes off by up to about half a day. While this is not surprising given the large distance between the source and the receptor, it means that the two sources could not be clearly separated, especially since the FLEXPART emission sensitivity often also covered both sites for the same arrival times at ZEP. Assuming a unit emission at those two locations and scaling the resulting simulated mole fractions at ZEP to the observed enhancements above background, we estimated the emission strength for the two sites together for each event (see Sect. 4.7). Five of the ten pollution events could be approximately reproduced by this method and required a flux of 0.18 ± 0.06 Gg yr^{-1}, while the sixth event required ~0.54 Gg yr^{-1}. Averaged for all six events 0.24 ± 0.15 Gg yr^{-1} would be required. Either of these fluxes would be significant, representing 9 ± 3 %, 26 %, and 12 ± 7 % of global emissions, respectively, compared to ~6 % of estimated global PTFE production in Russia. The uncertainty of this estimate is large because only a few events were observed and not all of them were reproduced equally well by FLEXPART. Similar to eastern Asia, the largest c-C_4F_8 pollution event also showed enhancements of HFC-23 pointing to TFE/HFP/PTFE chemistry as source (see Fig. S15), but other halogenated compounds were also elevated.

Deleted: T

Deleted: s

Comment [JM138]: *Rev. #1: L713 What is the main purpose of this direct c-C4F8 production?*

Deleted: S12

Deleted: PTFE production

Deleted: HCFC-22 and HFC-23

Comment [JM139]: *Rev. #1: L729 Which ones did PFC-318 correlate best with (also for other pollution events in Asia etc)?*

Deleted: the production of

6 Summary and conclusions

We determine the atmospheric histories of c-C_4F_8 (PFC-318, perfluorocyclobutane) in both hemispheres based on measurements of archived, in situ, and firn air samples in conjunction with the CSIRO firn model, the AGAGE 12-box model, and two global inversion frameworks. Compared to previous studies, our work extends the Southern Hemisphere record from 1978 back to 1900 and from 2008 until 2017 and adds a Northern Hemisphere record, all reported with improved precisions for air archive measurements (~1–2 %) and a lower uncertainty (2 %) of the SIO-14 gravimetric calibration scale. We find global c-C_4F_8 atmospheric mole fractions near zero (< 0.02 ppt) from 1900 until the early 1960s, after which they rose sharply, reaching 0.45 ppt in 1980, 0.74 ppt in 1990, 0.97 ppt in 2000, 1.29 ppt in 2010, and 1.66 ppt in 2017. Global c-C_4F_8 emissions started to increase in the 1960s from near zero to ~1.2 ± 0.1 (1σ) Gg yr^{-1} in the late 1970s to the late 1980s. After this, emissions declined to ~0.77 ± 0.03 Gg yr^{-1} in the mid-1990s to early 2000s. After this emissions again increased, reaching ~2.20 ± 0.05 Gg yr^{-1} in 2017. These global emissions are significantly larger than what can be compiled from available bottom-up inventory information (70 ± 17 times, 1990–1996, 29 ± 5 times, 1997–2010, 15 ± 1 times, 2011–2014).

Deleted: better

Deleted: versus ≤ 7 %

Deleted: 8

Comment [JM140]: *Rev. #1: L740-741 How much larger?*

Using the NAME-HB regional inverse method and observations at Gosan station we find that emissions from eastern Asia rose from ~0.36 Gg yr^{-1} in 2010 to ~0.73 Gg yr^{-1} in 2016 and 2017, representing 31 ± 4 % of global emissions, predominantly from eastern China. Strong c-C_4F_8 emissions are found from heavily industrialized provinces south/southwest of Beijing and near the Yangtze River Delta. In contrast, emissions from western Japan, South Korea, and Taiwan are small, suggesting that their large semiconductor industries are not major c-C_4F_8 emitters. While we cannot categorically exclude emissions from other industrial sources, overall, the strong c-C_4F_8 emissions in eastern China and their spatial pattern are roughly consistent with emissions from production of TFE/HFP/PTFE/FEP and other fluorochemicals. A significant fraction of global PTFE production (53–67 % in 2015) occurs in China and, as indicated by the second largest producer of PTFE in China, the c-C_4F_8 by-product from the underlying HCFC-22 pyrolysis process is not recovered or abated, but rather emitted to the atmosphere.

Deleted: O

Deleted: polymer

Based on samples collected over the Indian subcontinent in mid-2016, we determine emissions of 0.14 (0.09–0.20) Gg yr^{-1} c-C_4F_8 from Northern and Central India (NCI), ~6.8 (4.4–9.7) % of global emissions. Within the limitations of the inversion, the determined emission map is also roughly consistent with emissions from TFE/PTFE production.

Deleted: Even clearer than in China,

Using the InTEM regional inverse method and measurements at four western European stations, we only find small NW European emissions of ~0.02 ± 0.01 Gg yr^{-1} c-C_4F_8 from 2013–2017 (~1 % of global emissions), in contrast to an estimate of 14 % of global PTFE production capacity in 2015. The inversion also points to facilities which may produce PTFE and FEP and semiconductor fabrication plants though the picture is less clear.

Deleted: /or

No obvious correlation between population density and c-C_4F_8 emissions is found in Eastern Asia, NCI, and NW Europe, indicating that incineration of waste containing fluoropolymers is not a major source of c-C_4F_8.

Based on data from two Australian stations and an Inter Species Correlation method, Australian c-C_4F_8 emissions are estimated to be small, perhaps ~0.7 % of global c-C_4F_8 emissions. We find no evidence for c-C_4F_8 production from three large aluminum smelters in SE Australia.

Deleted: two

Based on a few c-C_4F_8 pollution events observed at Zeppelin station and a rough FLEXPART analysis, we estimate that emissions from two Russian facilities known to produce PTFE and halocarbons including c-C_4F_8 itself could be ~0.24 ± 0.15 Gg yr^{-1}. While this could a represent significant fraction of global emissions (possibly ranging from 5 to 26 %), uncertainties are very large.

In summary, for the year 2016, we find global c-C_4F_8 emissions of 2.06 ± 0.10 Gg yr^{-1}, with 0.73 ± 0.12 Gg yr^{-1} from parts of eastern Asia (36 % of the global total), 0.14 (0.09–0.20) Gg yr^{-1} from Northern and Central India (6.8 %), ~0.024 ± 0.013 Gg yr^{-1} from North Western Europe (~1 %), and ~0.015 Gg yr^{-1} from Australia (~0.7 %).

Current monitoring capabilities of the AGAGE network leave large areas with potential c-C_4F_8 emission sources un- or under-monitored, e.g. most of the U.S., India, Russia, western China, and eastern Japan, where various semiconductor facilities and fluorochemical and fluoropolymer production plants are located.

Deleted:

While many possible uses and emission sources of c-C_4F_8 are found in the literature and though we cannot categorically exclude unknown industrial sources, the start of significant c-C_4F_8 emissions around the 1960s may well be related to the initial synthesis of PTFE in 1938 with commercial production of PTFE ("Teflon") by DuPont commencing in 1947 (Gangal and Brothers, 2015) via pyrolysis of HCFC-22, with c-C_4F_8 as a by-product/intermediate. It seems unlikely that process control or abatement to minimize c-C_4F_8 by-production were in place in the early decades of PTFE production and c-C_4F_8 by-product was probably emitted to the atmosphere, explaining the steep increase in global emissions reconstructed here. With the advent of UNFCCC by-product reporting requirements in the 1990s, concern about climate change and product stewardship, abatement, and perhaps collection of *c*-C_4F_8 for use in the semiconductor industry where it can be easily abated, it is conceivable that fugitive *c*-C_4F_8 in developed countries (UNFCCC Annex 1) overall were reduced, explaining the observed stabilization and reduction of global emissions in the 1980s and 1990s. Similar efforts to contain and destroy by-product emissions of fluorocarbons, e.g. HFCs, from the 1980s to the 2000s are documented in the Toxics Release Inventory (https://www.epa.gov/toxics-release-inventory-tri-program) Program of the US EPA and the European Pollutant Release and Transfer Register. Concurrently, production of PTFE in China increased rapidly, e.g. from 2000 to 2005 by ~26 % yr^{-1}, followed by a slowdown to ~14% yr^{-1} from 2005 to 2015 and perhaps ~8 % yr^{-1} from 2015 onward, reaching an estimated 53–67 % of global production in 2015 (see Tables S2, 3, and 4). Without any emission reduction requirements, it is conceivable that fugitive emissions of *c*-C_4F_8 from TFE/HDP/PTFE/FEP production in China, and other developing (UNFCC non-Annex 1) countries, today dominate global emissions. The 2010 to 2016 rise in rates of eastern Chinese (eastern Asian) *c*-C_4F_8 emissions of ~15 % yr^{-1} (~13 % yr^{-1}) determined here are compatible to these PTFE production increase rates of 14 to 8 % yr^{-1} in China. Barring other developments, we predict that *c*-C_4F_8 emissions will continue to rise and that *c*-C_4F_8 will become the second most important PFC emitted to the global atmosphere in terms of CO_2-eq. emissions within a year or two. While the 2017 radiative forcing of *c*-C_4F_8 (~0.52 mW m^{-2}) is very small compared to that of CO_2, emissions *c*-C_4F_8 and other perfluorinated compounds with similarly long lifetimes and high radiative efficiencies essentially permanently alter the radiative budget of Earth. The fact that significant emissions of ~1.16 Gg yr^{-1} of global emissions (56 %) exist outside of the monitored regions clearly shows that observational capabilities and reporting requirements need to be improved to understand global and country-wide emissions of PFCs and other synthetic greenhouse gases and ozone depleting substances.

Deleted: , in agreement with our analysis

Deleted: uivalent

Deleted: ,

Deleted:

7 Author contributions

JM contributed to archive, firn, and in situ measurements, interpreted the data, and prepared the manuscript with contributions from all co-authors. CMT provided CSIRO firn model and CSIRO global inversion results and interpretation. MR provided Bristol global inversion results. LMW provided NAME-HB model runs and emission estimated for East Asia, DS and ALG provided the same for India. AJM and LMW provided InTEM model runs and emissions for Europe. AS and NE provided FLEXPART model runs and guided estimation of Russian emissions. DS and ALG provided the aircraft data from India. CMT, MR, LMW, AJM, DS, ALG, AS, and PJF contributed significantly to the text. LPS, DJI, TA, JM, PJF, PBK provided and oversaw CSIRO air archive and NH archive measurements. MKV, SP, SL, M-KP, COJ, LPS, PBK, SOD, PGS, DY, PBK, KMS, OH, BM, CL, JK, JA, MM, SR, and BY oversaw station operations and provided quality controlled measurement data. PJF provided the estimate of Australian emissions. CMH provided gravimetric calibration and calibration propagation for the whole AGAGE network. PKS wrote the software to run all instruments and analyze all measurement data. MKV, BH, CB, VP, DME, and JS provided firn data and were instrumental in their interpretation. AMcC provided insight into UNFCCC reporting and bottom-up inventories as well as industrial processes. EM and MC greatly helped with the gathering of locations of semiconductor facilities. RGP and RFW provided overall project oversight.

8 Acknowledgments

Development of the Medusa GC/MS systems, calibrations, and measurements at the Scripps Institution of Oceanography, La Jolla as well as operations of Trinidad Head, CA were carried out as part of the international AGAGE research program and supported by the NASA Upper Atmospheric Research Program in the US with grants NNX07AE89G and NNX16AC98G to MIT, NNX07AF09G, NNX07AE87G, NNX16AC96G, and NNX16AC97G to SIO. In the UK, the Department for Business, Energy & Industrial Strategy (BEIS) provided support through contract 1028/06/2015 to the University of Bristol for Mace Head, Ireland, for Tacolneston, UK and to the UK Met Office for InTEM analysis. The National Oceanic and Atmospheric Administration (NOAA) in the US provided support to the University of Bristol for operations at Ragged Point, Barbados through contract RA-133-R15-CN-0008 and supported operations at Cape Matatula, American Samoa. Operations in Australia were supported by the Commonwealth Scientific and Industrial Research Organization (CSIRO), the Bureau of Meteorology (Australia), the Department of Environment and Energy (Australia), and Refrigerant Reclaim Australia. Operations at Jungfraujoch were supported by the Swiss National Program HALCLIM/CLIMGAS-CH (Swiss Federal Office for the Environment, FOEN) and by the International Foundation High Altitude Research Stations Jungfraujoch and Gornergrat (HFSJG). Operations at Zeppelin were supported by the Norwegian Environment Agency. Operations at Monte Cimone were supported by the National Research Council of Italy and the Italian Ministry of Education, University and Research through the Project of National Interest Nextdata. Operations at Gosan were supported by the National Strategic Project-Fine particle of the National Research Foundation of Korea (NRF) funded by the Ministry of Science and ICT (MSIT), the Ministry of Environment (ME), and the Ministry of Health and Welfare(MOHW) (No. NRF-2017M3D8A1092225). Operations at Shangdianzi were supported by the National Nature Science Foundation of China (41575114). We are indebted to the staff and scientists at AGAGE and other sites for their continuing contributions to produce high quality measurements of atmospheric trace gases. Firn air sampling at Law Dome was supported by the Australian Antarctic Division, Australian Antarctic Science Program, and Australia's Nuclear Science and Technology Organisation. We acknowledge the members of the firn air sampling teams at South Pole in 2001 and at NEEM in 2008. Firn air sampling at Summit station was supported through NSF grants ARC-1203779 and ARC-1204084, with airlift support from the 109th New York Air National guard. We thank E. J. Dlugokencky and the National Oceanic and Atmospheric Administration (NOAA) Earth System Research Laboratory (ESRL) Global Monitoring Division (GMD) Carbon Cycle Greenhouse Gases (CCGG) group for measurements which were instrumental for characterizing the Summit13 firn site. We also thank C.D. Keeling (deceased) and R.F. Keeling (SIO) for air samples. We thank Dr. T. Saito for helpful discussions. Matthew Rigby was supported in part by advanced research fellowships from the UK Natural Environment Research Council (NERC, NE/1021365/1). Luke Western was supported by NERC grant NE/M014851/1. Anita L. Ganesan was funded under a NERC Independent Research Fellowship (NE/L010992/1). We acknowledge the contribution of NERC, the Ministry of Earth Sciences, Government of India and the Principal Investigators of 'Drivers of the South Asian Monsoon' aircraft campaign in India. Funding for the measurements used here were made possible by NERC grant NE/I027282/1. We thank two anonymous reviewers for their very helpful comments.

Deleted: and

Deleted: UK Natural Environment Research Council

Deleted: the UK National Environmental Research Council (

Deleted:)

References

Acerboni, G., Beukes, J. A., Jensen, N. R., Hjorth, J., Myhre, G., Nielsen, C. J., and Sundet, J. K.: Atmospheric degradation and global warming potentials of three perfluoroalkenes, Atmos. Environ., 35, 24, 4113-4123, 10.1016/S1352-2310(01)00209-6, 2001.

Adolph, A. C., and Albert, M. R.: Gas diffusivity and permeability through the firn column at Summit, Greenland: measurements and comparison to microstructural properties, The Cryosphere, 8, 1, 319-328, 10.5194/tc-8-319-2014, 2014.

Arnold, T., Mühle, J., Salameh, P. K., Harth, C. M., Ivy, D. J., and Weiss, R. F.: Automated measurement of nitrogen trifluoride in ambient air, Anal. Chem., 84, 11, 4798−4804, 10.1021/ac300373e, 2012.

Arnold, T., Manning, A. J., Kim, J., Li, S., Webster, H., Thomson, D., Mühle, J., Weiss, R. F., Park, S., and O'Doherty, S.: Inverse modelling of CF_4 and NF_3 emissions in East Asia, Atmos. Chem. Phys., 18, 18, 13305-13320, 10.5194/acp-18-13305-2018, 2018.

Aydin, M., Saltzman, E. S., De Bruyn, W. J., Montzka, S. A., Butler, J. H., and Battle, M.: Atmospheric variability of methyl chloride during the last 300 years from an Antarctic ice core and firn air, Geophys. Res. Lett., 31, 2, L02109, 10.1029/2003GL018750, 2004.

Battle, M., Bender, M., Sowers, T., Tans, P. P., Butler, J. H., Elkins, J. W., Ellis, J. T., Conway, T., Zhang, N., Lang, P., and Clarke, A. D.: Atmospheric gas concentrations over the past century measured in air from firn at the South Pole, Nature, 383, 6597, 231-235, 1996.

Bezuidenhoudt, A., Sonnendecker, P. W., and Crouse, P. L.: Temperature and pressure effects on the product distribution of PTFE pyrolysis by means of qualitative, in-line FTIR analysis, Polym. Degrad. Stab., 142, 79-88, 10.1016/j.polymdegradstab.2017.05.025, 2017.

Broyer, E., Bekker, A. Y., and Ritter, A. B.: Kinetics of the pyrolysis of chlorodifluoromethane, Ind. Eng. Chem. Res., 27, 1, 208-211, 10.1021/ie00073a039, 1988.

Buizert, C., Martinerie, P., Petrenko, V. V., Severinghaus, J. P., Trudinger, C. M., Witrant, E., Rosen, J. L., Orsi, A. J., Rubino, M., Etheridge, D. M., Steele, L. P., Hogan, C., Laube, J. C., Sturges, W. T., Levchenko, V. A., Smith, A. M., Levin, I., Conway, T. J., Dlugokencky, E. J., Lang, P. M., Kawamura, K., Jenk, T. M., White, J. W. C., Sowers, T., Schwander, J., and Blunier, T.: Gas transport in firn: multiple-tracer characterisation and model intercomparison for NEEM, Northern Greenland, Atmos. Chem. Phys., 12, 9, 4259-4277, 10.5194/acp-12-4259-2012, 2012.

Buznik, V. M.: Fluoropolymer chemistry in Russia: Current situation and prospects, Russ. J. Gen. Chem., 79, 3, 520-526, 10.1134/s1070363209030335, 2009.

Cai, B., Liu, H., Kou, F., Yang, Y., Yao, B., Chen, X., Wong, D. S., Zhang, L., Li, J., Kuang, G., Chen, L., Zheng, J., Guan, D., and Shan, Y.: Estimating perfluorocarbon emission factors for industrial rare earth metal electrolysis, Resources, Conservation and Recycling, 136, 315-323, 10.1016/j.resconrec.2018.04.018, 2018.

Chinoy, P. B., and Sunavala, P. D.: Thermodynamics and kinetics for the manufacture of tetrafluoroethylene by the pyrolysis of chlorodifluoromethane, Ind. Eng. Chem. Res., 26, 7, 1340-1344, 10.1021/ie00067a013, 1987.

Christophorou, L. G., and Olthoff, J. K.: Electron interactions with c-C_4F_8, J. Phys. Chem. Ref. Data, 30, 2, 449-473, 2001.

Chung, M. O., and Bai, C.: Thermodynamic property variation of nonazeotropic refrigerant mixtures (NARMs) in the temperature gliding zone, Chemical Engineering Communications, 180, 1, 1-17, 10.1080/00986440008912199, 2000.

Cunnold, D. M., Prinn, R. G., Rasmussen, R. A., Simmonds, P. G., Alyea, F. N., Cardelino, C. A., Crawford, A. J., Fraser, P. J., and Rosen, R. D.: The Atmospheric Lifetime Experiment, 3. Lifetime Methodology and Application to 3 Years of $CFCl_3$ Data, J. Geophys. Res., 88, C13, 8379-8400, 1983.

Cunnold, D. M., Weiss, R. F., Prinn, R. G., Hartley, D., Simmonds, P. G., Fraser, P. J., Miller, B., Alyea, F. N., and Porter, L.: GAGE/AGAGE measurements indicating reductions in global emissions of CCl_3F and CCl_2F_2 in 1992-1994, J. Geophys. Res., 102, D1, 1259-1269, 1997.

Cunnold, D. M., Steele, L. P., Fraser, P. J., Simmonds, P. G., Prinn, R. G., Weiss, R. F., Porter, L. W., O'Doherty, S., Langenfelds, R. L., Krummel, P. B., Wang, H. J., Emmons, L., Tie, X. X., and Dlugokencky, E. J.: In situ measurements of atmospheric methane at GAGE/AGAGE sites during 1985-2000 and resulting source inferences, J. Geophys. Res., 107, D14, 10.1029/2001JD001226, 2002.

Dunse, B. L., Derek, N., Fraser, P. J., Krummel, P. B., and Steele, L. P.: Australian and global HFC, PFC, sulfur hexafluoride nitrogen trifluoride and sulfuryl fluoride emissions, Report prepared for Australian Government Department of the Environment and Energy, CSIRO Oceans and Atmosphere, Aspendale, Australia, iv, 33 pp. http://www.environment.gov.au/protection/ozone/publications/csiro-report-australian-global-sgg, 2018.

Engel, A., M. Rigby (Lead Authors), Burkholder, J. B., Fernandez, R. P., Froidevaux, L., Hall, B. D., Hossaini, R., Saito, T., Vollmer, M. K., B. Yao (Coauthors), Altas, E., Bernath, P., Blake, D. R., Dutton, G., Krummel, P., Laube, J. C., Mahieu, E., Montzka, S. A., Mühle, J., Nedoluha, G., O'Doherty, S. J., Oram, D. E., Pfeilsticker, K., Prinn, R. G., Quack, B., Simpson, I. J., R.F. Weiss (Contributors), Liang, Q., and S. Reimann (Review Editors): Update on Ozone-Depleting Substances (ODSs) and Other Gases of Interest to the Montreal Protocol (Chapter 1), in: Scientific Assessment of Ozone Depletion: 2018, Global Ozone Research and Monitoring Project–Report No. 58, World Meteorological Organization, Geneva, Switzerland, 2018.

Fraser, P., Steele, P., and Cooksey, M.: PFC and Carbon Dioxide Emissions from an Australian Aluminium Smelter Using Time-Integrated Stack Sampling and GC-MS, GC-FID Analysis, in: Light Metals 2013, John Wiley & Sons, Inc., 871-876, 2013.

Fraser, P. J., Dunse, B. L., Manning, A. J., Walsh, S., Wang, R. H. J., Krummel, P. B., Steele, L. P., Porter, L. W., Allison, C., O'Doherty, S., Simmonds, P. G., Mühle, J., Weiss, R. F., and Prinn,

R. G.: Australian carbon tetrachloride emissions in a global context, Environ. Chem., 11, 1, 77-88, 10.1071/EN13171, 2014.

Fraser, P. J., Pearman, G. I., and Derek, N.: CSIRO Non-carbon Dioxide Greenhouse Gas Research. Part 1: 1975-90, Hist. Rec. Aust. Sci., 29, 1, 1-13, 10.1071/HR17016, 2018.

Fuller, E. N., Schettler, P. D., and Giddings, J. C.: A new method for prediction of binary gas-phase diffusion coefficients, Industrial & Engineering Chemistry, 58, 5, 18-27, 10.1021/ie50677a007, 1966.

Ganesan, A. L., Rigby, M., Zammit-Mangion, A., Manning, A. J., Prinn, R. G., Fraser, P. J., Harth, C. M., Kim, K. R., Krummel, P. B., Li, S., Mühle, J., O'Doherty, S. J., Park, S., Salameh, P. K., Steele, L. P., and Weiss, R. F.: Characterization of uncertainties in atmospheric trace gas inversions using hierarchical Bayesian methods, Atmos. Chem. Phys., 14, 8, 3855-3864, 10.5194/acp-14-3855-2014, 2014.

Gangal, S. V., and Brothers, P. D.: Perfluorinated Polymers, in: Kirk-Othmer Encyclopedia of Chemical Technology, 2015.

Harnisch, J., Wing, I. S., Jacoby, H. D., and Prinn, R. G.: Primary Aluminum Production: Climate Policy, Emissions and Costs, Massachusetts Institute of Technology, Report #44, 1998.

Harnisch, J.: Reactive Fluorine Compounds, in: Reactive Halogen Compounds in the Atmosphere Vol. 4 Part E, The Handbook of Environmental Chemistry, Springer Berlin/Heidelberg, 81-111, 1999.

Harnisch, J.: Atmospheric perfluorocarbons: sources and concentrations, in: Non-CO_2 greenhouse gases: scientific understanding, control and implementation, edited by: Ham, J. v., Baede, A., Meyer, L., and Ybema, R., Kluwer Academic Publishers, Netherlands, 205-210, 2000.

Hastings, W. K.: Monte Carlo sampling methods using Markov chains and their applications, Biometrika, 57, 1, 97-109, 10.1093/biomet/57.1.97, 1970.

Holliday, R. D., and Henry, J. L.: Anode polarization fluorocarbon formation in aluminum reduction cells, J. Ind. Eng. Chem., 51, 10, 1289-1292, 1959.

Ivy, D. J., Arnold, T., Harth, C. M., Steele, L. P., Mühle, J., Rigby, M., Salameh, P. K., Leist, M., Krummel, P. B., Fraser, P. J., Weiss, R. F., and Prinn, R. G.: Atmospheric histories and growth trends of C_4F_{10}, C_5F_{12}, C_6F_{14}, C_7F_{16} and C_8F_{18}, Atmos. Chem. Phys., 12, 9, 4313-4325, 10.5194/acp-12-4313-2012, 2012.

Ji, L., Lu, S., Yang, J., Du, C., Chen, Z., Buekens, A., and Yan, J.: Municipal solid waste incineration in China and the issue of acidification: A review, Waste Management & Research, 34, 4, 280-297, 10.1177/0734242x16633776, 2016.

Jianming, S.: Synthesis of Hexafluoropropene by Co-pyrolysis Reaction of Tetrafluoroethylene with Octafluorocyclobutane, Masters Degree, Department of Chemical Engineering, Zhajiang University, Hangzhou, China, 2006.

Jones, A. R., Thomson, D. J., Hort, M., and Devenish, B.: The UK Met Office's next-generation atmospheric dispersion model, NAME III, in: Air Pollution Modelling and Its Application XVII, edited by: Borrego, C., and Norman, A.-L., 580-589, 2007.

Kannan, G. K., Gupta, M., and Chandra Kapoor, J.: Estimation of gaseous products and particulate matter emission from garden biomass combustion in a simulation fire test chamber, Atmos. Environ., 39, 3, 563-573, 2005.

Kass, W.: Tracing Technique in Geohydrology, CRC Press, 1998.

Kim, J. H., Oh, C. H., Lee, N. E., and Yeom, G. Y.: Effect of N_2O to C_4F_8/O_2 on global warming during silicon nitride plasma enhanced chemical vapor deposition (PECVD) chamber cleaning using a remote inductively coupled plasma source, Jpn. J. Appl. Phys. Part 2 - Lett., 41, 12B, L1495-L1498, 10.1143/jjap.41.l1495, 2002.

Kokkoris, G., Goodyear, A., Cooke, M., and Gogolides, E.: A global model for C_4F_8 plasmas coupling gas phase and wall surface reaction kinetics, J. Phys. D: Appl. Phys., 41, 19, 195211, 10.1088/0022-3727/41/19/195211, 2008.

Langenfelds, R. L., Krummel, P. B., Fraser, P. J., Steele, L. P., Ward, J., and Somerville, N. T.: Archiving of Cape Grim air, Baseline Atmospheric Program Australia 2009-2010, Melbourne, Australia, 2014, edited by: Derek, N., Krummel, P. B., and Cleland, S. J., pp. 44-45, Australian Bureau of Meteorology and CSIRO Marine and Atmospheric Research.

Lewis, R. J., Sr.: Food additives handbook, Chapman & Hall, New York, 1989.

Liu, X., Wang, J., Wang, Y., Zhang, Z., and Xiao, D.: Analysis of the insulation characteristics of c-C_4F_8/CO_2 gas mixtures by the Monte Carlo method, Journal of Physics D: Applied Physics, 41, 1, 015206, 2008.

Lovelock, J. E.: Atmospheric Fluorine Compounds as Indicators of Air Movements, Nature, 230, 5293, 379-&, 1971.

Lunt, M. F., Rigby, M., Ganesan, A. L., and Manning, A. J.: Estimation of trace gas fluxes with objectively determined basis functions using reversible-jump Markov chain Monte Carlo, Geosci. Model Dev., 9, 9, 3213-3229, 10.5194/gmd-9-3213-2016, 2016.

Mackay, D., Shiu, W. Y., Ma, K. C., and Lee, S.: Handbook of Physical-Chemical Properties and Environmental Fate for Organic Chemicals, 2006.

Maione, M., Giostra, U., Arduini, J., Furlani, F., Graziosi, F., Lo Vullo, E., and Bonasoni, P.: Ten years of continuous observations of stratospheric ozone depleting gases at Monte Cimone (Italy) — Comments on the effectiveness of the Montreal Protocol from a regional perspective, Sci. Total Environ., 445-446, 155-164, 10.1016/j.scitotenv.2012.12.056, 2013.

Matsunaga, N., Hori, M., and Nagashima, A.: Mutual diffusion coefficients of halogenated-hydrocarbon refrigerant-air systems, High Temp.-High Press, 25, 63-70, 1993.

Matsunaga, N., Hori, M., and Nagashima, A.: Measurements of the mutual diffusion coefficients of gases by the Taylor method, 7th report, measurements on the SF_6-air, SF_6-N_2, SF_6-O_2, CFC12-N_2, CFC12-O_2, HCFC22-N_2 and HCFC22-O_2 systems, Trans. Jpn. Soc. Mech. Eng. B., 68, 550–555, 2002.

Matsunaga, N., Hori, M., and Nagashima, A.: Measurements of the mutual diffusion coefficients of carbon tetrafluoride and methyl bromide in air, nitrogen and oxygen, Proc. 26th Jpn. Symp. Therm. Props, 26, 499–501, 2005.

Metropolis, N., Rosenbluth, A. W., Rosenbluth, M. N., Teller, A. H., and Teller, E.: Equation of State Calculations by Fast Computing Machines, J. Chem. Phys., 21, 6, 1087-1092, 10.1063/1.1699114, 1953.

Miller, B. R., Weiss, R. F., Salameh, P. K., Tanhua, T., Greally, B. R., Mühle, J., and Simmonds, P. G.: Medusa: A sample preconcentration and GC/MS detector system for in situ measurements of atmospheric trace halocarbons, hydrocarbons, and sulfur compounds, Anal. Chem., 80, 5, 1536-1545, 10.1021/ac702084k, 2008.

Morisaki, S.: Simultaneous thermogravimetry-mass spectrometry and pyrolysis--gas chromatography of fluorocarbon polymers, Thermochimica Acta, 25, 2, 171-183, 1978.

Morris, R. A., Miller, T. M., Viggiano, A. A., Paulson, J. F., Solomon, S., and Reid, G.: Effects of electron and ion reactions on atmospheric lifetimes of fully fluorinated compounds, J. Geophys. Res., 100, D1, 1287-1294, 1995.

Mühle, J., Ganesan, A. L., Miller, B. R., Salameh, P. K., Harth, C. M., Greally, B. R., Rigby, M., Porter, L. W., Steele, L. P., Trudinger, C. M., Krummel, P. B., O'Doherty, S., Fraser, P. J., Simmonds, P. G., Prinn, R. G., and Weiss, R. F.: Perfluorocarbons in the global atmosphere: tetrafluoromethane, hexafluoroethane, and octafluoropropane, Atmos. Chem. Phys., 10, 11, 5145-5164, 10.5194/acp-10-5145-2010, 2010.

Myhre, G., D. Shindell (Coordinating Lead Authors), Bréon, F.-M., Collins, W., Fuglestvedt, J., Huang, J., Koch, D., Lamarque, J.-F., Lee, D., Mendoza, B., Nakajima, T., Robock, A., Stephens, G., Takemura, T., and Zhang, H.: Anthropogenic and Natural Radiative Forcing, in: Climate Change 2013: The Physical Science Basis. Contribution of Working Group I to the Fifth Assessment Report of the Intergovernmental Panel on Climate Change, Chapter 8, edited by: Stocker, T. F., Qin, D., Plattner, G.-K., Tignor, M., Allen, S. K., Boschung, J., Nauels, A., Xia, Y., Bex, V., and Midgley, P. M., Cambridge University Press, Cambridge, United Kingdom and New York, NY, USA, 2013.

O'Doherty, S., Simmonds, P. G., Cunnold, D. M., Wang, H. J., Sturrock, G. A., Fraser, P. J., Ryall, D., Derwent, R. G., Weiss, R. F., Salameh, P., Miller, B. R., and Prinn, R. G.: In situ chloroform measurements at Advanced Global Atmospheric Gases Experiment atmospheric research stations from 1994 to 1998, J. Geophys. Res., 106, D17, 20429-20444, 2001.

O'Doherty, S., Rigby, M., Mühle, J., Ivy, D. J., Miller, B. R., Young, D., Simmonds, P. G., Reimann, S., Vollmer, M. K., Krummel, P. B., Fraser, P. J., Steele, L. P., Dunse, B., Salameh, P. K., Harth, C. M., Arnold, T., Weiss, R. F., Kim, J., Park, S., Li, S., Lunder, C., Hermansen, O., Schmidbauer, N., Zhou, L. X., Yao, B., Wang, R. H. J., Manning, A. J., and Prinn, R. G.: Global emissions of HFC-143a (CH_3CF_3) and HFC-32 (CH_2F_2) from in situ and air archive atmospheric observations, Atmos. Chem. Phys., 14, 17, 9249-9258, 10.5194/acp-14-9249-2014, 2014.

Oram, D.: Trends of long-lived anthropogenic halocarbons in the Southern Hemisphere and model calculations of global emissions, P.D. thesis, University of East Anglia, Norwich, U.K., 1999.

Oram, D. E., Mani, F. S., Laube, J. C., Newland, M. J., Reeves, C. E., Sturges, W. T., Penkett, S. A., Brenninkmeijer, C. A. M., Röckmann, T., and Fraser, P. J.: Long-term tropospheric trend of octafluorocyclobutane (c-C_4F_8 or PFC-318), Atmos. Chem. Phys., 12, 1, 261-269, 10.5194/acp-12-261-2012, 2012.

Prinn, R. G., Weiss, R. F., Fraser, P. J., Simmonds, P. G., Cunnold, D. M., Alyea, F. N., O'Doherty, S., Salameh, P., Miller, B. R., Huang, J., Wang, R. H. J., Hartley, D. E., Harth, C., Steele, L. P., Sturrock, G., Midgley, P. M., and McCulloch, A.: A history of chemically and radiatively important gases in air deduced from ALE/GAGE/AGAGE, J. Geophys. Res., 105, D14, 17751-17792, 10.1029/2000jd900141, 2000.

Prinn, R. G., Huang, J., Weiss, R. F., Cunnold, D. M., Fraser, P. J., Simmonds, P. G., McCulloch, A., Harth, C., Salameh, P., O'Doherty, S., Wang, R. H. J., Porter, L., and Miller, B. R.: Evidence for substantial variations of atmospheric hydroxyl radicals in the past two decades, Science, 292, 5523, 1882-1888, 2001.

Prinn, R. G., Weiss, R. F., Arduini, J., Arnold, T., DeWitt, H. L., Fraser, P. J., Ganesan, A. L., Gasore, J., Harth, C. M., Hermansen, O., Kim, J., Krummel, P. B., Li, S., Loh, Z. M., Lunder, C. R., Maione, M., Manning, A. J., Miller, B. R., Mitrevski, B., Mühle, J., O'Doherty, S., Park, S., Reimann, S., Rigby, M., Saito, T., Salameh, P. K., Schmidt, R., Simmonds, P. G., Steele, L. P., Vollmer, M. K., Wang, R. H., Yao, B., Yokouchi, Y., Young, D., and Zhou, L.: History of chemically and radiatively important atmospheric gases from the Advanced Global Atmospheric Gases Experiment (AGAGE), Earth Syst. Sci. Data, 10, 2, 985-1018, 10.5194/essd-10-985-2018, 2018.

Raju, R., Kudo, D., Kubo, Y., Inaba, T., and Shindo, H.: Warming potential reduction of C_4F_8 using inductively coupled plasma, Japanese Journal of Applied Physics Part 1-Regular Papers Short Notes & Review Papers, 42, 1, 280-285, 10.1143/jjap.42.280, 2003.

Ravishankara, A. R., Solomon, S., Turnipseed, A. A., and Warren, R. F.: Atmospheric lifetimes of long-lived halogenated species, Science, 259, 5092, 194-199, 1993.

Rigby, M., Ganesan, A. L., and Prinn, R. G.: Deriving emissions time series from sparse atmospheric mole fractions, J. Geophys. Res., 116, D8, D08306, 10.1029/2010jd015401, 2011.

Rigby, M., Prinn, R. G., O'Doherty, S., Montzka, S. A., McCulloch, A., Harth, C. M., Mühle, J., Salameh, P. K., Weiss, R. F., Young, D., Simmonds, P. G., Hall, B. D., Dutton, G. S., Nance, D., Mondeel, D. J., Elkins, J. W., Krummel, P. B., Steele, L. P., and Fraser, P. J.: Re-evaluation of the lifetimes of the major CFCs and CH_3CCl_3 using atmospheric trends, Atmos. Chem. Phys., 13, 5, 2691-2702, 10.5194/acp-13-2691-2013, 2013.

Rigby, M., Prinn, R. G., O'Doherty, S., Miller, B. R., Ivy, D., Mühle, J., Harth, C. M., Salameh, P. K., Arnold, T., Weiss, R. F., Krummel, P. B., Steele, L. P., Fraser, P. J., Young, D., and Simmonds, P. G.: Recent and future trends in synthetic greenhouse gas radiative forcing, Geophys. Res. Lett., 41, 7, 2623-2630, 10.1002/2013gl059099, 2014.

Saito, T., Yokouchi, Y., Stohl, A., Taguchi, S., and Mukai, H.: Large emissions of perfluorocarbons in East Asia deduced from continuous atmospheric measurements, Environ. Sci. Technol., 44, 11, 4089-4095, 10.1021/es1001488, 2010.

Sasaki, K., Kawai, Y., Suzuki, C., and Kadota, K.: Absolute density and reaction kinetics of fluorine atoms in high-density c-C_4F_8 plasmas, Journal of Applied Physics, 83, 12, 7482-7487, 1998.

Say, D., Ganesan, A. L., Lunt, M. F., Rigby, M., O'Doherty, S., Harth, C., Manning, A. J., Krummel, P. B., and Bauguitte, S.: Emissions of CFCs, HCFCs and HFCs from India, Atmos. Chem. Phys. Discuss., 2019, 1-30, 10.5194/acp-2018-1146, 2019.

Siegemund, G., Schwertfeger, W., Feiring, A., Smart, B., Behr, F., Vogel, H., McKusick, B., and Kirsch, P.: Fluorine Compounds, Organic, in: Ullmann's Encyclopedia of Industrial Chemistry, 2016.

Simmonds, P. G., Rigby, M., McCulloch, A., Vollmer, M. K., Henne, S., Mühle, J., O'Doherty, S., Manning, A. J., Krummel, P. B., Fraser, P. J., Young, D., Weiss, R. F., Salameh, P. K., Harth, C. M., Reimann, S., Trudinger, C. M., Steele, P., Wang, R. H. J., Ivy, D. J., Prinn, R. G., Mitrevski, B., and Etheridge, D. M.: Recent increases in the atmospheric growth rate and emissions of HFC-23 (CHF_3) and the link to HCFC-22 ($CHClF_2$) production, Atmos. Chem. Phys., 18, 6, 4153-4169, 10.5194/acp-18-4153-2018, 2018.

Smith, A. M., Levchenko, V. A., Etheridge, D. M., Lowe, D. C., Hua, Q., Trudinger, C. M., Zoppi, U., and Elcheikh, A.: In search of in-situ radiocarbon in Law Dome ice and firn, Nuclear Instruments and Methods in Physics Research Section B: Beam Interactions with Materials and Atoms, 172, 1–4, 610-622, 10.1016/S0168-583X(00)00280-9, 2000.

Sowers, T., Bernard, S., Aballain, O., Chappellaz, J., Barnola, J.-M., and Marik, T.: Records of the $\delta^{13}C$ of atmospheric CH_4 over the last 2 centuries as recorded in Antarctic snow and ice, Global Biogeochem. Cycles, 19, GB2002, 10.1029/2004GB002408, 2005.

Stanley, K. M., Grant, A., O'Doherty, S., Young, D., Manning, A. J., Stavert, A. R., Spain, T. G., Salameh, P. K., Harth, C. M., Simmonds, P. G., Sturges, W. T., Oram, D. E., and Derwent, R. G.: Greenhouse gas measurements from a UK network of tall towers: technical description and first results, Atmos. Meas. Tech., 11, 3, 1437-1458, 10.5194/amt-11-1437-2018, 2018.

Stohl, A., Forster, C., Frank, A., Seibert, P., and Wotawa, G.: Technical note: The Lagrangian particle dispersion model FLEXPART version 6.2, Atmos. Chem. Phys., 5, 2461-2474, 2005.

Stohl, A., Seibert, P., Arduini, J., Eckhardt, S., Fraser, P., Greally, B. R., Lunder, C., Maione, M., Mühle, J., O’Doherty, S., Prinn, R. G., Reimann, S., Saito, T., Schmidbauer, N., Simmonds, P. G., Vollmer, M. K., Weiss, R. F., and Yokouchi, Y.: An analytical inversion method for determining regional and global emissions of greenhouse gases: Sensitivity studies and application to halocarbons, Atmos. Chem. Phys., 9, 5, 1597-1620, 10.5194/acp-9-1597-2009, 2009.

Sturges, W. T., Penkett, S. A., Lee, J. M., and Sturges, K. E.: Stratospheric distribution and lifetime of halogenated hydrocarbons; Final report to the European Commission, Contract EV5V-CT92-0078, Unversity of East Anglia, Norwich, 1995.

Sturges, W. T., Oram, D. E., Penkett, S. A., Fraser, P. J., and Engel, A.: Long-lived halogenated compounds in the stratosphere, in: Non-CO_2 Greenhouse Gases: Scientific Understanding, Control, and Implementation, edited by: van Ham, J., Baede, A. P. M., Meyer, L. A., and Ybema, R., Kluwer Academic Publishers, The Netherlands, 239-240, 2000.

Sturrock, G. A., Etheridge, D. M., Trudinger, C. M., Fraser, P. J., and Smith, A. M.: Atmospheric histories of halocarbons from analysis of Antarctic firn air: Major Montreal Protocol species, J. Geophys. Res., 107, D24, 4765, 10.1029/2002JD002548, 2002.

Tabereaux, A. T.: Anode Effects, PFCs, Global Warming, and the Aluminum-Industry, J. Miner. Met. Mater. Soc., 46, 11, 30-34, 1994.

Travnicek, W.: A study of light halgenated hydrocarbons in stratospheric air samples using CG-MS, diploma thesis, Dept. Jülich, Fachhochschule Aachen, Germany, Aachen, 1998.

Trudinger, C. M., Enting, I. G., Etheridge, D. M., Francey, R. J., Levchenko, V. A., Steele, L. P., Raynaud, D., and Arnaud, L.: Modeling air movement and bubble trapping in firn, J. Geophys. Res., 102, D6, 6747-6763, 10.1029/96jd03382, 1997.

Trudinger, C. M., Etheridge, D. M., Rayner, P. J., Enting, I. G., Sturrock, G. A., and Langenfelds, R. L.: Reconstructing atmospheric histories from measurements of air composition in firn, J. Geophys. Res., 107, D24, 4780, 10.1029/2002JD002545, 2002.

Trudinger, C. M., Enting, I. G., Rayner, P. J., Etheridge, D. M., Buizert, C., Rubino, M., Krummel, P. B., and Blunier, T.: How well do different tracers constrain the firn diffusivity profile?, Atmos. Chem. Phys., 13, 3, 1485-1510, 10.5194/acp-13-1485-2013, 2013.

Trudinger, C. M., Fraser, P. J., Etheridge, D. M., Sturges, W. T., Vollmer, M. K., Rigby, M., Martinerie, P., Mühle, J., Worton, D. R., Krummel, P. B., Steele, L. P., Miller, B. R., Laube, J., Mani, F. S., Rayner, P. J., Harth, C. M., Witrant, E., Blunier, T., Schwander, J., O'Doherty, S., and Battle, M.: Atmospheric abundance and global emissions of perfluorocarbons CF_4, C_2F_6 and C_3F_8 since 1800 inferred from ice core, firn, air archive and in situ measurements, Atmos. Chem. Phys., 16, 18, 11733-11754, 10.5194/acp-16-11733-2016, 2016.

Tsai, W. T.: Fate of Chloromethanes in the Atmospheric Environment: Implications for Human Health, Ozone Formation and Depletion, and Global Warming Impacts, Toxics, 5, 4, 10.3390/toxics5040023, 2017.

van der Walt, I. J., Neomagus, H. W. J. P., Nel, J. T., Bruinsma, O. S. L., and Crouse, P. L.: A kinetic expression for the pyrolytic decomposition of polytetrafluoroethylene, J. Fluor. Chem., 129, 4, 314-318, 10.1016/j.jfluchem.2008.01.003, 2008.

Victor, D. G., and MacDonald, G. J.: A model for estimating future emissions of sulfur hexafluoride and perfluorocarbons, Climatic Change, 42, 4, 633-662, 1999.

Vollmer, M. K., Mühle, J., Trudinger, C. M., Rigby, M., Montzka, S. A., Harth, C. M., Miller, B. R., Henne, S., Krummel, P. B., Hall, B. D., Young, D., Kim, J., Arduini, J., Wenger, A., Yao, B., Reimann, S., O'Doherty, S., Maione, M., Etheridge, D. M., Li, S., Verdonik, D. P., Park, S., Dutton, G., Steele, L. P., Lunder, C. R., Rhee, T. S., Hermansen, O., Schmidbauer, N., Wang, R. H. J., Hill, M., Salameh, P. K., Langenfelds, R. L., Zhou, L., Blunier, T., Schwander, J., Elkins, J. W., Butler, J. H., Simmonds, P. G., Weiss, R. F., Prinn, R. G., and Fraser, P. J. C. J. D.: Atmospheric histories and global emissions of halons H-1211 ($CBrClF_2$), H-1301 ($CBrF_3$), and H-2402 ($CBrF_2CBrF_2$), J. Geophys. Res., 121, 7, 3663-3686, 10.1002/2015jd024488, 2016.

Vollmer, M. K., Young, D., Trudinger, C. M., Mühle, J., Henne, S., Rigby, M., Park, S., Li, S., Guillevic, M., Mitrevski, B., Harth, C. M., Miller, B. R., Reimann, S., Yao, B., Steele, L. P., Wyss, S. A., Lunder, C. R., Arduini, J., McCulloch, A., Wu, S., Rhee, T. S., Wang, R. H. J., Salameh, P. K., Hermansen, O., Hill, M., Langenfelds, R. L., Ivy, D., O'Doherty, S., Krummel, P. B., Maione, M., Etheridge, D. M., Zhou, L., Fraser, P. J., Prinn, R. G., Weiss, R. F., and Simmonds, P. G.: Atmospheric histories and emissions of chlorofluorocarbons CFC-13 ($CClF_3$), ΣCFC-114 ($C_2Cl_2F_4$), and CFC-115 (C_2ClF_5), Atmos. Chem. Phys., 18, 2, 979-1002, 10.5194/acp-18-979-2018, 2018.

Vollmer, M. K., Bernard, F., Mitrevski, B., Steele, L. P., Trudinger, C. M., Reimann, S., Langenfelds, R. L., Krummel, P. B., Fraser, P. J., Etheridge, D. M., Curran, M. A. J., and Burkholder, J. B.: Abundances, emissions, and loss processes of the long-lived and potent greenhouse gas octafluorooxolane (octafluorotetrahydrofuran, c-C_4F_8O) in the atmosphere, Atmos. Chem. Phys., 19, 6, 3481-3492, 10.5194/acp-19-3481-2019, 2019.

Walters, D. N., Williams, K. D., Boutle, I. A., Bushell, A. C., Edwards, J. M., Field, P. R., Lock, A. P., Morcrette, C. J., Stratton, R. A., Wilkinson, J. M., Willett, M. R., Bellouin, N., Bodas-Salcedo, A., Brooks, M. E., Copsey, D., Earnshaw, P. D., Hardiman, S. C., Harris, C. M., Levine, R. C., MacLachlan, C., Manners, J. C., Martin, G. M., Milton, S. F., Palmer, M. D., Roberts, M. J., Rodríguez, J. M., Tennant, W. J., and Vidale, P. L.: The Met Office Unified Model Global Atmosphere 4.0 and JULES Global Land 4.0 configurations, Geosci. Model Dev., 7, 1, 361-386, 10.5194/gmd-7-361-2014, 2014.

Zhihong, W., Seidel, S., Kokorin, A., and Rand, S.: Chapter 3.6, PFC, HFC, SF6 emissions from semiconductor manufacturing, in: IPCC Good Practice Guidance and Uncertainty Management in National Greenhouse Gas Inventories, IGES, Hayama, Japan, 2001.

Tables

Table 1. Availability of *c*-C_4F_8 in situ, flask, firn, and aircraft air measurements, measurements sites, and instrumentation

Station/Site	Network	Lat.	Lon.	Medusa no.	Data availability[*]
Zeppelin (ZEP), Ny-Ålesund, Svalbard	AGAGE	78.9	11.9	19	09/2010–12/2017
NEEM08 firn, Greenland	–	77.5	-51.1	9	Extracted 07/2008
Summit13 firn, Greenland	–	72.7	-38.6	7	Extracted 05/2013
Mace Head (MHD), Ireland	AGAGE	53.3	-9.9	2	06/2010–12/2017
Tacolneston (TAC), United Kingdom	UK DECC/AGAGE	52.5	1.1	13	05/2013–12/2017
Jungfraujoch (JFJ), Switzerland	AGAGE	46.5	8.0	12	11/2008–12/2017
Monte Cimone (CMN), Italy	AGAGE/ICO-CV	44.2	10.7	ADS-GC/MS	05/2013–12/2017
Trinidad Head (THD), USA	AGAGE	41.0	-124.1	4	06/2010–12/2017
Shangdianzi (SDZ), China	AGAGE/CMA	40.7	117.1	17	05/2010–08/2012, 15/2015–04/2017, 09/2017–12/2017
Gosan (GSN), South Korea	AGAGE/KNU	33.3	126.2	10	06/2010–09/2016, 04/2017–09/2017, 12/2017–12/2017
La Jolla (SIO), USA	AGAGE	32.9	-117.3	1	11/2009–08/2013, 01/2014–12/2017
NH flasks	SIO & other	33–46	-72 – -124	7, 1, 9	10/1973–04/2016
Aircraft flask samples, India	FAAM/UoB	9–28	72–86	21	06/2016–07/2016
Ragged Point (RPB), Barbados	AGAGE	13.2	-59.4	5	06/2010–06/2014, 10/2014–12/2017
Cape Matatula (SMO), American Samoa	NOAA/AGAGE	-14.2	-170.6	6	08/2010–12/2017
Aspendale (ASA), Australia	AGAGE	-38.0	145.1	9	04–10/2010, 05–07/2011, 05/2015–12/2017
Cape Grim (CGO), Australia	AGAGE	-40.7	144.7	3	09/2010–12/2017
CGAA flasks, Australia	CSIRO/BoM	-40.7	144.7	9, 7	04/1978–12/2010
DSSW20K firn, Antarctica[+]	–	-66.7	112.8	7	Extracted 12/1997
SPO01 firn, Antarctica	–	-90.0	-119	9	Extracted 01/2001

[*] Shorter interruptions are excluded.

AGAGE: Advanced Global Atmospheric Gases Experiment (Prinn et al., 2018).

NEEM08: Firn air samples collected in 2008 at the Northern Greenland Eemian Ice Drilling Project, Greenland were collected by the University of Copenhagen, Denmark, the NEEM consortium, and the Commonwealth Scientific and Industrial Research Organisation (CSIRO) (Buizert et al., 2012).

Summit13: Firn samples collected in 2013 near Summit station, Greenland by the University of Rochester and Oregon State University.

UK DECC: The Tacolneston (TAC) site is part of the UK Deriving Emissions linked to Climate Change network (Stanley et al., 2018).

DSSW20K: Firn samples collected in December 1997 at Dome Summit South West 20 km, Law Dome by CSIRO, the Australian Antarctic Division (AAD), and the Australian Nuclear Science and Technology Organisation (ANSTO) (see Trudinger et al., 2016 and citations therein).

SPO01: Firn samples collected in 2001 at South Pole, Antarctica, by Bowdoin College, the National Oceanic and Atmospheric Administration (NOAA), the University of Colorado and the National Science Foundation (NSF) (Aydin et al., 2004; Sowers et al., 2005).

ICO-OV: Measurements at the Italian Climate Observatory “O. Vittori” Monte Cimone (CMN) were performed with a commercial Adsorption-Desorption System with gas chromatograph and mass spectrometer (ADS-GC/MS) (Maione et al., 2013).

CMA: China Meteorological Administration.

KNU: Kyungpook National University, South Korea.

SIO & other: Most archived northern hemispheric (NH) samples were collected by the Scripps Institution of Oceanography, La Jolla and measured on Medusa 7.

FAAM/UoB: Air samples over India and the Indian Ocean were taken aboard the UK’s FAAM (Facility for Airborne Atmospheric Measurements) BAe-146 research aircraft and analyzed on Medusa 21 at University of Bristol (UoB) (Say et al., 2019).

CGAA: Cape Grim Air Archive samples were collected by the CSIRO Oceans and Atmosphere and the Bureau of Meteorology (BoM), Australia predominantly measured on the Aspendale Medusa 9 at CSIRO (Langenfelds et al., 2014; Fraser et al., 2018).

Table 2. Regional *c*-C_4F_8 emissions derived for eastern Asia from Gosan measurements (NAME-HB inversion) and comparison to global emissions (Gg yr^{-1}, kt yr^{-1})

	Eastern China[#]	Western Japan[#]	South Korea	North Korea	Taiwan[#]	Σ eastern Asia	Global[+]	Global - Σ eastern Asia
2010	0.30 ± 0.07	0.02 ± 0.01	0.019 ± 0.008	0.008 ± 0.004	0.008 ± 0.005	0.36 ± 0.07	1.40 ± 0.11	1.04 ± 0.13
2011	0.35 ± 0.07	0.02 ± 0.01	0.016 ± 0.007	0.006 ± 0.003	0.007 ± 0.005	0.41 ± 0.07	1.52 ± 0.10	1.12 ± 0.12
2012	0.41 ± 0.06	0.02 ± 0.01	0.009 ± 0.005	0.004 ± 0.002	0.010 ± 0.008	0.45 ± 0.06	1.61 ± 0.08	1.16 ± 0.10
2013	0.46 ± 0.09	0.02 ± 0.01	0.017 ± 0.007	0.007 ± 0.004	0.008 ± 0.005	0.51 ± 0.09	1.67 ± 0.09	1.15 ± 0.13
2014	0.54 ± 0.06	0.03 ± 0.01	0.039 ± 0.009	0.009 ± 0.004	0.009 ± 0.006	0.62 ± 0.06	1.76 ± 0.09	1.14 ± 0.11
2015	0.59 ± 0.09	0.02 ± 0.01	0.041 ± 0.010	0.011 ± 0.005	0.011 ± 0.009	0.68 ± 0.09	1.88 ± 0.10	1.21 ± 0.13
2016	0.67 ± 0.12	0.02 ± 0.01	0.022 ± 0.010	0.009 ± 0.005	0.009 ± 0.006	0.73 ± 0.12	2.06 ± 0.10	1.33 ± 0.16
2017	0.68 ± 0.13	0.02 ± 0.01	0.014 ± 0.011	0.006 ± 0.005	0.010 ± 0.009	0.73 ± 0.13	2.20 ± 0.11	1.47 ± 0.17
	China	Japan	South Korea	North Korea	Taiwan	Sum		
a priori[*]	0.42 ± 0.05	0.09 ± 0.01	0.032 ± 0.002	0.010 ± 0.001	0.009 ± 0.001	0.56 ± 0.05		
	Eastern China	Western Japan						
a priori[*]	0.185	0.0294						

[+] Global emissions are the average of the emissions determined by the CSIRO and the Bristol inversion in this work.

[#] Eastern China contains the provinces Anhui, Beijing, Hebei, Henan, Jiangsu, Liaoning, Shandong, Shanghai, Shanxi, Tianjin and Zhejiang. Western Japan contains the prefectures Chugoku, Kansai, Shikoku and Okawa and Kyushu. Due to the lower sensitivities of the inversion in western China, eastern Japan, and parts of Taiwan, where potential source industries are located, we cannot exclude further emissions in these regions and therefore total emissions are probably larger.

[*] Saito et al. (2010) emission estimates based on atmospheric measurements from November 2007 to September 2009 were used as a priori information and were spread for each country uniformly over the area of each country. The resulting a priori estimates for eastern China and western Japan are additionally listed for comparison with the inversion results for these regions.

Gosan measurements started in June 2010 with most complete coverages from 2011 to 2015.

Figures

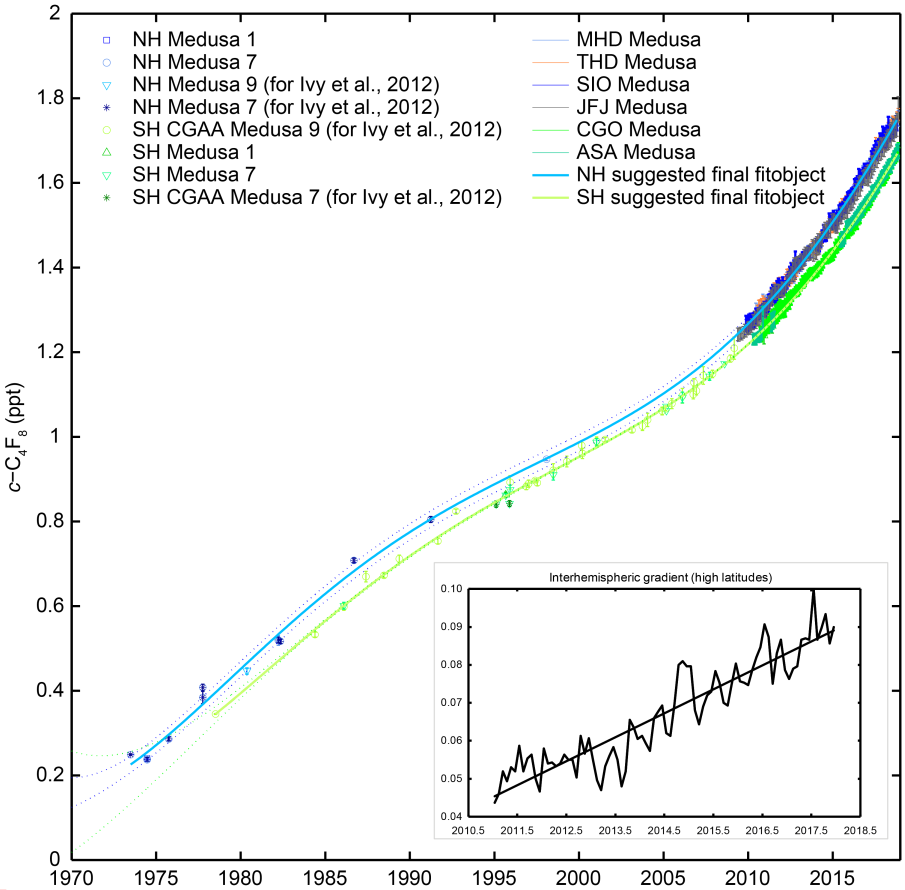

Figure 1. c-C_4F_8 mole fractions reconstructed from the late 1970s to 2018 from archived air samples and in situ measurements in both hemispheres. Cape Grim Air Archive (CGAA) and archived NH air samples are shown with symbols in shades of green and blue, respectively, reflecting different data subsets. For recent years, in situ measurements are shown as pollution removed monthly means for extra-tropical stations in the NH (MHD in light blue, THD in orange, SIO in darker blue, JFJ in grey) and in the SH (CGO in lighter green, ASA in pale green). Shown are the final data after an iterative filtering process described in the main text. The final suggested fits are shown as bold light green (SH) and bold light blue (NH) polynomial fits. Confidence bands (2σ) are shown as dotted lines. Results for the tropical stations, RPB and SMO, the Asian stations, GSN and SDZ, and the Arctic station, ZEP, are omitted here for clarity. For individual samples, error bars reflect measurement precisions. For monthly means, error bars represent standard deviations. The inset shows the interhemispheric gradient from in situ measurements at high latitudes (MHD, THD, SIO, and CGO) from 2011 to 2017

Deleted:

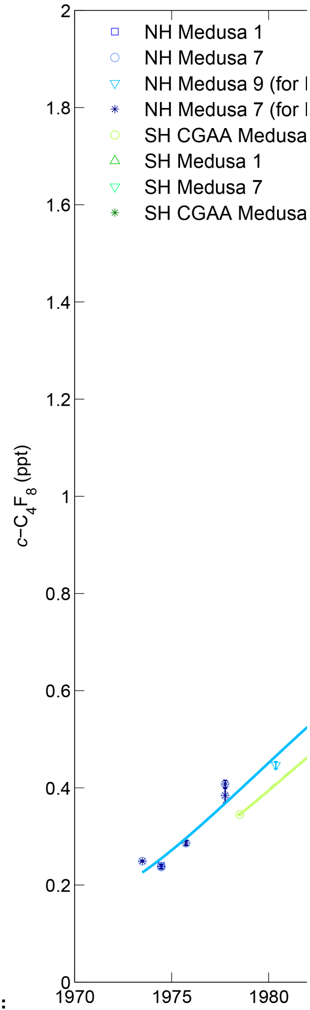

Comment [JM141]: *Rev. #1: L1236 Figure 1 is mostly demonstrating quality assurance purposes and one cannot see most station data anyway as it is on top of each other. As the long-term trend is shown again in Figures 3 and 4 I suggest moving it to the supplement.*

See our reply.

Rev. #2: Figure 1 caption: What are the error bars?

Rev #2: Figures 1 is nicely formatted, but the formatting is inconsistent with that applied in Figures 2-4. Moreover Figure 5 has a completely different formatting style. This figure formatting ought to be "harmonized".

See our reply.

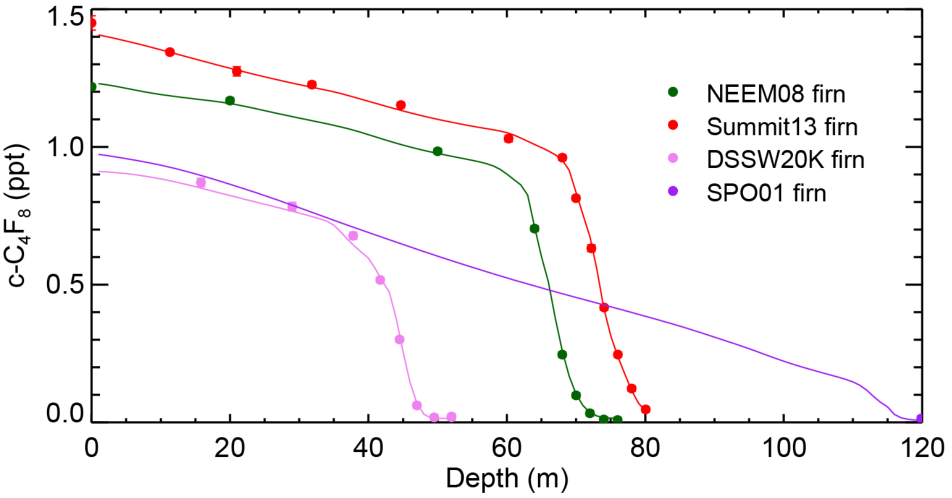

Figure 2. Depth profile of *c*-C_4F_8 measured dry-air molar mole fractions (parts per trillion, ppt) in air extracted from polar firn at NEEM08 (Northern Greenland, dark green) and Summit13 (Greenland, red) in the NH and DSSW20K (Eastern Antarctica, pink) and SPO01 (South Pole, purple) in the SH, together with the simulated depth profiles for each site (dark green, red, pink, and purple lines) that correspond to the emissions inferred by the CSIRO inversion. The modelled depth profiles for each site (solid lines) are based on the inversion of measurements from all firn sites, archive, and in situ data. Measurement precisions (1σ) are shown as error bars and are generally smaller than the plotting symbol.

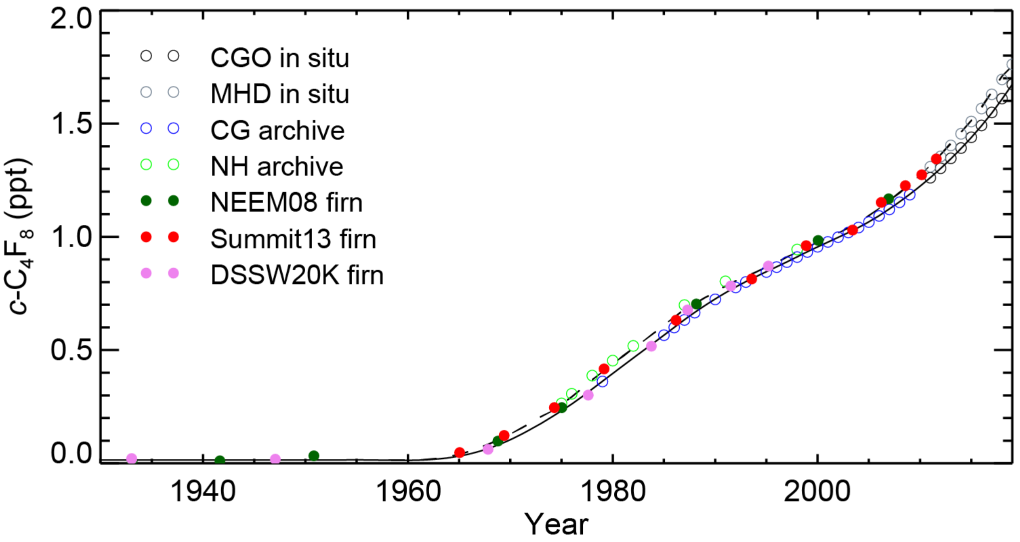

Figure 3. Historic atmospheric *c*-C_4F_8 mole fractions reconstructed for the extra-tropical Northern and Southern Hemispheres from air extracted from polar firn (full circles, NEEM08 in dark green, Summit13 in red, DSSW20K in

Deleted: ¶

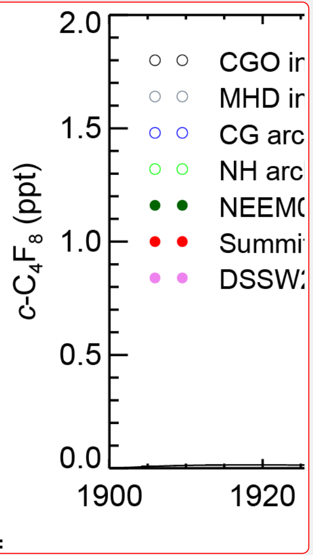

Deleted:

Comment [JM142]: *Rev. L1256 Is it necessary to show years from 1900 if the first data point is after 1930? What is the uncertainty of the calculated effective ages?*

pink, against mean or effective ages; SPO01 with mean age of ~1890 is not shown), annual values from spline fits to Cape Grim Air Archive (CG archive, open blue circles) and in situ measurements at Cape Grim (CGO, open black circles), archived air samples (NH archive, open green circles) and in situ measurements at Mace Head (MHD, open grey circles). Also shown are reconstructed abundances based on optimized emissions determined by the CSIRO inversion for the extra-tropical SH (black line) and NH (dashed black line).

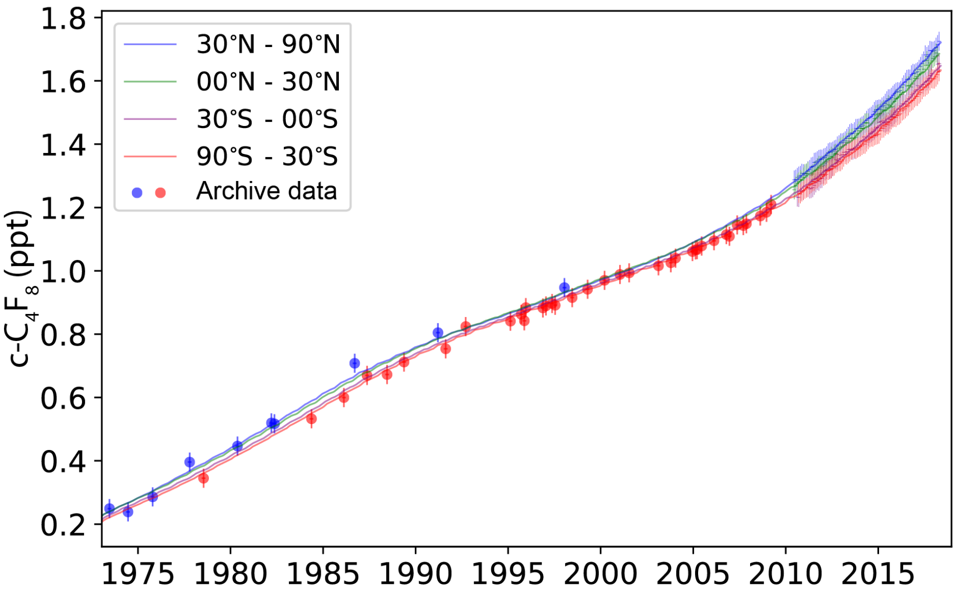

Figure 4. Historic *c*-C_4F_8 mole fractions from archive samples in both hemispheres (filled circles) and pollution-free monthly mean in situ data from AGAGE background sites (MHD and THD in blue, RPB in green, SMO in purple and CGO in green, vertical bars, bar size represents variability of monthly means) are shown together with the Bristol inversion results for the four latitudinal bands represented by these background sites (30° N–90° N, 0° N–30° N, 0° S–30° S and 30° S–90° S, solid lines of same color).

Deleted:

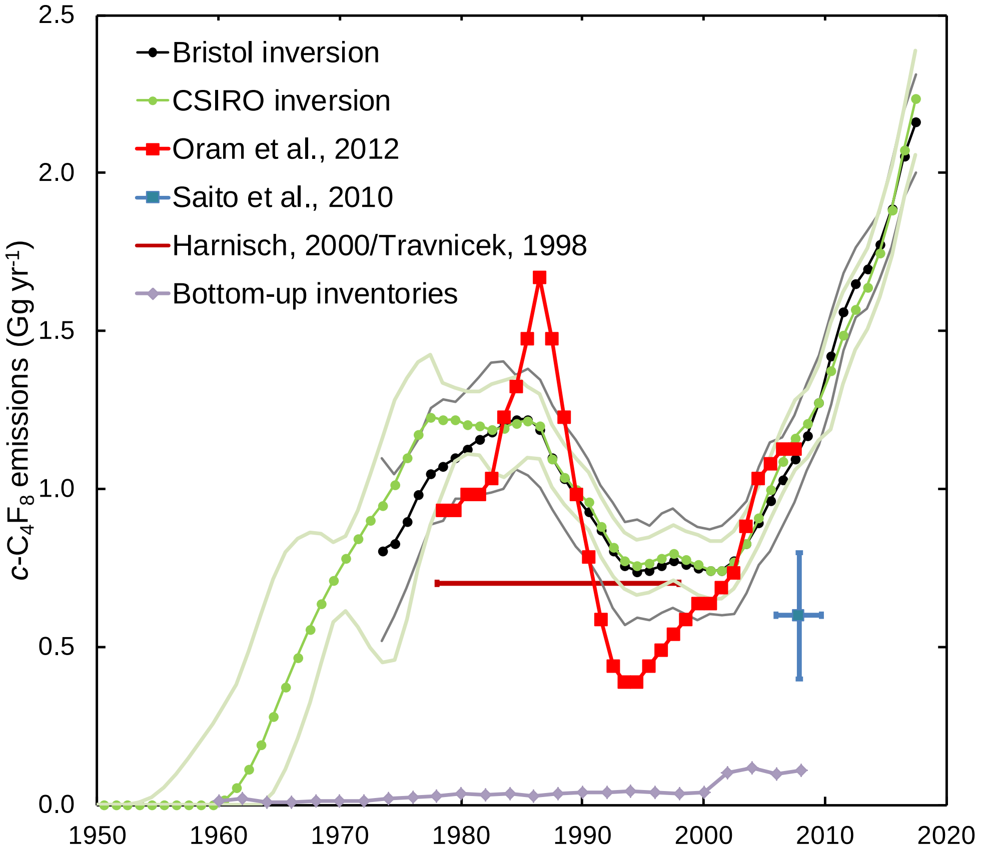

Figure 5. Global c-C_4F_8 emissions reconstructed by the CSIRO inversion (green dots and line, light green 2 σ uncertainty bands) from 1950 and by the Bristol inversion (black dots and line, grey 1 σ uncertainty bands) from the early 1970s to present. In situ and archive data are used in both inversions, while firn air data are only used in the CSIRO inversion. Emission estimates by Oram et al., 2012 (red), Saito et al., 2010 (blue), Harnisch, 2000/Travnicek, 1998 (brown) and from available bottom-up inventory information (grey) are shown for comparison.

Deleted:

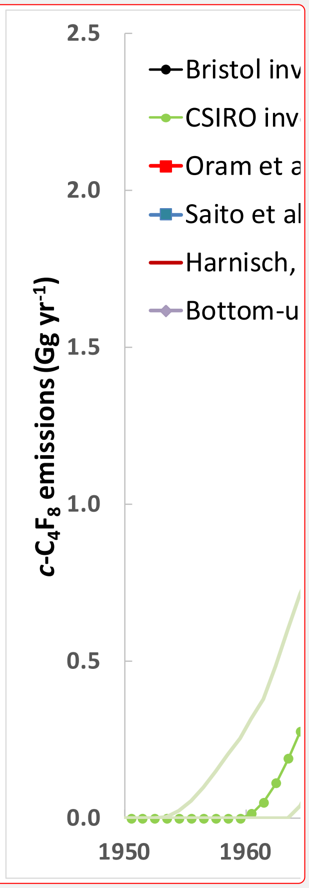

Comment [JM143]: *Figures 1 is nicely formatted, but the formatting is inconsistent with that applied in Figures 2-4. Moreover Figure 5 has a completely different formatting style. This figure formatting ought to be "harmonized".*

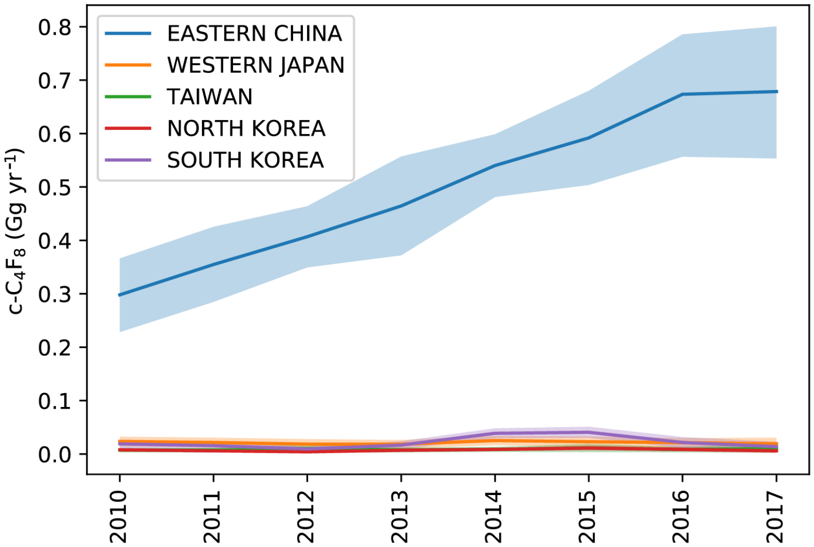

Figure 6. *c*-C_4F_8 emission in eastern Asia as determined by the NAME-HB regional inversion of measurements at the Gosan station, Jeju Island, South Korea are dominated by emissions from eastern China (blue), followed by emissions from western Japan (orange). Emissions from South Korea (violet) are much smaller, but show a small maximum in 2014 and 2015. Emissions from Taiwan (green) and North Korea (red) also small. Shadings represent uncertainty bands of emissions.

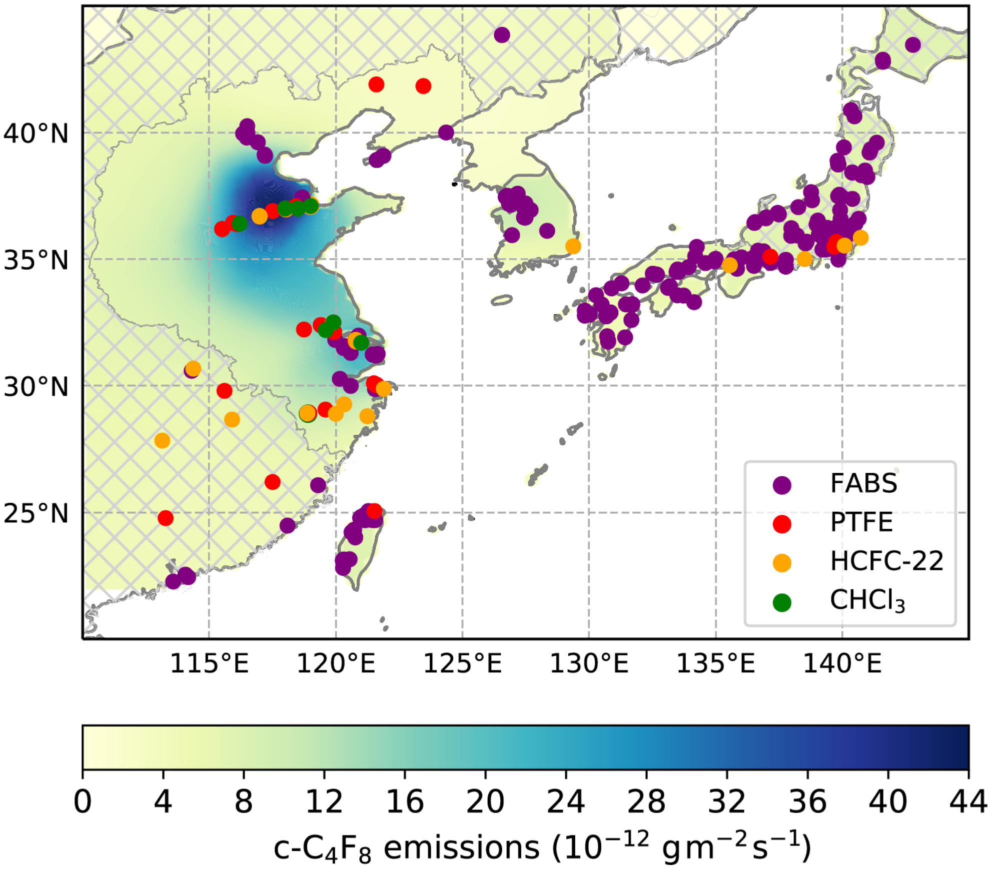

Figure 7. Mean *c*-C_4F_8 emission strength (shades of green and blue, 10^{-12} g m^{-2} s^{-1}) in eastern Asia from 2010 to 2017 determined by the NAME-HB inversion from measurements at the Gosan station, Jeju Island, South Korea. The hatching indicates areas for which emissions are not reported due to relatively low sensitivities of the inversion. Emissions predominantly occur in the densely industrialized Shandong, Tianjin and parts of Henan and Hebei provinces south/southwest of Beijing as well as in Shanghai and neighboring provinces Jiangsu (to the north), Anhui (to the west) and Zhejiang (to the south) of the Yangtze River Delta region. Shown are industries with potential *c*-C_4F_8 emissions: Semiconductor fabrication plants (FABS, purple dots, en.wikipedia.org/wiki/List_of_semiconductor_fabrication_plants, www.10stripe.com/featured/map/semiconductor-fabs.php and other sources) and TFE/HFP/PTFE/FEP production facilities (PTFE, red dots, www.qianzhan.com/analyst/detail/220/170629-c33a2ca7.html and other sources). HCFC-22 (orange dots) and chloroform ($CHCl_3$, green dots) production facilities are shown as the TFE and HFP monomers needed to produce PTFE and FEP fluoropolymers are produced via pyrolysis of HCFC-22 and *c*-C_4F_8 is an intermediate/by-product in this process, while HCFC-22 is manufactured from $CHCl_3$.

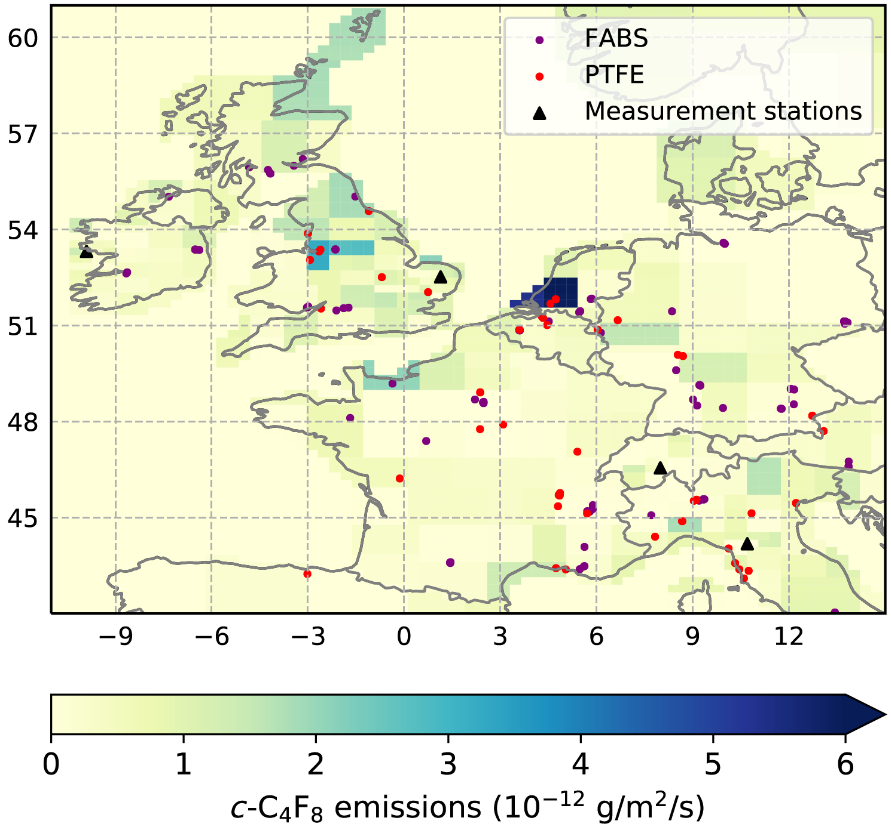

Figure 8. Mean c-C_4F_8 emission strength (shades of green and blue, 10^{-12} g m^{-2} s^{-1}) in North Western Europe (42° N to 59° N and -11° E to 15° E) from 2013–2017 determined by the InTEM inversion from measurements at four sites (Mace Head, Ireland, Tacolneston, United Kingdom, Jungfraujoch, Switzerland, and Monte Cimone, Italy, black triangles). Also shown are potential industrial emitters of c-C_4F_8. Locations of potential TFE/HFP/PTFE/FEP production facilities (red dots) are based on company websites (3M, Chemours, Daikin, DuPont, Saint-Gobain, and Solvay) and are much less certain than the corresponding location information for eastern Asia. Also shown are semiconductor fabrication plants (purple dots, en.wikipedia.org/wiki/List_of_semiconductor_fabrication_plants, www.10stripe.com/featured/map/semiconductor-fabs.php, and other sources).

Comment [JM144]: Updated due to mistake in setup for European inversion.

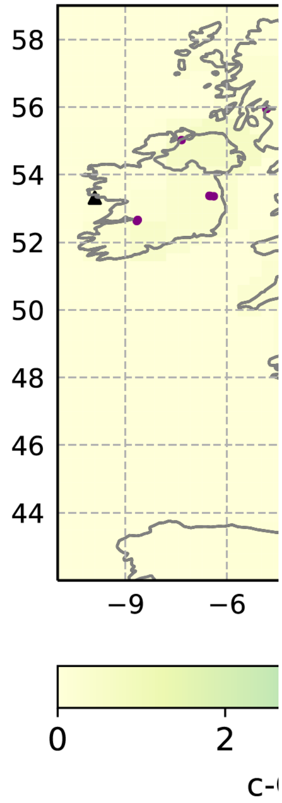

Deleted:

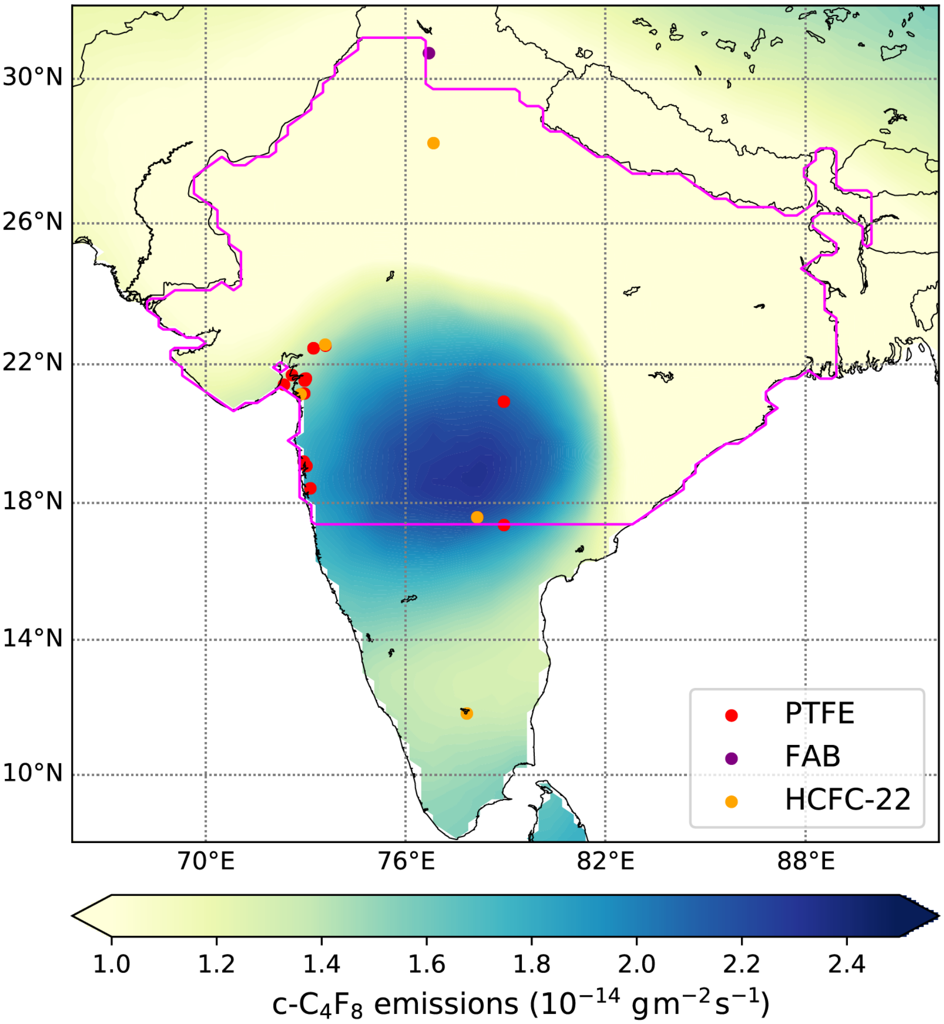

Figure 9. Mean *c*-C_4F_8 emission strength (shades of green and blue, 10^{-14} g m^{-2} s^{-1}) over the Indian subcontinent for June and July 2016 determined by the NAME-HB inversion based on air samples taken on-board UK's FAAM (Facility for Airborne Atmospheric Measurements) BAe-146 research aircraft. Also shown are the locations of one semiconductor fabrication plant (FAB, purple dot) and several potential TFE/HFP/PTFE/FEP production facilities (PTFE, red dots, Solvay/CYTEC, Hindustan Fluorocarbons, and Gujarat Fluorochemicals facilities) as potential *c*-C_4F_8 sources. HCFC-22 (orange dots) production facilities are also shown as the TFE and HFP monomers needed to produce PTFE and FEP fluoropolymers are produced via pyrolysis of HCFC-22 and *c*-C_4F_8 is an intermediate/by-product in this process. The outline of the Northern and Central India (NCI) model domain is shown as a pink line.

Perfluorocyclobutane (PFC-318, *c*-C_4F_8) in the global atmosphere

Mühle et al., acp-2019-267

Supplemental text, figures, and tables

AGAGE in situ data are available at

http://agage.mit.edu/data

http://cdiac.ess-dive.lbl.gov/ndps/alegage.html

CSIRO and Bristol inversion results, firn data, etc. are given in

Muhle et al. c-C4F8 acp-2019-267 Supplemental tables.xlsx

Details on data quality assurance for the measurements of archived air samples of the extra-tropical Southern Hemisphere (SH, Cape Grim Air Archive, CGAA) and extra-tropical Northern Hemisphere (NH)

To reconstruct the atmospheric history of *c*-C_4F_8 in the extra-tropical SH, 41 unique CGAA samples (collected 1978–2009, Langenfelds et al., 2014) were measured at CSIRO in 2011 (Ivy et al., 2012). Three CGAA tanks were measured at the beginning, in the middle, and towards the end of the measurements at CSIRO, with agreements within typical precisions or better (0.01–0.02 ppt). In addition, 8 SH samples were measured at SIO which were sub-sampled from CGAA parent tanks (fill dates 1986–2008, 0.60–1.17 ppt) into evacuated stainless steel (SS) tanks (4.5 L, Essex Industries, USA) with a vacuum manifold and pressure regulator shown not to produce any *c*-C_4F_8 artefacts. They were measured at SIO on Medusa 7 to take advantage of the more sensitive MSD and to evaluate the agreement with Medusa 9 measurements at CSIRO. Four of these CGAA subsamples measured at SIO agreed within precisions (delta mole fractions, Δx = 0.00–0.01 ppt, ratio = 1.0047, R^2 = 0.9994) with their CGAA parents measured at CSIRO, 2 subsamples showed a larger differences (0.018 and 0.027 ppt). The measurements of the seventh subsample and its CGAA parent were rejected, perhaps due to problems during the subsampling or with the parent tank. While we did not measure the CGAA parent of the eighth subsample at CSIRO, we found agreement (Δx = 0.01 ppt) with another CGAA tank of similar air age (Δt = 63 days) measured at CSIRO. Four additional SH samples (fill dates 1995–2010, 0.84–1.25 ppt) were measured at SIO. Three were also in very good agreement with CGAA samples of similar fill date measured at CSIRO ($\Delta x < 0.006$ ppt, Δt = 7–23 days) and one showed a larger difference (Δx = 0.05 ppt).

Comment [JM11]: *Rev. #1: L214-249 It is commendable that the authors have carried out these tests. However, the high number of statistical outliers is worrying and casts some doubt on the derived longterm trends, in particular the early parts. Adding uncertainty ranges to the fits based on a) the samples that were included but showed discrepancies between Medusas and b) the sparsity of the measurements, might help here. In addition, I recommend moving this rather technical paragraph to the supplement.*

MOVED FROM SECTION 2.2 following the reviewer's suggestion.

Comment [JM12]: *Rev. #1*: eigth

To reconstruct the atmospheric history in the extra-tropical NH, 126 unique air samples mostly filled at SIO and THD (1973–2016) were measured at SIO. Additionally, 3 NH samples (filled in 1980 and 1999) were measured at CSIRO. Two of these tanks measured at CSIRO were filled together at SIO in 1999 with 2 tanks measured at SIO and the agreement is excellent (Δx = <0.007 ppt). The third tank, filled in 1980 at Cape Meares, Oregon, agreed within 0.034 ppt with another NH tank (filled at SIO within 9 days) measured at SIO. Despite this larger difference, the overall good agreement of NH and SH samples measured at SIO and CSIRO shows that measurements on the involved instruments were comparable and that calibration scales were properly propagated.

Details on bottom-up emission inventories (UNFCCC, EDGAR, NIRs, WSC) for *c*-C_4F_8

Amongst the countries reporting to the United Nations Framework Convention on Climate Change (UNFCCC) (2016), a few countries report *c*-C_4F_8 emissions, most notably France, the USA, and Russia, and the global total ranges from 7 (1993) to 26 (2011) t yr^{-1} (0.007–0.026 Gg yr^{-1}, 1 t = 1 metric ton = 1 tonne = 0.001 Gg). Several countries also or exclusively report emissions of an unspecified mix of PFCs as a sum of CO_2-equivalent (CO_2-eq.) emissions (using global warming potentials, GWP), which may contain *c*-C_4F_8 emissions, most notably Japan (3,260 (2013) – 19,900 (1997) Gg CO_2-eq.), followed by much smaller amounts from France (~139 (2000) – 518 (2012) Gg CO_2-eq.) and a few other European countries.

Based on the National Inventory Report (NIR) for France, their reported emissions of unspecified mix of PFCs, all from category 2G2 (SF_6 and PFCs from other product use), does not contain any *c*-C_4F_8.

Based on the NIR for the Netherlands and Austria, category 2E1 (integrated circuit (IC) or semiconductor (SC) production) could contribute a few to a few ten t yr^{-1} of *c*-C_4F_8 per country if all emissions of unspecified mix of PFCs were *c*-C_4F_8, which is very unlikely. More likely seems that the GWP weighted mix of fugitive emissions from category 2E1 from these countries is similar to the mix for category 2E1 from European countries which report individual emissions for category 2E1. For the European Union, *c*-C_4F_8 represents ~0–8 % of the GWP weighted PFC mix (CF_4, C_2F_6, C_3F_8, *c*-C_4F_8) from 2E1. If the Netherlands and Austria emit 8 % of GWP weighted mix of PFCs in category 2E1 as *c*-C_4F_8, this would sum up to at most a few t yr^{-1}.

The United Kingdom NIR details that their unspecified PFC mix emissions are all from category 2B9 (fluorochemical production) and refers to the UK environmental agency's pollution inventory (https://data.gov.uk/dataset/pollution-inventory). Judging from this inventory and our knowledge of the listed PFC sources, they most likely do not emit any *c*-C_4F_8 and thus category 2B9 does not contain any *c*-C_4F_8 emissions for the UK.

The Japanese NIR details that their emissions of unspecified mix of PFCs stems from categories 2B9, 2E (SC, liquid crystals, and photovoltaic production), and 2F5 (solvents use). For Japan, category 2F5 is comprised of C_5F_{14} and C_6F_{16} emissions, but no *c*-C_4F_8. *c*-C_4F_8 emissions from category 2E can be estimated using purchased amounts of *c*-C_4F_8 from the NIR and IPCC emission estimation methods (IPCC, 2006) and are likely at most a few t yr^{-1}. If all of Japan's emissions from category 2B9 (fugitive emissions from fluorochemical production) were *c*-C_4F_8, this could equate to several tens to two hundred t yr^{-1}. However, more likely is that the PFC emissions from category 2B9 are due to fugitive emissions from PFC production in Japan, and that their mix is similar to the PFC mix used in Japan for the electronics industries (2E) of CF_4, C_2F_6, C_3F_8, and *c*-C_4F_8. As detailed in the NIR, *c*-C_4F_8 used in category 2E represents 0–7 % of the total PFC mix (CO_2-eq.), which would equate to a few t yr^{-1} from category 2B9. The Netherlands also lists unspecified PFC mix emissions from category 2B9. If we assume a similar mix as for Japan, this would contribute less than 0.6 t yr^{-1} of *c*-C_4F_8.

Two countries report emissions of an unspecified mix of HFCs and PFCs and other fluorinated compounds to the UNFCCC, the United States of America (293 (1990) – 9449 (2014) Gg CO_2-eq.) and Germany (152 (2014) – 5773 (1995) Gg CO_2-eq.). The German NIR details that their emissions of unspecified mix of PFCs and HFCs and other fluorinated compounds is comprised of various HFCs, hydrofluoroethers (HFE), C_3F_8, higher PFCs, perfluorinated polyether (PFPE), anesthetics, and SF_6 from categories 2B9 and 2H3 (Others), but not c-C_4F_8.

The US reports c-C_4F_8 emissions of a few t yr^{-1} from category 2E1 (IC or SC production). The NIR details that the US emissions of unspecified mix of PFCs and HFCs and other fluorinated compounds stems from category 2F6 (product uses as substitutes of ozone depleting substances (ODSs), other applications). From the description of category 2F and subcategory 2F6 it seems likely that c-C_4F_8 is at most a minor component of category 2F6 which is comprised of various HFCs, HFOs, C_4F_{10}, and a diverse collection of PFCs and PFPEs employed for solvent applications. Based on this one may conclude that no additional c-C_4F_8 emissions occur. However, data from the US EPA (https://www.epa.gov/sites/production/files/2018-10/ghgrp_i_freq_request_data_8_19_2018.xlsx, accessed Jan 2019) details that c-C_4F_8 emissions from three fluorochemical production facilities in the eastern US ranged from 29 to 62 t yr^{-1} from 2011 to 2017. At least two of these facilities are known to produce TFE, HFP, and/or PTFE and it is likely that these facilities use the process via pyrolysis of HCFC-22, with c-C_4F_8 as an intermediate/by-product, which probably is the source of these reported emissions. These c-C_4F_8 emissions, which are ~8 times larger than the emissions listed c-C_4F_8 emissions from category 2E, are currently not reported in category 2B9 (fluorochemical production). The US EPA intends to report these emissions once emissions for the years 1990 to 2010 have been estimated (currently only data from 2011 onward exists) to fulfil UNFCCC reporting requirements to estimate emissions for each year since 1990 (US EPA, personal communication). It is unclear if these c-C_4F_8 emissions are currently reported in the unspecified mix of PFCs and HFCs and other fluorinated compounds.

In summary, data submitted to UNFCCC probably represent 10–30 t yr^{-1} (0.01–0.03 Gg yr^{-1}) of c-C_4F_8 emissions, with 25–30 t yr^{-1} (0.025–0.030 Gg yr^{-1}) from 2011 to 2014. After adding the US emissions from fluorochemical production listed by the US EPA, this increases substantially to 50–83 t yr^{-1} (0.05–0.083 Gg yr^{-1}) from 2011 to 2014. It seems that large uncertainties remain due to difficulties disentangling the emissions of unspecified mixes of PFCs and mixes of HFCs/PFCs/other fluorinated compounds and perhaps unquantified or unaccounted for emissions.

The Emissions Database for Global Atmospheric Research (EDGAR) aims to estimate global emissions, including from countries not reporting to the UNFCCC, most notably China, South Korea, and Taiwan which may have significant c-C_4F_8 emissions from their electronics and PTFE industries. EDGAR v4.2 (EDGAR, 2010) estimates global c-C_4F_8 emission from three sources (SC production, solvent use, fire extinguisher use), but only until 2010. From 1970 to 1985, EDGAR reports no c-C_4F_8 emissions, followed by a rise to a few t yr^{-1} in the early 1990s and to ~25 t yr^{-1} (~0.025 Gg yr^{-1}) in 2008, followed by a decline to ~20 t yr^{-1} (0.02 Gg yr^{-1}) in 2010.

For Japan, c-C_4F_8 emissions reported by EDGAR are broadly consistent with those calculated from the UNFCCC NIR (see above) from the electronics industry alone (category 2E, assuming an increasing fraction of abatement from 2005 forward); therefore the potential emissions from category 2B9 (fugitive emissions from fluorochemical production) estimated above do not seem to be included in EDGAR.

For South Korea a NIR with data until 2013 can also be obtained (http://www.gir.go.kr/eng/). EDGAR c-C_4F_8 emission estimates are broadly consistent with those estimated from the South Korean NIR using IPCC methodologies for the electronics industries (category 2E), a few t yr^{-1} until 2010.

For Taiwan we received c-C_4F_8 emissions from their NIR (Chang-Feng Ou-Yang, personal communications). Emissions reported by EDGAR are consistently lower than given in the NIR, at most a t yr^{-1} versus a few t yr^{-1} (since

2001) to ~20 t yr^{-1} (2014). The Taiwanese NIR only includes emissions from SC, IC, and memory production, potentially excluding other emission sources, such as from LCD/TFT production. For China, Malaysia, and Singapore, EDGAR lists only very small emissions of less than a t yr^{-1}. Particularly for China this seems unlikely due to its large electronics and PTFE industries, potential c-C_4F_8 sources.

The World Semiconductor Council (WSC) estimates PFC emissions from their member industries in China, Taiwan, Europe, Japan, South Korea, United States, which range from 14 t yr^{-1} in 2012 to 24 t yr^{-1} in 2016.

Based on the available information discussed above we constructed a bottom-up inventory. First, we added for each year and each country emissions reported to UNFCCC and the estimated portion from unspecified mix of PFCs. For 2011 to 2014 we also added the U.S. emissions from fluorocarbon production reported by US EPA. Then we calculated the maximum for each year and each country from these augmented UNFCCC data, US EPA, EDGAR, and estimates from the NIRs, as detailed above. Globally these add up to 10–30 t yr^{-1} (0.01–0.03 Gg yr^{-1}) from 1990 to 1999, 30–40 t yr^{-1} (0.03–0.04 Gg yr^{-1}) from 2000 to 2010, and 100–116 t yr^{-1} (~0.1 Gg yr^{-1}) from 2011 to 2014 (with a substantial fraction due to the U.S. emissions from fluorocarbon production reported by US EPA). WSC emissions discussed above corresponds to ~16 % of these global emissions for the years 2012 to 2014.

Details on the tuning of the CSIRO firn model for the Summit13 site

We use firn air data for 11 tracers from the Summit13, Greenland site (CO_2, CH_4, N_2O, SF_6, CFC-11, CFC-12, CFC-113, CH_3CCl_3, HFC-134a, HCFC-141b, and HCFC-142b), to calibrate the diffusivity-depth profile and other diffusivity-related parameters in the CSIRO firn model using established methods. The firn model includes molecular diffusion throughout the firn (Schwander et al., 1993), and dispersion in the lock-in zone (Buizert and Severinghaus, 2016). The model gives the best match to observations with dispersion in the lock-in zone peaking at around 0.1 m^2 yr^{-1}, consistent with Buizert et al. (2013) and Buizert and Severinghaus (2016), although there were also cases within the 68 % confidence interval that had no lock-in zone dispersion. We tested the use of eddy diffusion for convective mixing near the surface, but the best fit to observations was obtained without is, so it was not used in the final calibration. A melt layer was observed at Summit, due to melting that occurred in July 2012. The melt layer corresponds to a depth of around 60 cm but there were extensive percolated melt features down to around 1.5 m. The melt layer was included in the CSIRO firn model as described in Trudinger et al. (2013). Model layers in the CSIRO firn model move with the ice, and the timing of model layer generation at the surface was chosen so that the influence of the melt layer began in July 2012, and extended down to a model layer boundary that reached around 1.4 m at the time of firn sampling. The model produced the best fit to observations with reduction of diffusion by the melt layer of around 90 % (this value depends on the location of the model layers with time). We generated an ensemble of diffusivity parameters corresponding to a 68 % confidence interval as described in Trudinger et al. (2013), to use this to incorporate firn model uncertainty into the inversion.

Figure S1 shows the optimized diffusivity-depth profile and the modelled depth profiles for the calibration tracers. The atmospheric histories used to force the firn model were those compiled in Buizert et al. (2012) (based on Martinerie et al., 2009) for most tracers for calibration of firn models for the NEEM site, with extension to 2013 using in situ measurements from either Summit in the NOAA network (for CO_2 and CH_4) or Mace Head in the AGAGE network, with correction between the calibration scales used by NOAA and AGAGE where required. For

Deleted: ¶
¶
¶
¶
¶
¶
¶
¶

Deleted: ¶
¶
¶
Supplemental figures¶

Comment [JM13]: *Rev. #1: Figure S1 The caption is actually an entire section and should perhaps have its own heading.*

Deleted: Figure S1. Tuning of the CSIRO firn model for the Summit13 site: CO_2 diffusivity on linear and log scales, and concentration profiles of CO_2, CH_4, N_2O, SF_6, CFC-11, CFC-12, CFC-113, CH_3CCl_3, HFC-134a, HCFC-141b, and HCFC-142b, as well as the $\delta^{15}N_2$ profile. The solid black lines show the case with the closest match to all observations used for diffusivity calibration. The dotted black lines show the upper and lower ranges of all cases that correspond approximately to a 68 % confidence interval. The blue curves show some representative cases within the 68 % confidence interval that are used in the CSIRO inversion to incorporate firn model uncertainty. In a) and b), the black and blue lines show molecular diffusivity, while in b), the red lines show dispersion in the lock-in zone (the red solid line is our best case, red dot

N_2O, we used the NOAA record at Summit, extended prior to 1998 based on the Law Dome (SH) ice core record (Rubino et al., 2019) and the reconstruction by Prokopiou et al. (2017). For HCFC-141b and HCFC-142b, we compiled atmospheric histories using measurements from Mace Head from late 1994, and extrapolated back to zero before this. Due to the lack of information on atmospheric histories of these HCFCs before 1994, the deepest few measurements of these tracers were not used for calibration (indicated by the grey symbols in Fig. S1). We used larger uncertainties for N_2O measurements prior to the in situ record due to the higher uncertainty in the atmospheric record. We excluded the deep CO_2 measurements from calibration, because at another NH site, NEEM, all models in the firn model intercomparison by Buizert et al., 2012 significantly underestimated CO_2 in the deep firn; the reason for this is not currently understood but could be due to in situ production or fractionation as discussed by Buizert et al. $\delta^{15}N_2$ is shown in Figure S1 but was not used for calibration because it is very sensitive to thermal effects at Summit that are not included in the firn model and not important for *c*-$C_4F_{8.}$

Buizert, C., Martinerie, P., Petrenko, V. V., Severinghaus, J. P., Trudinger, C. M., Witrant, E., Rosen, J. L., Orsi, A. J., Rubino, M., Etheridge, D. M., Steele, L. P., Hogan, C., Laube, J. C., Sturges, W. T., Levchenko, V. A., Smith, A. M., Levin, I., Conway, T. J., Dlugokencky, E. J., Lang, P. M., Kawamura, K., Jenk, T. M., White, J. W. C., Sowers, T., Schwander, J., and Blunier, T.: Gas transport in firn: multiple-tracer characterisation and model intercomparison for NEEM, Northern Greenland, Atmos. Chem. Phys., 12, 9, 4259-4277, 10.5194/acp-12-4259-2012, 2012.

Buizert, C., Sowers, T., and Blunier, T.: Assessment of diffusive isotopic fractionation in polar firn, and application to ice core trace gas records, Earth Planet. Sci. Lett., 361, 110-119, 10.1016/j.epsl.2012.11.039, 2013.

Buizert, C., and Severinghaus, J. P.: Dispersion in deep polar firn driven by synoptic-scale surface pressure variability, The Cryosphere, 10, 5, 2099-2111, 10.5194/tc-10-2099-2016, 2016.

Martinerie, P., Nourtier-Mazauric, E., Barnola, J.-M., Sturges, W. T., Worton, D. R., Atlas, E., Gohar, L. K., Shine, K. P., and Brasseur, G. P.: Long-lived halocarbon trends and budgets from atmospheric chemistry modelling constrained with measurements in polar firn, Atmos. Chem. Phys., 9, 12, 3911-3934, DOI 10.5194/acp-9-3911-2009, 2009.

Prokopiou, M., Martinerie, P., Sapart, C. J., Witrant, E., Monteil, G., Ishijima, K., Bernard, S., Kaiser, J., Levin, I., Blunier, T., Etheridge, D., Dlugokencky, E., van de Wal, R. S. W., and Röckmann, T.: Constraining N2O emissions since 1940 using firn air isotope measurements in both hemispheres, Atmos. Chem. Phys., 17, 7, 4539-4564, 10.5194/acp-17-4539-2017, 2017.

Rubino, M., Etheridge, D. M., Thornton, D. P., Howden, R., Allison, C. E., Francey, R. J., Langenfelds, R. L., Steele, P. L., Trudinger, C. M., Spencer, D. A., Curran, M. A. J., Van Ommen, T. D., and Smith, A. M.: Revised records of atmospheric trace gases CO_2, CH_4, N_2O and $\delta^{13}CO_2$ over the last 2000 years from Law Dome, Antarctica, Earth Syst. Sci. Data Discuss., 2018, 1-30, 10.5194/essd-2018-146, 2018.

Schwander, J., Barnola, J. M., Andrie, C., Leuenberger, M., Ludin, A., Raynaud, D., and Stauffer, B.: The Age of the Air in the Firn and the Ice at Summit, Greenland, J. Geophys. Res., 98, D2, 2831-2838, 1993.

Trudinger, C. M., Enting, I. G., Rayner, P. J., Etheridge, D. M., Buizert, C., Rubino, M., Krummel, P. B., and Blunier, T.: How well do different tracers constrain the firn diffusivity profile?, Atmos. Chem. Phys., 13, 3, 1485-1510, 10.5194/acp-13-1485-2013, 2013.

Details on the production of HFO-1234yf from HCFC-22 with potential *c*-C_4F_8 by-product emissions

The hydrofluoroolefin HFO-1234yf ($CF_3CF=CH_2$) is a fourth generation refrigerant replacing HFC-134a in mobile air conditioning (MAC) (Vollmer et al., 2015). It can be produced starting out with similar chemistry that is used for the production of PTFE/FEP, that is the pyrolysis of HCFC-22 to TFE and HFP (Lim et al., 2017), with *c*-C_4F_8 as a by-product that may be vented to the atmosphere. Even though this route to produce HFO-1234yf is not continuous, requiring several batch operations, it is the preferred route in China and India due to the existing large scale HCFC-22, TFE, and HFP production capacities. Honeywell has licensed Navin Fluorine International (NFIL, Surat, Gujarat, India) in 2016 to produce HFO-1234yf (www.coolingpost.com/world-news/honeywell-licences-r1234yf-production-in-india, accessed 2019/07/01). This facility is one of the PTFE producing facilities shown in Fig. 9 in Western India. Honeywell has also licensed the Juhua Group Corporation in China in 2016 to produce HFO-1234yf (www.springerprofessional.de/betriebsstoffe/honeywell-laesst-1234yf-auch-in-china-produzieren/10062482, accessed 2019/07/01, German, translate.google.com). The likely location of this HFC-1234yf production in China corresponds to one or both of to the two Juhua Group Corporation PTFE production facility shown in Fig. 7 in Zhejiang province. Other facilities licensed by Honeywell to produce HFO-1234yf using this route with potential *c*-C_4F_8 emissions may exist in East Asia, but any such production is relatively recent and cannot explain historic *c*-C_4F_8 emissions.

Lim, S., Kim, M. S., Choi, J.-W., Kim, H., Ahn, B. S., Lee, S. D., Lee, H., Kim, C. S., Suh, D. J., Ha, J.-M., and Song, K. H.: Catalytic dehydrofluorination of 1,1,1,2,3-pentafluoropropane (HFC-245eb) to 2,3,3,3-tetrafluoropropene (HFO-1234yf) using in-situ fluorinated chromium oxyfluoride catalyst, Catalysis Today, 293-294, 42-48, 10.1016/j.cattod.2016.11.017, 2017.

Vollmer, M. K., Reimann, S., Hill, M., and Brunner, D.: First Observations of the Fourth Generation Synthetic Halocarbons HFC-1234yf, HFC-1234ze(E), and HCFC-1233zd(E) in the Atmosphere, Environ. Sci. Technol., 49, 5, 2703-2708, 10.1021/es505123x, 2015.

Supplemental Figures

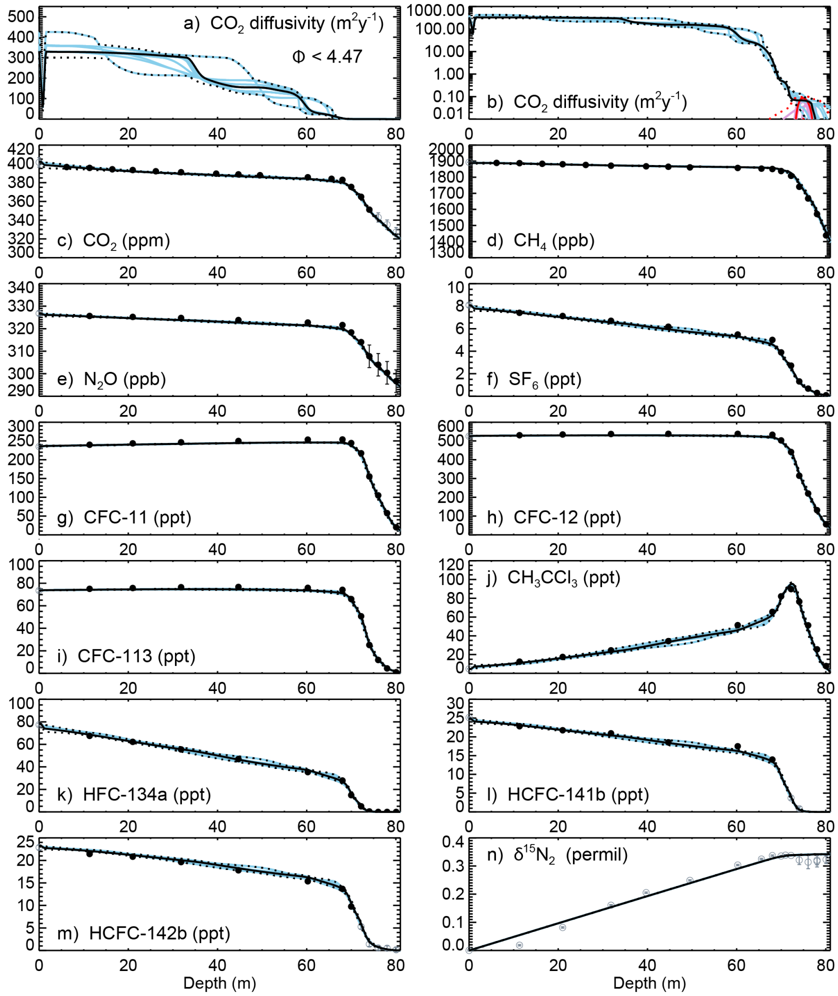

Figure S1. Tuning of the CSIRO firn model for the Summit13 site: CO_2 diffusivity on linear and log scales, and concentration profiles of CO_2, CH_4, N_2O, SF_6, CFC-11, CFC-12, CFC-113, CH_3CCl_3, HFC-134a, HCFC-141b, and HCFC-142b, as well as the $\delta^{15}N_2$ profile. The solid black lines show the case with the closest match to all observations used for diffusivity calibration. The dotted black lines show the upper and lower ranges of all cases that correspond approximately to a 68 % confidence interval. The blue curves show some representative cases within the 68 % confidence interval that are used in the CSIRO inversion to incorporate firn model uncertainty. In a) and b), the black and blue lines show molecular diffusivity, while in b), the red lines show dispersion in the lock-in zone (the red solid line is our best case, red dotted lines correspond to the 68 % confidence interval, and the pink lines show some representative cases). Measurements shown by black circles were used for calibration, and measurements shown by the grey circles were not used (see text).

Comment [JM14]: *Rev. #1: Figure S1 The caption is actually an entire section and should perhaps have its own heading.*

Moved here to clarify which part of the text is the caption.

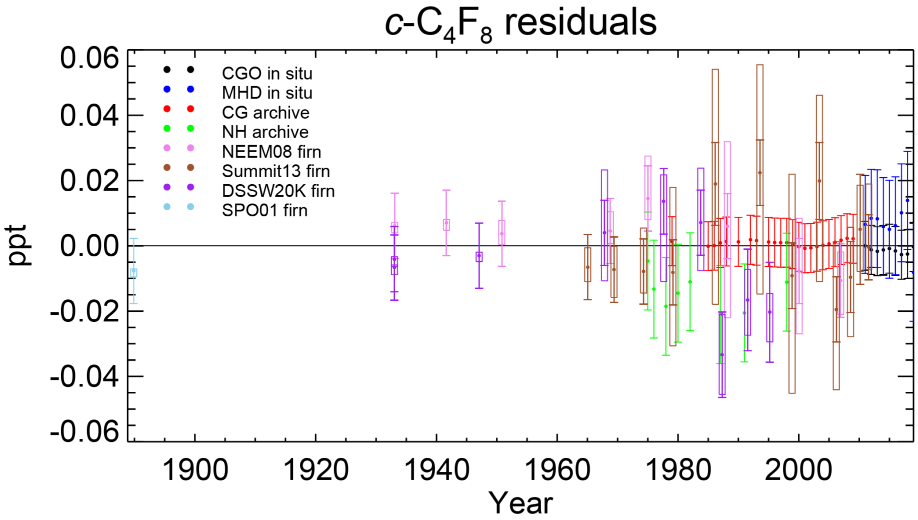

Figure S2. Residuals (model - observations) for the CSIRO inversion based on firn data and annual values from the smoothing spline in each hemisphere to in situ and archive data. The error bars show measurement errors used in the inversion (for the annual values this is the magnitude of correlated errors and for the firn data these are the measurement errors with a lower threshold of 0.01 ppt). The boxes show the range of uncertainties derived from the ensemble of Green's functions from the firn model.

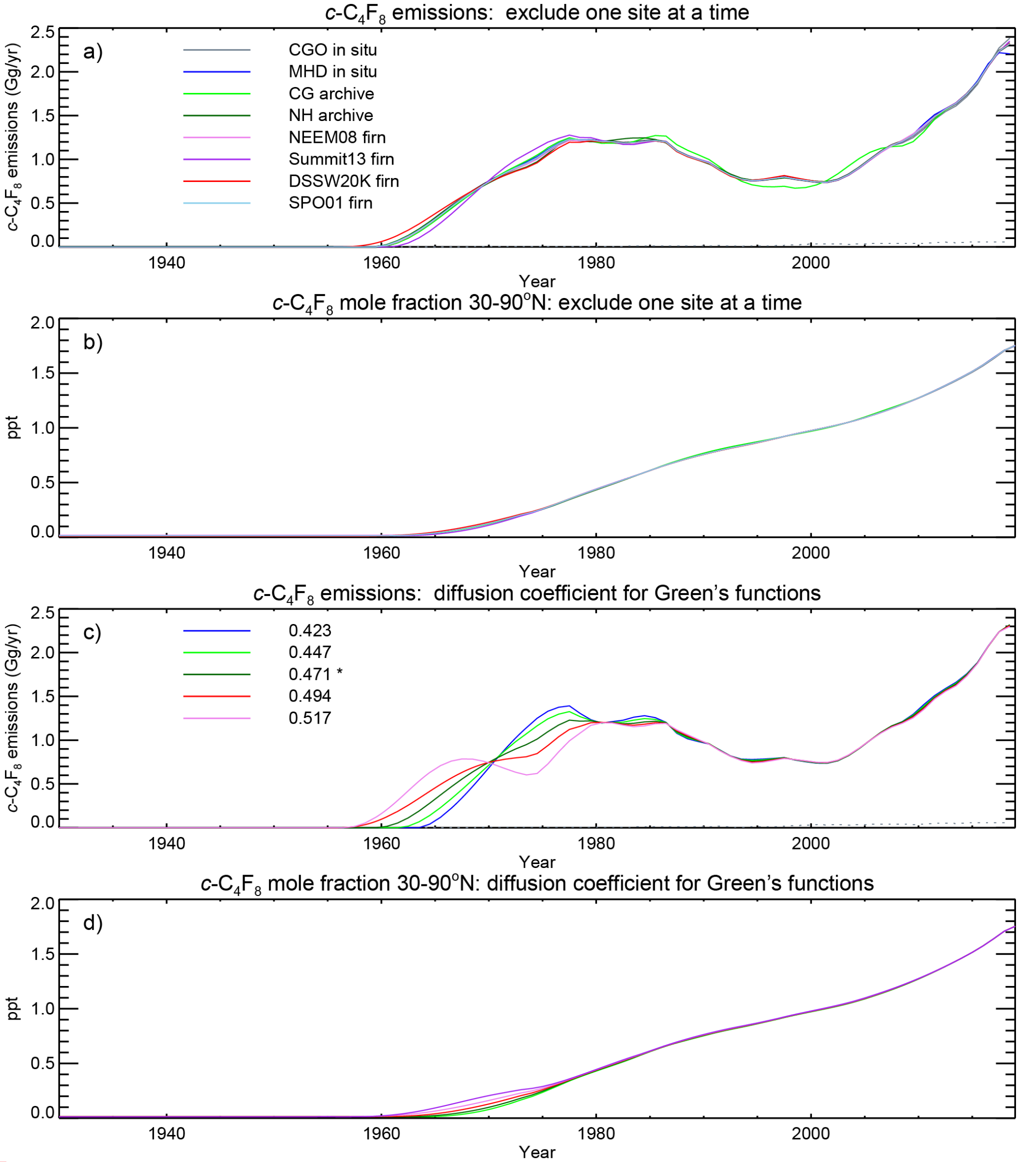

Figure S3. Sensitivity tests with the CSIRO inversion for removal of individual data subsets and uncertainty in the diffusion coefficient: a) inferred emissions with one firn site or in situ or archive part of the atmospheric record in each hemisphere left out at a time; b) same as a but inferred mixing ratios; c) inferred emissions for different values of the diffusion coefficient of c-C_4F_8 relative to CO_2, with values from -10 % to +10 %; d) same as c but inferred mixing ratios.

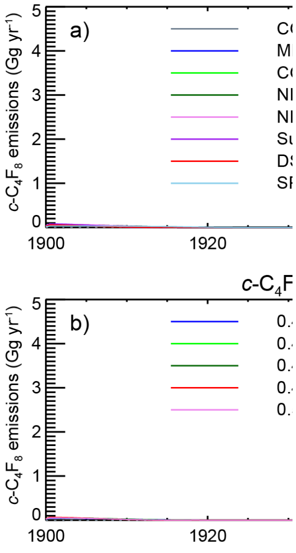

Deleted:

Comment [JM15]: *Rev. #1: Figure S3 There is quite some uncertainty in the 1960s and 70s. Has this been reflected in the emission uncertainties?*

Deleted: for

Deleted: towards

Deleted: variation of

Deleted: b

Deleted: ¶
¶
¶
¶
¶
¶
¶
¶
¶
¶
¶
¶
¶
¶
¶

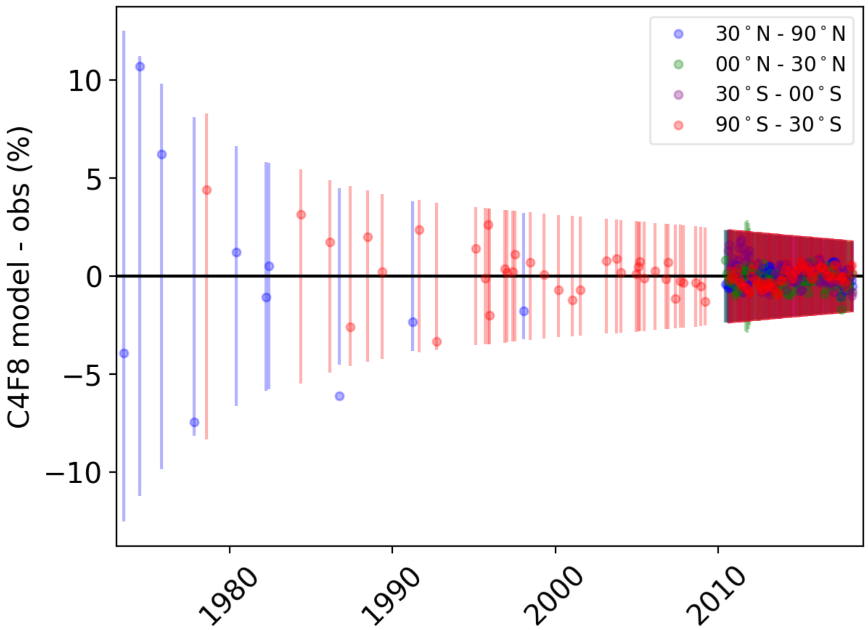

Figure S4. Residuals (model - observations) for the Bristol inversion based on archive and in situ data.

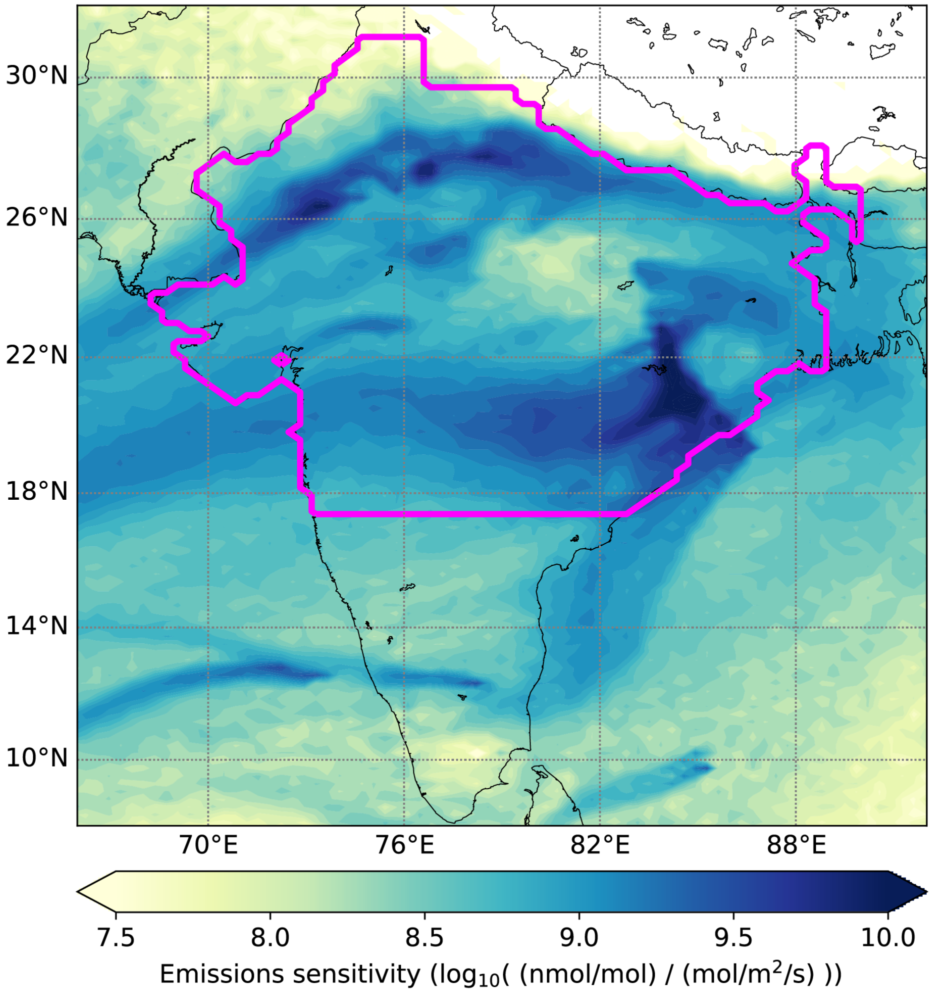

Figure S5 Emissions sensitivity averaged across all measurements made over the Indian subcontinent in June and July 2016. The region roughly corresponding to a maximum in emissions sensitivity is enclosed by the pink line. We denote this region as Northern and Central India (NCI).

Deleted: :

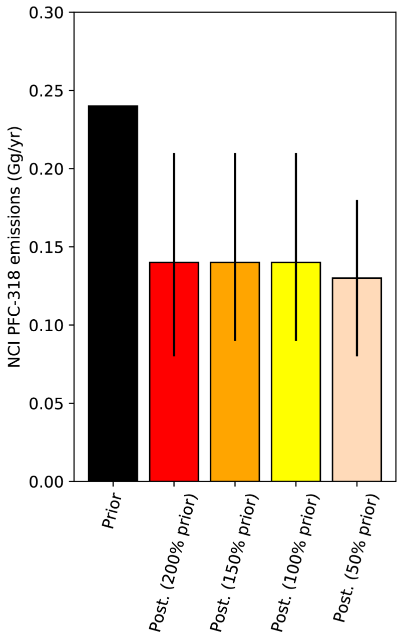

Figure S6 Sensitivity tests for the NAME-HB inversion for the Indian subcontinent. Emissions derived from priors of varying magnitudes (200% of the original prior, red bar, 150% of the original prior, orange bar, and 50% of the original prior, peach bar) indicate that *c*-C_4F_8 emissions determined for Northern and Central India are very insensitive to the choice of prior. The original prior (black bar) and posterior (yellow bar) estimates are also shown. For each estimate, error bars represent the 95% confidence interval of the posterior probability density function.

Deleted: :

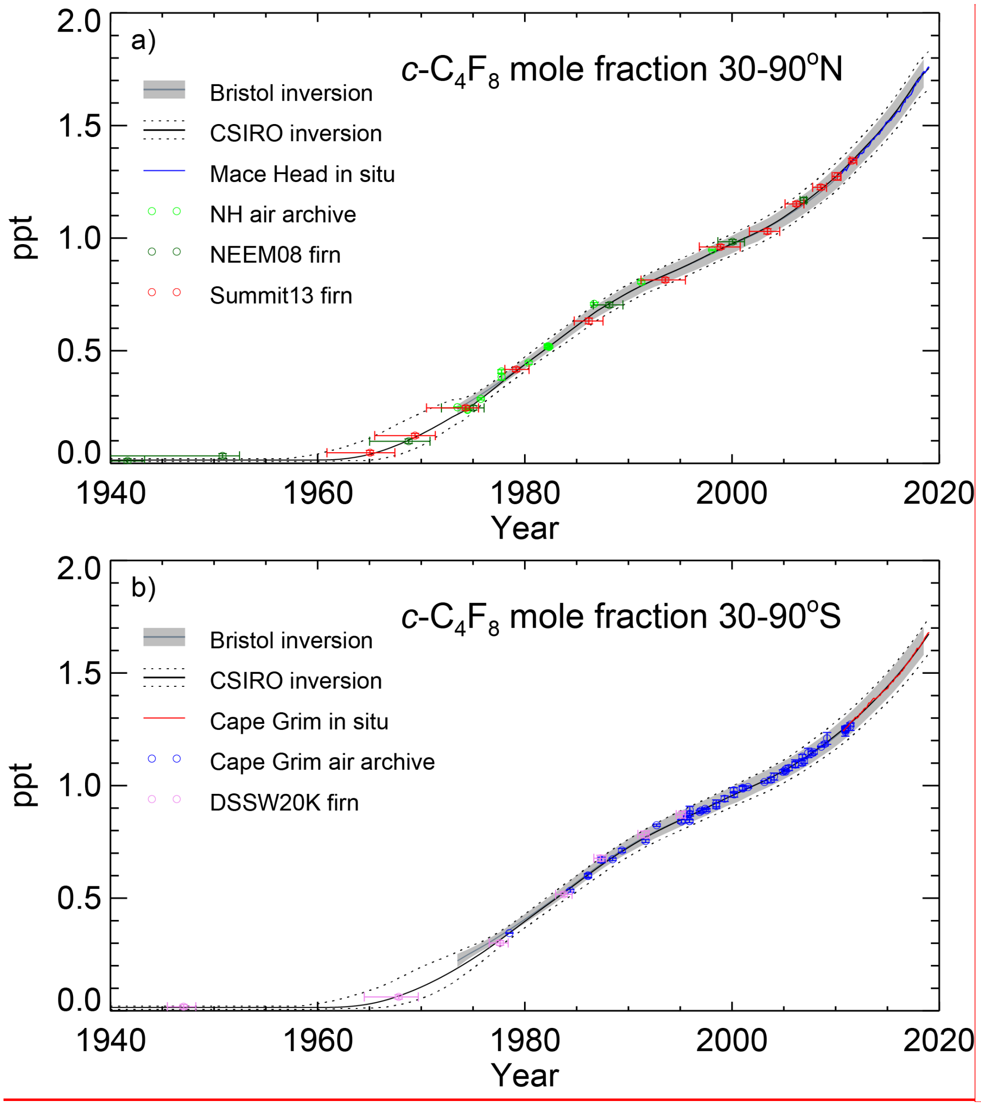

Figure S7. c-C_4F_8 extra-tropical mole fractions (ppt) reconstructed by the UB (grey line) and CSIRO (black line) inversions are shown with 2σ uncertainty bands (grey band and black dotted line, respectively) and the underlying in situ (pollution removed monthly means), archive, and firn air data: a) for 30-90°N MHD in situ (blue line), NH archive (light green circles), and the NH firn sites NEEM08 (dark green circles) and Summit13 (red circles); (b) for 30-90°S CGO in situ (red line), the Cape Grim air archive (CGAA, blue circles), and the SH firn site DSSW20K (pink circles); Firn samples are plotted against mean ages (before 1965) or effective ages (after 1965) with 2σ uncertainties as horizontal error bars. Vertical error bars represent precisions for archive and firn data. Uncertainties in monthly means for in situ data have been omitted for clarity (they are shown in Fig. 1).

Comment [JM16]: New Fig. S7 to show a) a direct comparison of the reconstructed mole fractions by the two inversions and b) the uncertainties in mean and effective ages as requested by reviewer #1.

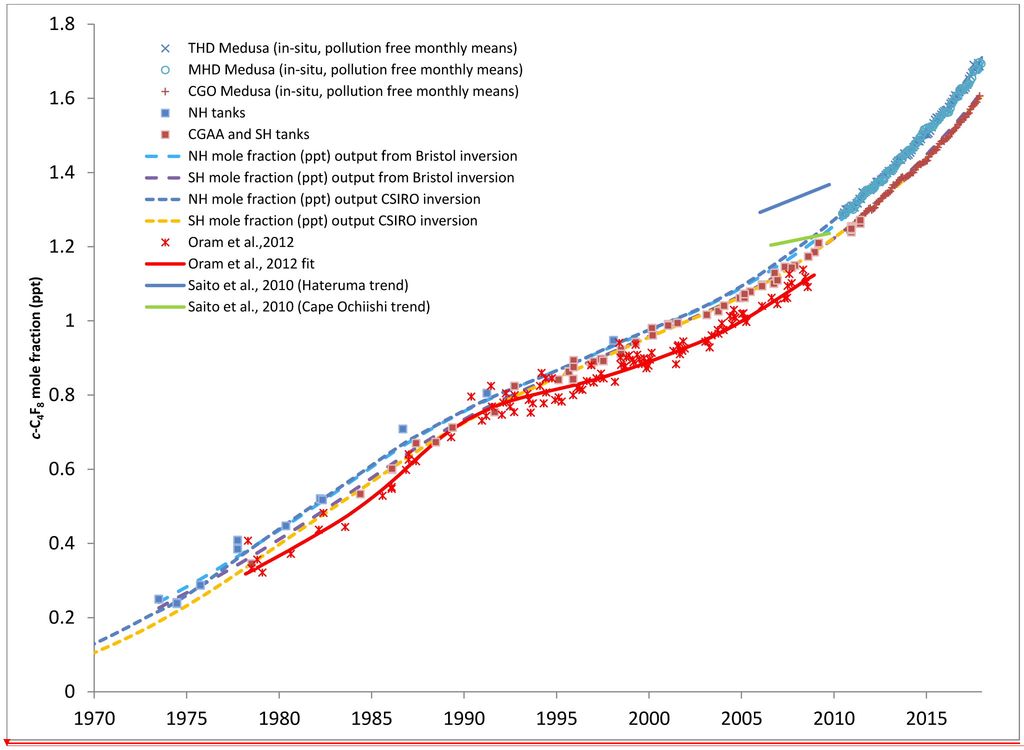

Figure S8. c-C$_4$F$_8$ mole fractions reconstructed here for the Northern (NH) and Southern Hemisphere (SH) compared to results from Oram et al., 2012 (SH only) and Saito et al., 2010. Measured c-C$_4$F$_8$ mole fractions from THD, MHD, and CGO Medusa (in situ, pollution-free monthly means, blue crosses and blue circles (NH), red pluses (SH) and NH (blue squares) and CGAA and SH tanks (red squares) are shown together with results from the Bristol (AGAGE 12-box, light blue (NH) and purple (SH) long dashes) and CSIRO (dark blue (NH) and orange (SH) short dashes) inversions. c-C$_4$F$_8$ mole fractions from Oram et al., 2012 (CGAA/SH only, red stars and red solid line) and Saito et al., 2010 (Hateruma island, blue solid line, Cape Ochiishi, green solid line, both NH) are shown for comparison.

Oram, D. E., Mani, F. S., Laube, J. C., Newland, M. J., Reeves, C. E., Sturges, W. T., Penkett, S. A., Brenninkmeijer, C. A. M., Röckmann, T., and Fraser, P. J.: Long-term tropospheric trend of octafluorocyclobutane (c-C$_4$F$_8$ or PFC-318), Atmos. Chem. Phys., 12, 1, 261-269, 10.5194/acp-12-261-2012, 2012.
Saito, T., Yokouchi, Y., Stohl, A., Taguchi, S., and Mukai, H.: Large emissions of perfluorocarbons in East Asia deduced from continuous atmospheric measurements, Environ. Sci. Technol., 44, 11, 4089-4095, 10.1021/es1001488, 2010.

Deleted: ¶

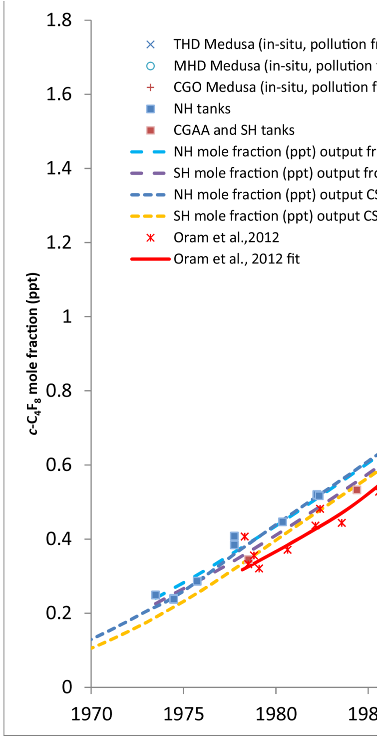

Comment [JM17]: *Rev. #1: Figure S7 Please also show the published observational data set of Saito et al.*

Deleted:

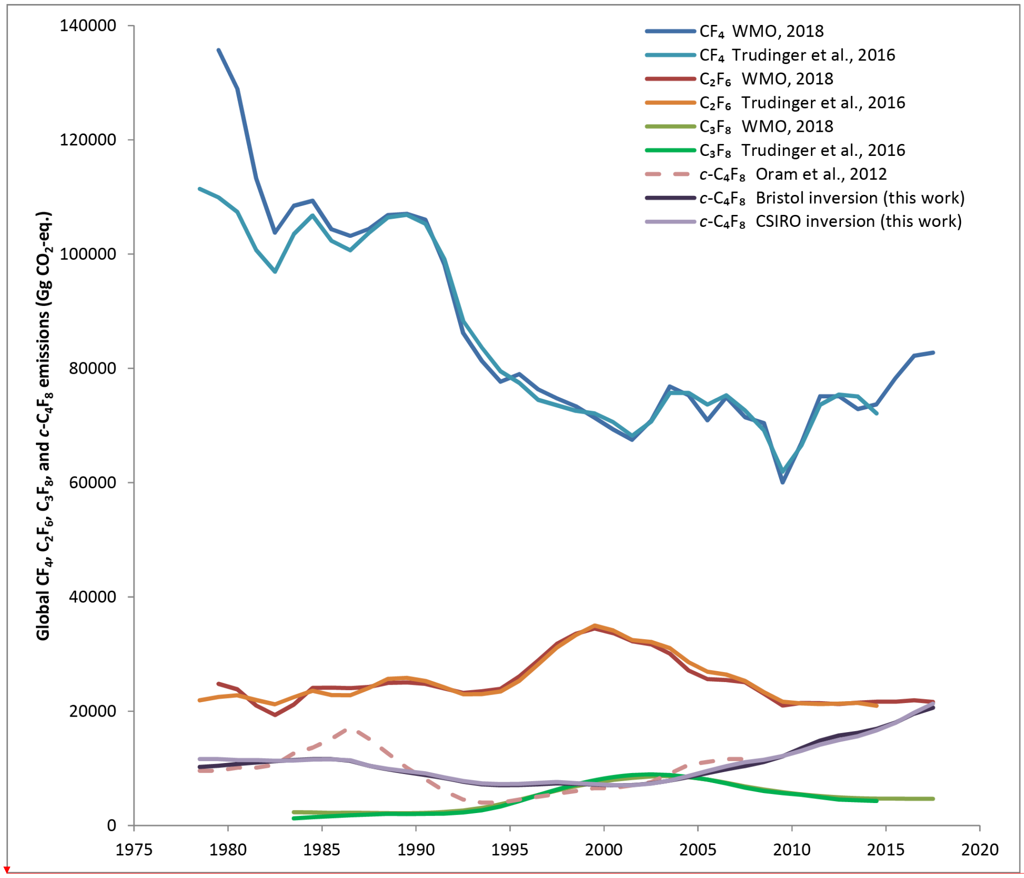

Deleted: ¶
¶
¶
¶
¶
¶

Figure S9. Global emissions of CF_4, C_2F_6, C_3F_8, and *c*-C_4F_8 expressed as carbon dioxide equivalent emissions (CO_2-eq.) emissions (using GWP_{100} of 6,630, 11,100, 8,900, and 9,540, respectively, Burkholder et al., 2018) (1.000.000 Gg CO_2-eq. = 1 billion tonnes CO_2-eq.). In 2017, *c*-C_4F_8 emissions have reached 0.021 billion tonnes of CO_2-equivalent compared to 0.083, 0.022, and 0.005 billion tonnes of CO_2-eq. for CF_4, C_2F_6, and C_3F_8.

Deleted: :

Burkholder, J. B. (Lead Author)., Hodnebrog, Ø., and Orkin, V. L. (Contributors).: Appendix A: Summary of Abundances, Lifetimes, Ozone Depletion Potentials (ODPs), Radiative Efficiencies (REs), Global Warming potentials (GWPs), and Global Temperature ChanGe Potentials (GTPs), in: Scientific Assessment of Ozone Depletion: 2018, Global Ozone Research and Monitoring Project–Report No. 58, World Meteorological Organization, Geneva, Switzerland, 2018.

Deleted: ¶

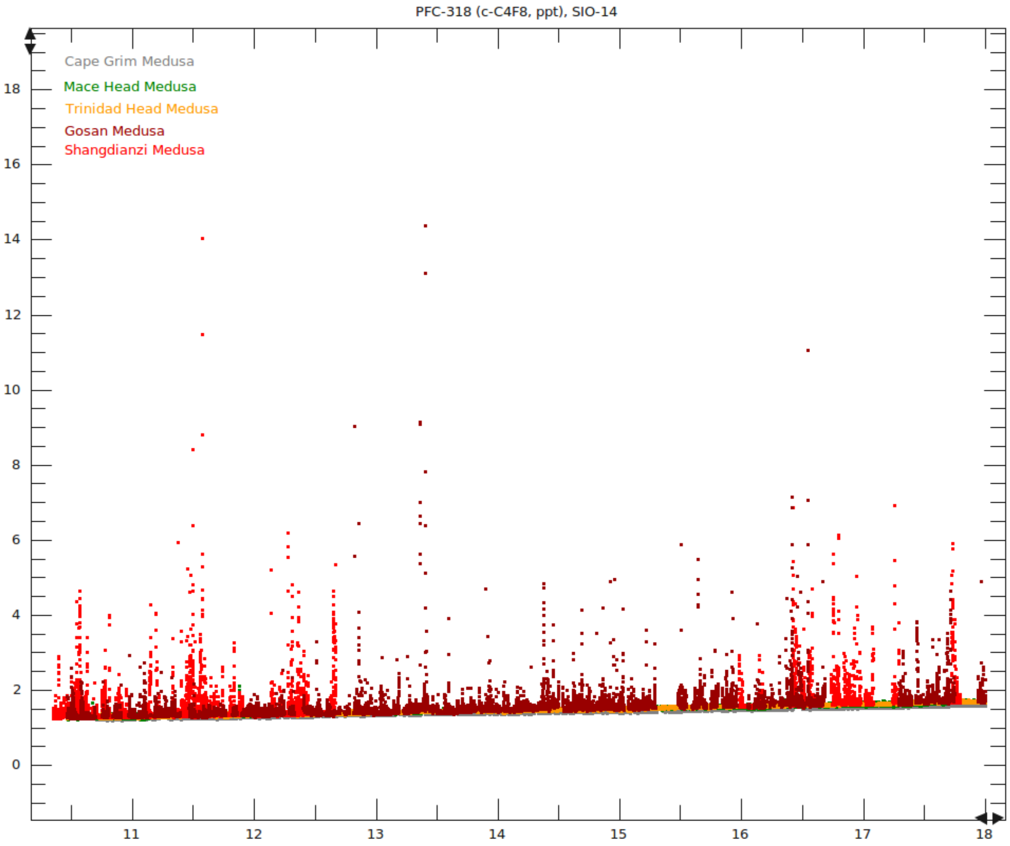

Figure S10. Magnitude of pollution events in East Asia. Among all stations of the AGAGE network, the two stations in eastern Asia, Gosan (brown) and Shangdianzi (red), show by far the most frequent and most pronounced pollution events of up to ~14 ppt above NH background (Mace Head, green, Trinidad Head, orange), indicating significant regional emissions. Measurements at Cape Grim, Australia (light grey), representing SH background, are also shown for comparison.

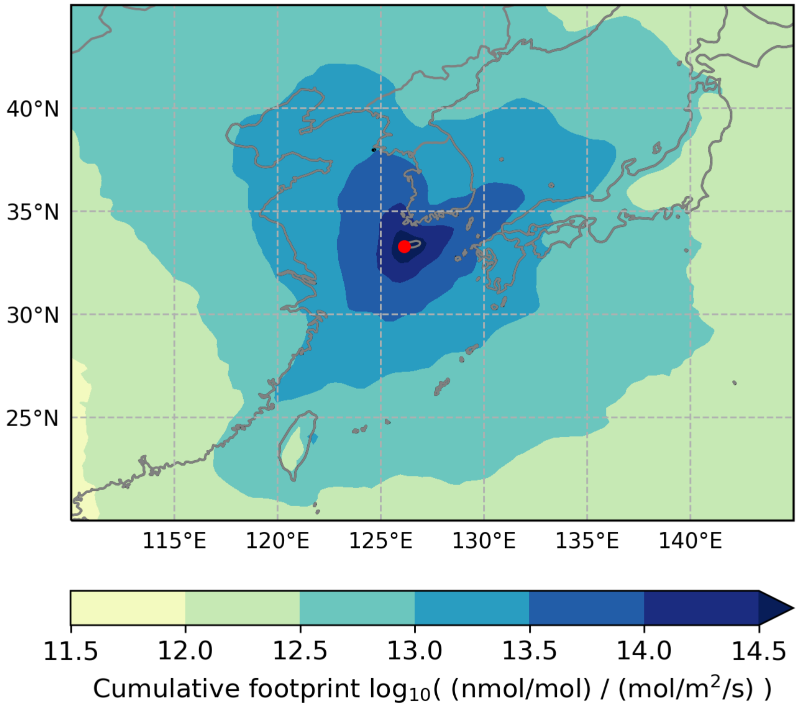

Figure S11. Cumulative footprint map for measurements at Gosan station, Jeju island, South Korea from 2010-2017 generated using the NAME transport model. The footprint indicates where the receptor station is sensitive to emissions. The sensitivity of the inversion generally decreases with distance to the receptor station resulting in relatively low sensitivity for emissions from western China, eastern Japan and Taiwan. Therefore, we report emissions for eastern China, western Japan, South Korea, North Korea, and parts of Taiwan. Eastern China contains the provinces Anhui, Beijing, Hebei, Henan, Jiangsu, Liaoning, Shandong, Shanghai, Shanxi, Tianjin and Zhejiang. Western Japan contains the prefectures Chugoku, Kansai, Shikoku and Okawa and Kyushu.

Deleted: :

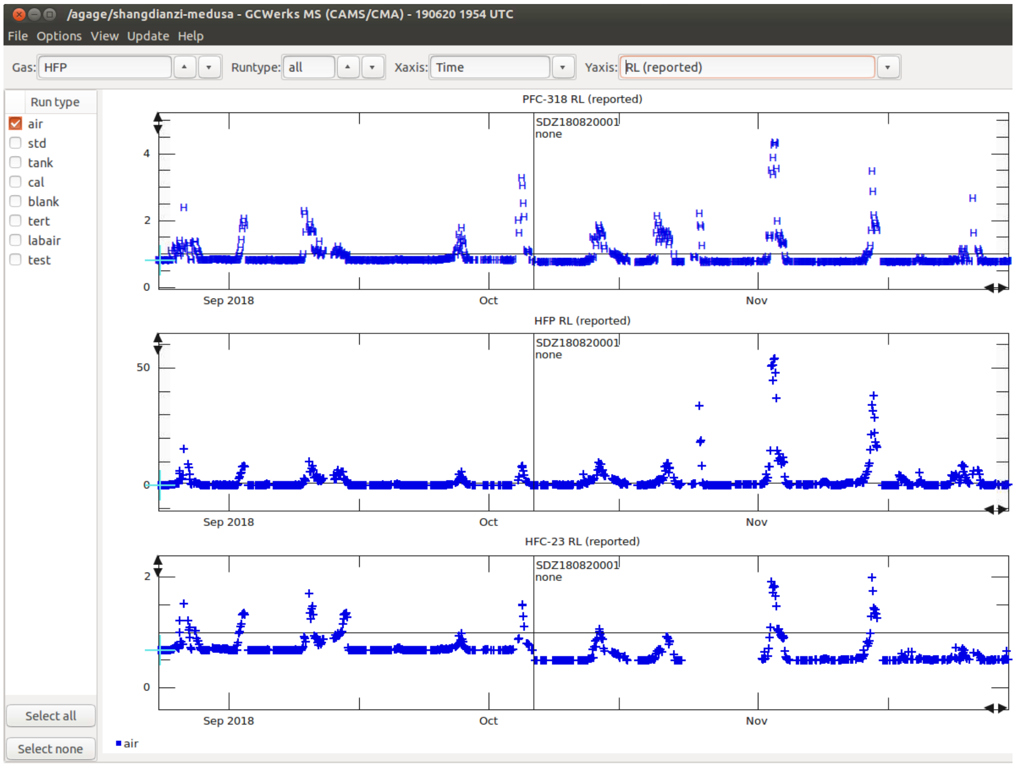

Gas: HFP
Runtype: all
Xaxis: Time
Yaxis: RL (reported)

Figure S12. Area responses of ambient air samples relative to those of the working standard (RL (reported)) for *c*-C_4F_8 (PFC-318), HFP (hexafluoropropylene), and HFC-23 measurements at SDZ.

HFP (hexafluoropropylene) is measured on m/z 131 and 150. On the Porabond Q column it elutes after HFC-125 and before CFC-115. We confirmed its identify with a spike of ~10 ppt HFP (87,422 area counts) at SIO. The working standard used at the time contained ~0.03–0.04 ppt HFP (270–380 area counts). Ambient air samples contained ~0.01 ppt HFP (98–123 area counts), just around estimated detection limit of ~0.01 ppt (3 times baseline noise). The low abundance in the working standards led to poor precisions of ~20%. From Nov. 2018 until present, ambient air at SIO typically showed 0–0.5 times (0–150 area counts) the response of the working standard used (reaching a few times to 2.5 times), indicating continuing miniscule ambient mixing ratios. HFP measurements at Aspendale (ASA) have not been calibrated, but the peak responses in ambient air from Feb. 2017 until present were almost always small (0–300 area counts), indicating similarly small ambient mixing ratios as at SIO. Occasional small pollution events have been observed at ASA, see Section 5.3.3. HFP measurements at GSN and SDZ were not calibrated, but several working standards showed significant peak responses (up to 2,500 and 4,000 area counts, respectively). From Aug. 2018 until present, HFP pollution events at SDZ always coincided with *c*-C_4F_8 and HFC-23 pollution events. Figure S12 shows examples of the good correlations observed among PFC-318 (*c*-C_4F_8), HFP, and HFC-23.

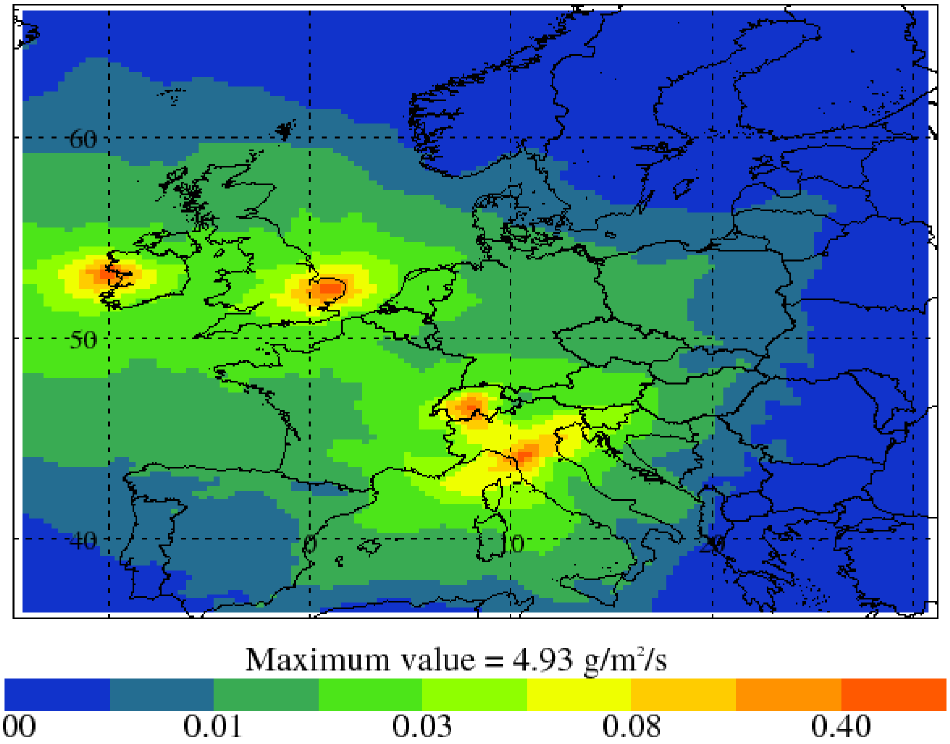

Figure S13: Cumulative footprint map for measurements at the Tacolneston, United Kingdom, Mace Head, Ireland, Jungfraujoch, Switzerland, and Monte Cimone, Italy stations for 2013. The sensitivity of the InTEM inversion is shown in arbitrary units. We report only estimated emissions from North Western Europe (42° N to 59° N and -11° E to 15° E) based on to the areas of highest sensitivity to the observations.

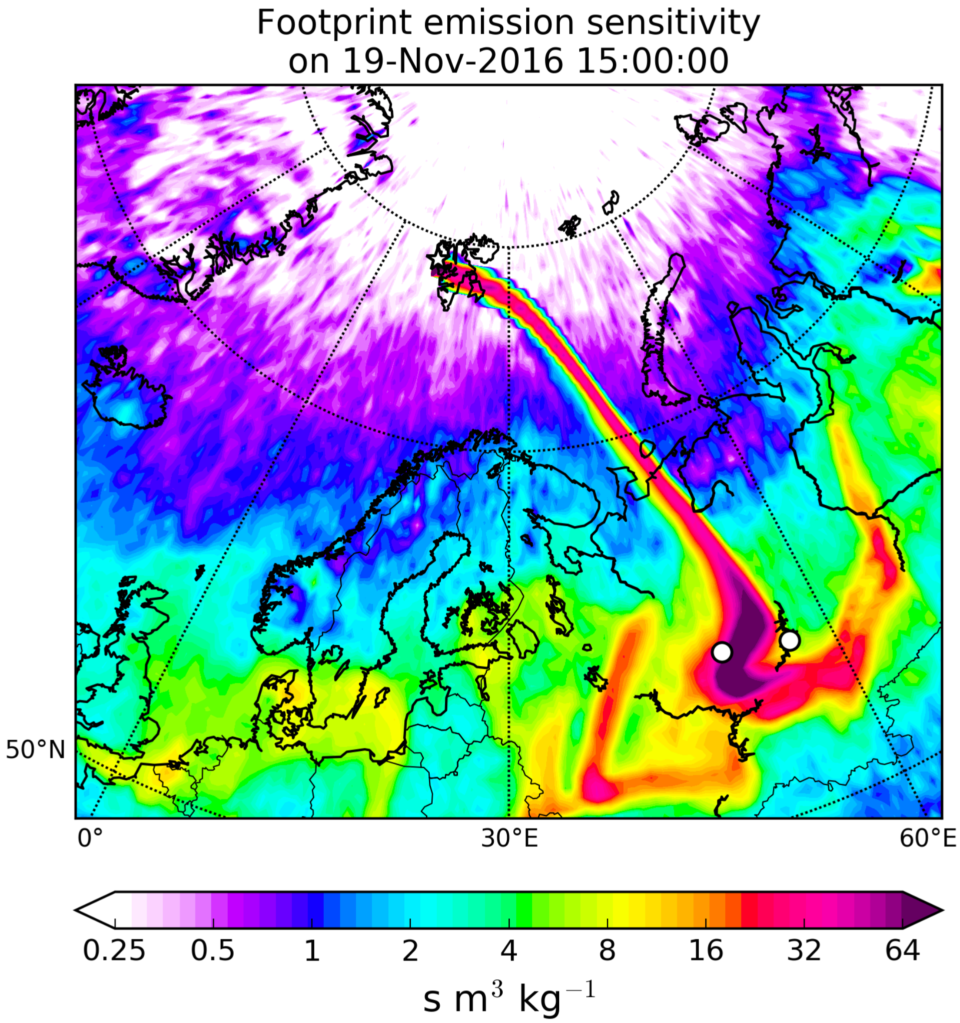

Figure S14. FLEXPART backward simulation for the strong c-$\mathrm{C_4F_8}$ pollution event observed at Zeppelin station on November 19, 2016 indicate that this pollution event may be the result of direct transport of air from two facilities which produce PTFE and halogenated chemicals including c-$\mathrm{C_4F_8}$ (HaloPolymer, Kirovo-Chepetsk, Kirov Oblast, 58.55° N and 49.99° E and Galogen Open Joint-Stock Company, Perm, Russia, 57.92° N and 56.14° E each site marked with a white dot) to the Zeppelin station (marked with a white star).

Deleted: ¶

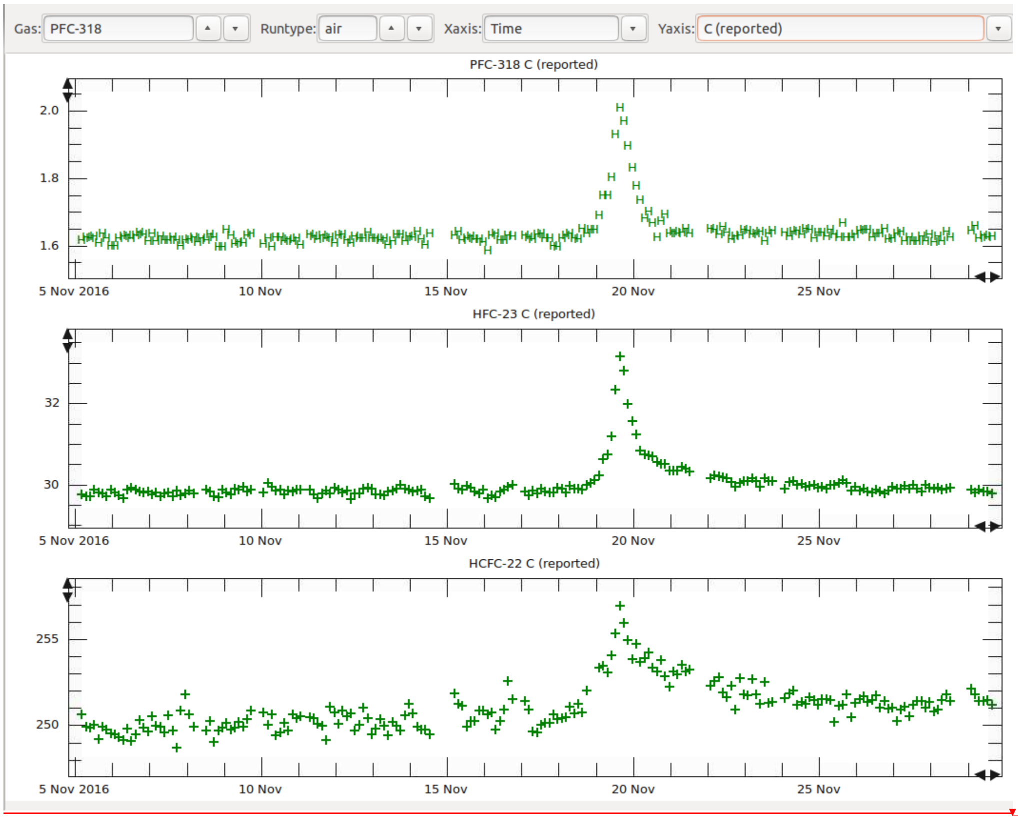

Gas: PFC-318
Runtype: air
Xaxis: Time
Yaxis: C (reported)

Figure S15. PFC-318 (c-C_4F_8), HFC-23, and HCFC-22 mixing ratios in ambient during the largest PFC-318 pollution event at ZEP.

The best correlation was observed between PFC-318 (c-C_4F_8) and HFC-23 mixing ratios (C (reported)). Other compounds, such as HCFC-22 (shown above), CFC-13, CH_2Cl_2, $CHCl_3$, or TCE showed weaker correlations. Most other halogenated compounds showed no obvious correlations.

Supplemental Tables

Table S1. The probability distributions assigned to the emissions and boundary conditions scaling and hyperparameters. Fixed parameters are those which have a fixed distribution that remain unchanged during the inversion. Hyperparameters represent the uncertainty in the uncertainties in the statistical model. These variable hyperparameters are estimated with their associated uncertainty within the NAME-HB inversion framework. This uncertainty translates into the total uncertainty in the posterior emissions estimates.

Parameter	Probability distribution	Fixed or variable?
Emissions and boundary conditions scaling	Log-normal(1,10)	Fixed
Model error (ppt)	Uniform(0.1, 10)	Variable
Correlation length scale (hours)	Uniform(1,120)	Variable
Number of Voronoi cells	Uniform(4,200)	Variable

Table S2. Chinese production of PTFE and FEP fluoropolymers (t yr^{-1}) and five year rise rates, including 2015–2020 forecast from the 13th Chinese five year plan

	2000	2005	2010	2011	2014	2015	2020*
PTFE	8,377	26,700	52,078	52,310	91,608	96,335	140,000
FEP			3,865		10,975	12,937	19,000
Fluoropolymers (total)			60,153		122,190	131,320	194,000
PTFE (% total)			87 %		75 %	73 %	72 %
FEP (% total)			6 %		9 %	10 %	10 %
% yr^{-1} increase		2000-2005	2005-2010			2010-2015	2015-2020*
PTFE		26 %	14 %			13 %	7.8 %
FEP						27 %	8.0 %

www.qianzhan.com/analyst/detail/220/170629-c33a2ca7.html, accessed Dec. 2018 (Chinese, translate.google.com)

*Forecast from the 13th Chinese five year plan.

Deleted: Source:

Table S3. Estimates of global PTFE market share by region

	2012[%]	2015[+]	2015[+]	2015[#]	2015[#]
North America	31 %	10 %	10 %	see RoW	
Europe	21 %	14 %	14 %	see RoW	
Asia Pacific (Total)	36 %	62 %		78 %	
China			53 %		67 %
Japan			9 %		11 %
Rest of World (RoW, Total)	12 %	14 %		22 %	22 %
India			8 %		
Russia			6 %		
Total	100 %	100 %	100 %	100 %	100 %

[%] Polytetrafluoroethylene (PTFE), Market Analysis, www.grandviewresearch.com, accessed Oct. 2018.

RoW is comprised of India and Russia.

[+] Polytetrafluoroethylene (PTFE), A Global Market Overview, www.industry-experts.com, accessed Jul. 2018.

RoW is comprised of India and Russia.

[#] www.qianzhan.com/analyst/detail/220/170629-c33a2ca7.html, accessed Dec. 2018 (Chinese, translate.google.com).

RoW is comprised of North America, Europe, India, and Russia.

In 2015, PTFE production in China was estimated to account for 53 - 67% of global PTFE production.

Table S4. Estimates of global PTFE market share by company

	2012[%]		2015[#]
DuPont	31.0 %	Dupont (Global incl. China)	13 %
Daikin	14.0 %	Daikin (Global incl. China)	13 %
Solvay	11.5 %	Solvay (China)	4 %
3M	9.0 %	3M	4 %
Others	31.0 %	Shangdong Dongyue Group	20 %
		Others (China)	30 %
		Others (Global excl. China)	11 %
Arkema SA	5.5 %		
Gujarat Fluorochemicals Ltd.	3.5 %		
		Asahi Glass (Japan)	5 %
Total	100.0 %		100 %

[%] Polytetrafluoroethylene (PTFE), Market Analysis, www.grandviewresearch.com, accessed Oct. 2018

[#] www.qianzhan.com/analyst/detail/220/170629-c33a2ca7.html, accessed Dec. 2018 (Chinese, translate.google.com).

DuPont incl. Chemours, Solvay incl. Solexis, 3M incl. Dyneon, and Asahi Glass incl. AGC.

Deleted: [+]

Comment [JM18]: Rev. #1: RoW is not exaplained and web pages should be cited with the date on which they were accessed.

Deleted: [+]

Deleted: [+]www.industry-experts.com¶